Analyzing Loricrin in Healthy and Periodontally Diseased Gingival Epithelium

by

Christopher Bryant Roy

A thesis submitted in partial fulfillment of the requirements for the degree of

Master of Science

Medical Sciences - Periodontology
University of Alberta

ABSTRACT

Introduction: Periodontitis is an inflammatory disease of the periodontium that leads to irreversible loss of periodontal ligament, cementum, and alveolar bone. Stage 3 and stage 4 grade C periodontitis (P3C/P4C) are the most severe forms of periodontitis according to the 2017 Classification of Periodontal and Peri-Implant Diseases and Conditions (Papapanou et al., 2018). Loricrin is an integral structural protein comprising more than 70% of the total protein mass in the outer keratinized layer of the epithelium (Nithya et al., 2015). Downregulated and/or mutant phenotypes of loricrin have been linked to inflammatory epithelial related disorders of the skin (Catunda et al., 2019). This suggests an important role of this protein in maintaining barrier function.

Hypothesis: If histological and immunohistological differences exist in the epithelium of Healthy versus P3C/P4C samples then this may suggest a pathogen-mediated epithelial barrier breach due to loss of loricrin.

Methods: A total of 15 gingival epithelium samples were collected during the study period. Discard tissue samples were collected from patients who underwent various periodontal procedures at the University of Alberta Periodontology Clinic. The samples were derived from 5 patients with gingival health, 5 patients with generalized periodontitis stage III grade C, and 5 patients generalized periodontitis IV grade C. The samples were immediately fixed in paraformaldehyde (PFA) and then embedded in paraffin. Each sample was then serially sectioned and mounted on slides for histological and immunohistological analysis. Hematoxylin and Eosin (H&E) staining was completed for a comprehensive expression of the gingival epithelium and connective tissue. Immunofluorescence analysis was completed using antibodies for Loricrin (Lor), Cytokeratin 1 (CK1), and Cytokeratin 14 (CK14). Immunostaining results

from these assays were compared and documented. Using ImageJ software [National Institutes of Health (NIH), Bethesda, MD, USA], the immunostaining intensity of loricrin was semi-quantitatively analyzed and compared amongst the tissue samples by two investigators independently.

Results: For Healthy, P3C, and P4C gingival samples, immunofluorescence assay expressed loricrin, CK1, and CK14 in a similar pattern. Loricrin was expressed predominantly in the stratum granulosum and corneum. Healthy gingival samples had a relatively wider loricrin expression. CK1 was observed in the stratum spinosum and granulosum. A general uniform immunofluorescent signaling trend was observed in the Healthy gingival samples relative to a more interrupted immunofluorescent signal for both P3C and P4C gingival samples. CK14 presented in the strata basale for all gingival sample types. A general uniformed immunofluorescent trend was present for CK14 with no observable distinction amongst the three types of samples.

Significance: The findings from this study suggest that the inflammatory condition of P3C and P4C epithelium may be attributable to a weaker loricrin phenotypic expression. Studies on the pathogenesis of periodontitis tend to focus on the host immune response and the microbiology of the disease. A weakened epithelial barrier and its role in the pathogenesis of periodontal disease necessitates further study.

PREFACE

This thesis is an original work by Christopher Bryant Roy. This project was approved by the University of Alberta Ethics Board (Pro00062112_REN6) under the name "The role of a Loricrin in aggressive periodontal disease". This study was funded by "Fund for Dentistry, Frederick Banting and Charles Best Canada Graduate Scholarship Doctoral and Master's Awards (CIHR)".

Techniques and experiments were done in collaboration with Dr. Maria Febbraio and Dr. Raisa Catunda. Intellectual and editorial contributions to this dissertation were done in collaboration with Dr. Febbraio. H&E and Immunofluorescence were completed and analyzed in collaboration with Dr. Raisa Catunda and Zahra Mantaka. All gingival tissue samples were collected by residents of the Graduate Periodontology Program at the University of Alberta.

ACKNOWLEDGEMENTS

Table of Contents

LIST OF ABBREVIATIONS	
CK	Cytokeratin
BSA	Bovine Serum Albumin
H&E	Hematoxylin and Eosin
IF	Immunofluorescence antibody staining
P3C	Stage III Grade C Periodontitis
P4C	Stage IV Grade C Periodontitis
PBS	Phosphate-buffered saline
RBC	Red blood cells

Chapter 1. Background

CHAPTER 1: Background

1.1 Periodontitis

Periodontitis is an inflammatory disease of the periodontium that leads to progressive and irreversible attachment loss of alveolar bone, cementum, and periodontal ligament. It is one of the leading causes of tooth loss that greatly impacts the quality of life, health, and function of a patient suffering from this disease. It is characterised as a chronic, multifactorial disease associated with a dysbiotic relationship between plaque bacteria and the host immune system (Papapanou et al., 2018). Epidemiological studies have identified the most severe forms of periodontitis as having an international prevalence of 11.2%; this translates into the 6th most prevalent disease, affecting approximately 743 million people (Tonetti et al, 2017). Periodontitis is distinguished from periodontal health by clinical, radiographic, and histological findings.

Clinical features (Salvi et al, 2015) of a patient diagnosed with periodontitis (Figure 1.1) include gingival epithelium that has an erythematous or cyanotic colour. The gingival epithelium consistency presents as spongy and edematous, with bulbous, rolled margins having swollen or absent papillae. The surface texture of the gingival epithelium appears shiny and smooth.

Figure 1.1 Clinical features of periodontitis.
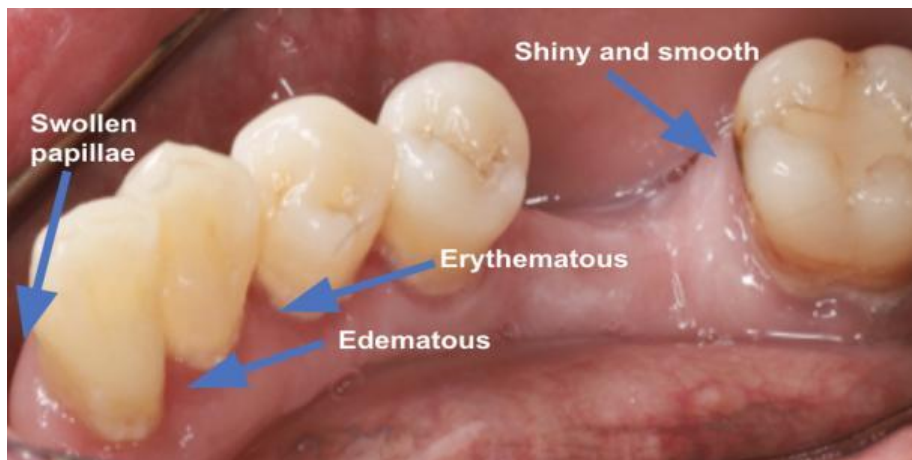
In contrast, hallmark features of periodontally healthy gingiva (Lindhe et al, 2015) include pink epithelium with or without racial pigmentation (Figure 1.2). The gingiva appears tightly adherent and well-adapted to the dentition, with knife-edge and scalloped gingival margins. Interdental papilla are present, well-defined, and fill the embrasure space. The gingival surface may present either with a matte or stippled orange peel appearance.

Figure 1.2 Clinical features of periodontal health.

Radiographically, early signs of periodontitis (Figure 1.3) may include loss of crestal definition. More severe disease will present with horizontal and vertical bone loss, with angular defects extending past the mid- to apical third of the root (Salvi et al, 2015). Additional radiographic findings include molar furcation bone loss and radiopacities suggestive of subgingival calculus. The presence of these structures further increases the level of difficulty for patients to eliminate plaque bacteria to improve their chances of improving periodontal health. The periodontal ligament may appear widened on the radiograph if occlusal trauma is present from parafunctional habits.

Figure 1.3 Radiographic features of periodontitis. A bitewing radiograph of a patient demonstrating some of the hallmark features of periodontitis.

Periodontal health presents radiographically (Figure 1.4) with well-defined crestal bone: the crest of the alveolar bone is typically within 2 mm of the cementoenamel junction (Hausmann et al, 1991). There is no furcation bone loss and calculus are typically not observed on these images.

Figure 1.4 Radiographic features of periodontal health. A periapical radiograph of a patient demonstrating some of the hallmark features of periodontal health.

At the histological level, the destructive process is observed by periodontal loss of attachment and inflammatory signs. This destructive process extends into the periodontal ligament and alveolar bone. Along the alveolar bone, osteoclasts are present in uneven resorption lacunae indicating active osteoclastic activity destruction of bone (Hienz et al., 2015). The sulcular and junctional epithelium appear hyperplastic, with the junctional epithelial margin migrating apically along the root surface, signifying attachment loss. As the periodontal lesion progresses, rete ridge elongation is observed into the gingival connective tissue (Murakami et al, 2018).

The host-microbial challenge in periodontitis triggers the immune system to release pro-inflammatory mediators. Proinflammatory cytokines and microbial virulence factors have been identified in the gingival crevicular fluid as biomarkers for periodontitis (Barros et al, 2016). The neuropeptide Substance P is released upon sensory nerve stimulation by these cytokines and virulence factors (Lundy and Linden, 2004). Substance P plays a role in the vasodilation of microvasculature in the periodontium (Cekici et al, 2014). Clinically, this vasodilation appears as erythema and edema (Chapple et al., 2018). This results in an increase of dense inflammatory cell infiltrates (Figure 1.5) where neutrophils appear within the periodontal pocket epithelium and plasma cells in the connective tissue (Page and Schroeder, 1976).

Figure 1.5 Histological features of periodontitis. A periodontitis gingival sample stained with H&E at 10x magnification demonstrate inflammatory cell infiltration within connective tissue.
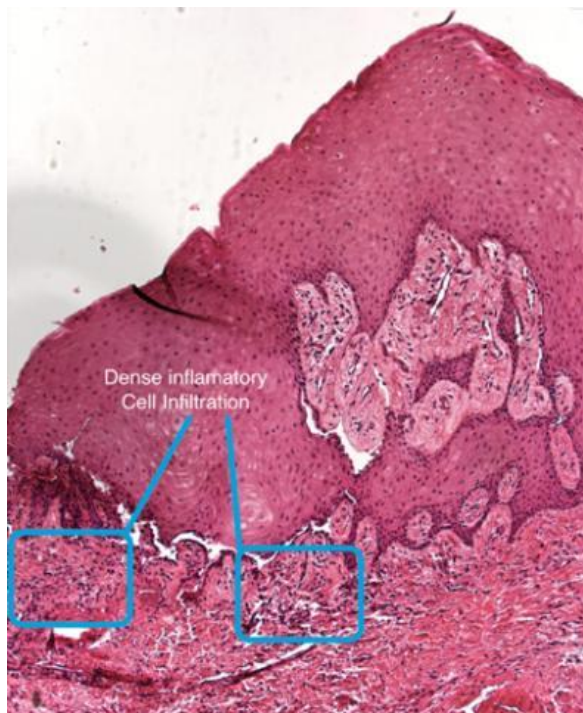
The histological features of healthy gingiva are represented in Figure 1.6. Macroscopically, the gingival epithelium surrounds the dentition and extends interproximal forming the interdental papillae (Lindhe et al, 2015) There is a smooth collar of junctional epithelium that attaches to the enamel and then terminates at the cementoenamel junction. Further, there is a densely collagenous lamina propria that includes a supra-alveolar fiber apparatus, blood and lymphatic vessels, and nerves. This uniformly dense collagen fiber network characteristically lacks or has minimal signs of inflammatory cell infiltration. Compatible with health, there may be a low-grade symbiotic microbial and antigenic challenge (Chapple et al., 2018).

Figure 1.6 Histological features of periodontal health. Depicted is a healthy gingival sample stained with H&E at 20x magnification. A stratified squamous epithelium is observed overlying a densely collagenous connective tissue with minimal inflammatory cell presence.
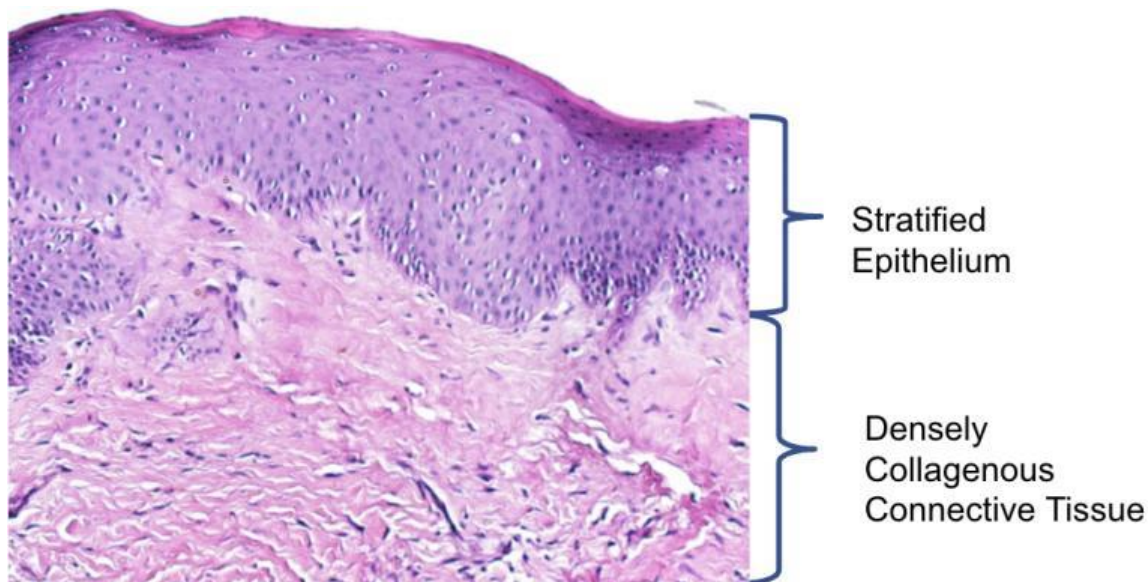
Distinguishing gingival health from periodontitis is important for an oral health practitioner. By recognizing clinical and radiological signs and symptoms of periodontal disease, this will guide a practitioner in formulating a diagnosis and an appropriate treatment plan. To better understand the pathogenesis of disease, it is important to further evaluate, at a histological level, the anatomy of the epithelium. This is where this important barrier serves as a first line of defence against bacteria and other microbes.

1.2 Gingival Epithelium Structure

The oral cavity consists of three types of mucosa, the lining mucosa (e.g., lips, floor mouth, cheeks), specialized mucosa (e.g. dorsal surface of the tongue), and masticatory mucosa (e.g. gingiva, palate). The two main types of stratified squamous epithelium of the lining mucosa are ortho- and para-keratinized. The distinguishing feature between these two types of keratinized tissue is presence or absence of nuclei in the stratum corneum. The predominant

keratinized epithelium type is parakeratinized epithelium. The presence of one type or another does not distinguish health from disease.

The oral epithelium is the primary barrier of the oral mucosa. As a barrier, it functions in protecting the oral cavity against microbial and toxic substance invasion, as well as mechanical trauma insults (Groeger & Meyle, 2019). Surrounding a tooth is a cuff of gingival epithelium (Figure 1.7) that also overlies the alveolar bone (Schroeder & Listgarten, 1997). The gingival epithelium extends coronally alongside an underlying connective tissue. This epithelium is further divided from the inferior portion that attaches directly to the tooth, known as the attached gingiva, from the more superior portion that is not attached and forms a sulcus known as the free gingiva. Apical to this sulcus are the supracrestal tissue attachment, the junctional epithelium and connective tissue, which physically connect to the tooth.

Figure 1.7 Schematic of gingival epithelium surrounding a tooth.
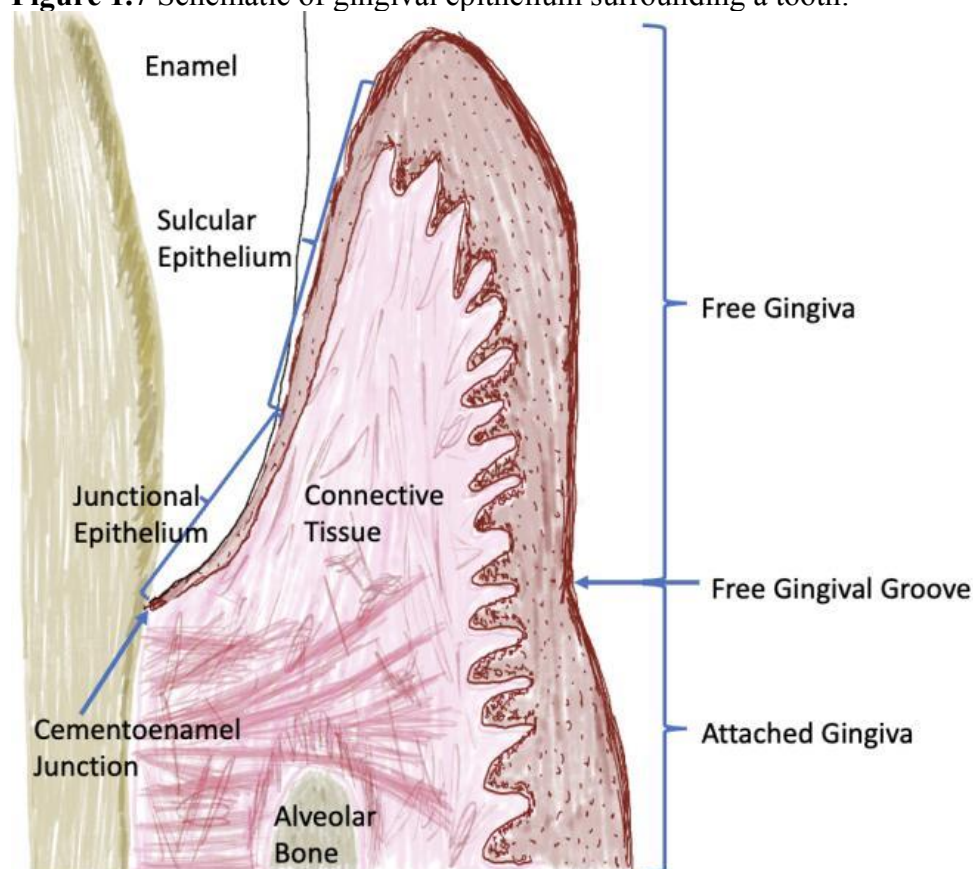
The gingival epithelial barrier consists of a stratified squamous epithelium with an underlying lamina propria connective tissue. Keratinocytes are the predominant cell type in the epithelium. As keratinocytes develop, they undergo a programmed cell death process. This maturation results in a terminally differentiated, complex, cross-linked protein structure known as the keratinized epithelium. The development of the epithelial barrier consists of several protein interactions that give the appearance of four strata (Figure 1.8) (Nanci, 2018):

1) Stratum basale: is the innermost layer of the epithelium. This is the germinative layer where keratinocytes actively undergo mitosis. The cells are found along the basement membrane and appear cuboidal in shape.

2) Stratum spinosum: also known as the prickle-cell layer due to the development of spinous processes around the cell. The cells are larger and ovoid in shape and the spinous processes represent desmosome intercellular contact points.

3) Stratum granulosum: cell contents appear more granular due to the production of a number of keratohyalin granules. The cell shape is slightly flattened. In this stratum, the cell membrane thickens and fusion between cells is observed.

4) Stratum corneum: cells and nuclei are condensed and flattened further in this outer layer of the epithelium. The organelles are lost, and keratinocytes contain several tonofilaments. If nuclei disappear then the epithelium is orthokeratinized. In contrast, if the nuclei are retained then the epithelium is parakeratinized. The stratum plays in an important barrier function role.

Figure 1.8 Strata of the gingival epithelium.
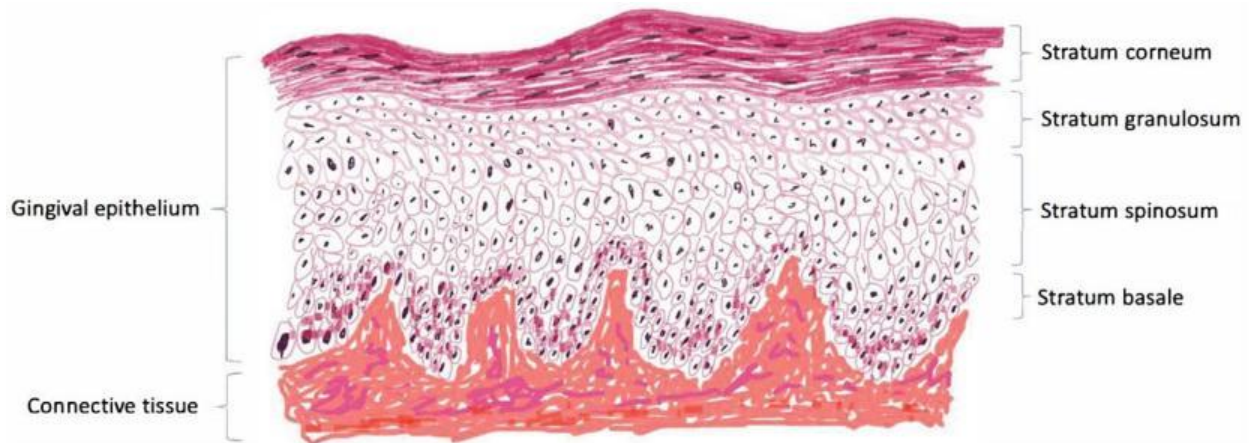
This epithelium can be further subdivided in the oral cavity depending on the presence or absence of keratin. Keratinized epithelium is tightly adherent to the underlying collagenous connective tissue and found along the hard palate and gingiva. In contrast, the non-keratinized form overlies a more elastic connective tissue support, found within the flexible buccal mucosa, labial mucosa, soft palate, and sublingual tissues. Junctional epithelium consists of non-keratinized epithelium and gingival epithelium consists of keratinized epithelium (Groeger & Meyle, 2019).

1.3 Key Epithelial Structural Proteins

The epithelium provides the first line of defense against bacterial challenge by virtue of its barrier integrity. Key specific epithelial proteins evaluated in this study were loricrin and cytokeratins. Cytokeratin 14 (CK 14) is expressed to the stratum basale, while CK 1 is expressed throughout the stratum spinosum and granulosum, and loricrin is found in the stratum corneum. These proteins are found distributed throughout the gingival epithelium and make up key components of the epithelial barrier. Akin to how mutant or downregulation of loricrin expression underlies certain skin disorders, mutant or downregulation of loricrin may contribute mechanistically to severe periodontitis. Severe periodontal disease is characterized by having

rapid attachment and bone loss. One of the possible reasons for the aggressivity, despite a thin

microbial presence, could be due to a compromised barrier resulting from dysregulation of

loricrin or other epithelial barrier proteins. We focussed on loricrin as an initial protein to

investigate due to its high abundance in cornified epithelium.

The formation of the keratinized envelope involves an intricate series of

transglutamination and crosslinking steps between structural proteins and lamellar body lipids

(Candi et al., 2005). Loricrin is an integral structural protein that makes up more than 70% of the

keratinized envelope (Nithya et al., 2015). A sequence of protein synthesis, covalent interactions,

enzymatic crosslinking with structural proteins, and lipid extrusion gives rise to the cornified

envelope (Figure 1.9). Loricrin becomes highly insoluble with further cross-linkages that leads to

stabilization and strengthening of the cornified envelope (Hohl et al, 1991). As such, loricrin

plays an important role of reinforcing this epithelial barrier in the stratum corneum.

Figure 1.9 Development of the cornified envelope barrier.
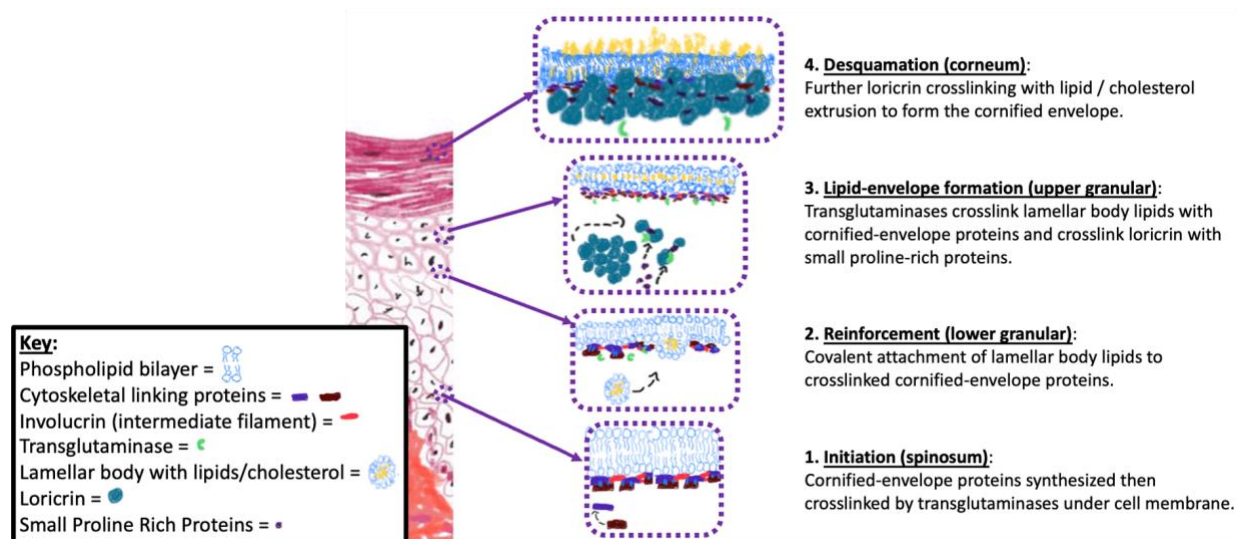
A recent systematic review by Catunda et al., 2019, hypothesized that epithelial disorders

may be due to changes in loricrin expression and subsequent barrier function alteration. The

results of this study found a 63% correlation between loricrin mutation and/or a 75% correlation

with loricrin downregulation with epithelial related disorders (Catunda et al., 2019). This study found the most common condition associated with loricrin mutations was loricrin keratoderma (Catunda et al., 2019). Further, atopic dermatitis was the most common condition where loricrin was downregulated (Catunda et al., 2019).

Individuals presenting with loricrin keratoderma characteristically present with parakeratotic hyperkeratosis of the soles and palms as well as digital constriction (Ishida-Yamamoto, 2003). This disorder is linked to a frameshift mutation at the C-terminus end of loricrin (Nithya et al, 2015). As a result, there is an increase in the more positively charged arginine addition to the primary structure (Hohl et al, 1991). This mutational change disrupts keratinocyte differentiation by creating an arginine-rich nuclear localization sequence leading to loricrin accumulation within the nucleus (Ishida-Yamamoto, 2003). As a result of loricrin accumulation within the nucleus, keratinocyte mitosis or apoptosis is observed causing a disorganization of the epithelium (Ishida-Yamamoto et al 1998).

The other epithelial related disorder linked to loricrin is atopic dermatitis. This condition is characterized by individuals exhibiting a chronic inflammatory skin condition predisposing them to skin infections (Bao et al, 2017). A molecular mechanism has been elucidated between the production of inflammatory cytokine interleukin-4 (IL-4) and the down-regulation of loricrin (Bao et al, 2017). In response to inflammation, the cytokine IL-4 production is elevated by Th2 lymphocytes, mast cells, and basophils stimulation (Silva-Filho et al, 2014). In an animal study by Bao et al (2017), loricrin transcription was downregulated as IL-4 was upregulated. The proposed molecular mechanism was a shared transcription pathway between these two proteins (Bao et al, 2017). An intracellular signal transducer and activator of transcription (STAT)-6 protein recruits a common coactivator, p300/CBP, during transcription (Bao et al, 2017). As the

demands of inflammation leads to an increased IL-4 synthesis, loricrin is outcompeted for this common co-activator leading to its downregulation (Bao et al, 2017). This may serve as a potential pathogenic molecular mechanism explaining possible epithelial barrier defects in periodontal disease.

Intermediate filaments of the epithelium are linked to barrier integrity and epithelial related disorders. All epithelial intermediate filament cytoskeletons are composed of keratins type I and type II (Magin et al, 2007). These proteins are derived from 65 functional genes and play a significant role in forming the epithelial cytoskeleton (Groeger & Meyle, 2019). The basic structure of a keratin is a heterodimer protein with a type I chain paired with a type II counterpart (Ganavi, 2014). The heterodimers continue to pair forming polypeptide chains stabilized by hydrophobic interactions to assemble into filaments. (Figure 1.10).

Figure 1.10 Keratin filament formation.
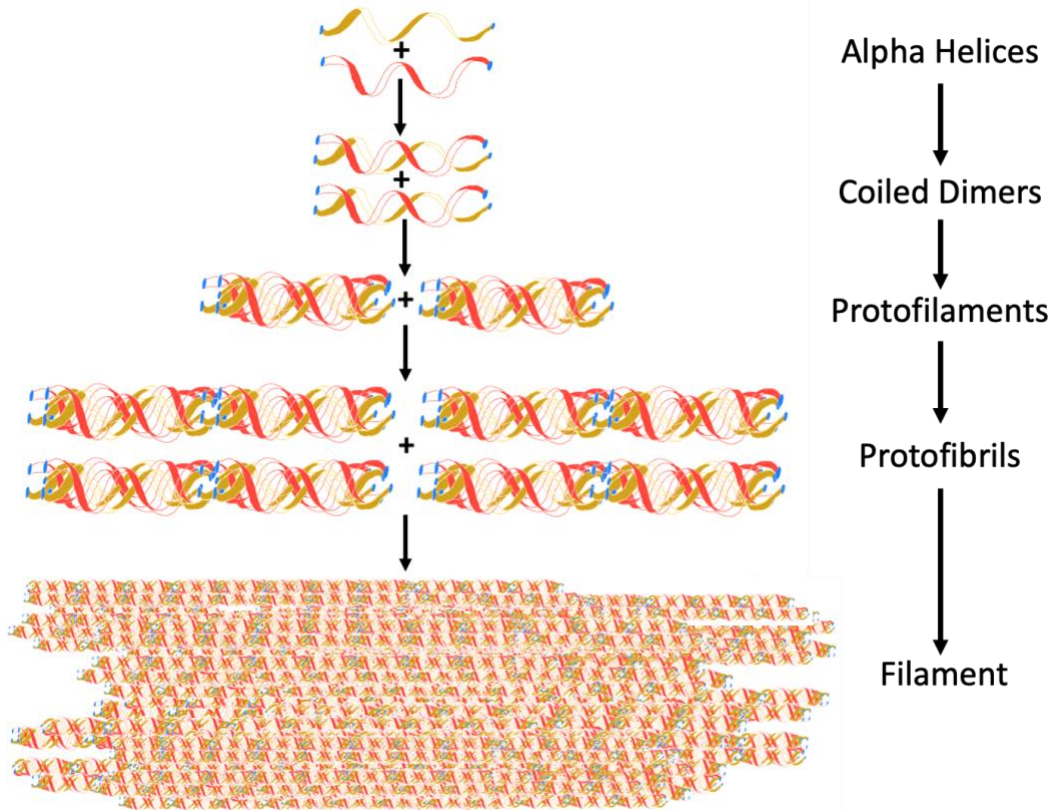
Cytokeratins will form tonofilaments that connect keratinocytes with desmosomes and hemidesmosomes of the epithelium (Magin et al, 2007). These tonofilament structures maintain epithelial tissue integrity by virtue of interactions between keratinocytes, the basal membrane, and/or the surrounding matrix (Magin et al, 2007). In addition to providing mechanical support and cellular architecture maintenance, keratins also aid in wound healing, intracellular transport, intercellular junction formation, and in regulating protein synthesis and cell growth (Ganavi, 2014). Cytoskeletal proteins are expressed in a highly specific manner in different epithelium types. These structural proteins can serve as biomarkers for epithelial integrity.

Over 30 disorders are related to genetic mutations of genes for intermediate filaments (Omary et al 2004). These disorders reflect a degradation in barrier. In addition to evaluating loricrin distribution in healthy and periodontitis tissue samples, the intermediate filaments cytokeratin 1 (CK 1) and CK 14 were analysed as a potential indicator of epithelial dysfunction. We chose CK 1 and CK 14 because they are differentially expressed. CK 1 is expressed to the stratum spinosum and granulosum, whereas CK 14 is found expressed to the stratum basale (Figure 1.11). CK 1 mutations are associated with the following epithelial-related disorders: epidermolytic hyperkeratosis; palmoplantar keratoderma; and monilethrix (Omary et al 2004). Similarly, CK 14 mutations are associated with the epithelial-related disorder epidermolysis bullosa simplex (Omary et al 2004).

Figure 1.11 CK1 and CK 14 expressed within epithelium.

Cytokeratin 1   **Cytokeratin 14**

Key:

● = keratinocyte with CK localization
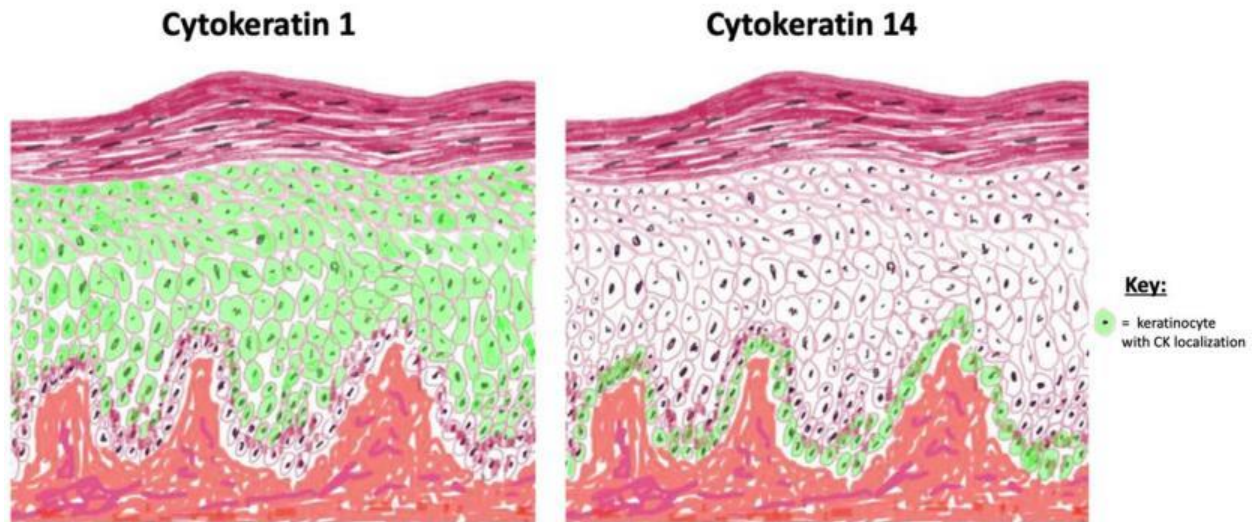
1.4 Hypothesis

If histological and immunohistological differences exist in the epithelium of healthy versus severe periodontal disease patients, then this may suggest a pathogen-mediated epithelial barrier breach due to loss of loricrin.

Chapter 2. Methodology

CHAPTER 2: Methodology

2.1 Ethics

All procedures related to the collection of human tissue samples were conducted in accordance with protocols approved by the University of Alberta Ethics Board (Pro00062112_REN6) under the name "The role of a Loricrin in aggressive periodontal disease". Patients undergoing various periodontal procedures at the University of Alberta Graduate Periodontal Clinic were invited to donate gingival tissue samples after having reviewed and signed the informed consent document (Appendix 1).

2.2 Gingival Sample Acquisition and Preparation for Analyses

2.2.1 Sample Acquisition from Patients at the Graduate Periodontal Clinic

Gingival discard samples were collected from patients undergoing various procedures at the University of Alberta Graduate Periodontal clinic. The tissue samples were derived from 25 male and 23 female patients. The samples were collected from the patients that underwent crown lengthening, osseous resective surgery (Figure 1), extractions, connective tissue grafts, free gingival grafts, orthodontic tooth exposure, and implant placement (Figure 2.1).

Figure 2.1 Example of a periodontal procedure where a gingival sample was collected.

From this collection of samples, 5 gingival healthy, 5 periodontitis stage III grade C (P3C), and 5 periodontitis stage IV grade C (P4C) discard samples were identified as having a sufficient quantity and quality for histological analysis. Diagnoses were completed by the

residents during patient initial examinations in accordance with the World Workshop

Periodontology 2017 classifications (Lang & Bartold, 2018; Papapanou et al., 2018). The tissues

were fixed in 10% formaldehyde (28908, Thermo Fisher Scientific) at 4°C overnight. The tissue

samples were rinsed with phosphate buffered saline (PBS) twice and then immersed in PBS in a

500 μL microfuge tube at 4°C until tissue processing was completed.

2.2.2 Dehydration and Processing

Tissue samples were transferred from the microfuge tube and placed in histologic slotted

cassettes (B851120OR, Epredia). The cassettes were then placed in a TP1020, Leica Biosystems

Automatic Benchtop Tissue Processor (Figure 2.2) to undergo a paraffin embedding tissue

processing cycle. Processing included a sequence of dehydration steps, beginning with two

changes in 70% ethanol for 1-hour, 96% ethanol for 1-hour, three changes in 100% ethanol over

3.5-hours, followed by three changes in xylene over 1.5-hours, and then two changes in paraffin

wax (58-60°C) over 2-hours (Berlin-Broner 2018).

Figure 2.2 Automated benchtop tissue processor.

2.2.3 Embedding

Using an EG1160, Leica Biosystems Embedding Center (Figure 2.3), each gingival tissue sample was embedded in paraffin wax (Histoplast Paraffin Wax, 22900700, Thermo Fisher Scientific). Where possible, samples were laterally oriented to permit analysis of the stratified squamous epithelium with underlying connective tissue.

Figure 2.3 EG1160, Leica Biosystems Embedding Center.

2.2.4 Microtome Sectioning

Sectioning of the embedded blocks was completed using an automated Leica microtome (Figure 2.4). The section thickness was set at 7 μm. The sectioned tissues were collected onto Superfrost Plus microscope slides (22037246, Thermo Fisher Scientific). Using a 40°C water bath, samples were oriented onto slides for further histological analyses.

Figure 2.4 HistoCore AUTOCUT, 14051956472, Leica Biosystems.

2.3 Hematoxylin and Eosin (H&E) Staining

As one of the principal histological stains for evaluating tissue samples, H&E technique was employed to investigate any morphological differences between the tissue types, specifically, the type of keratinized epithelium and presence of inflammatory signs within each sample. A modified H&E protocol from Gautier et al (2017) was performed in this study.

2.3.1 Sample Deparaffinization

Deparaffinization of the samples on the slides was performed by heating the slides to 65ºC in a Hi-Temp Vacuum Oven (3625A, ThermoFisher Scientific Hi-Temp Vacuum Oven, Figure 2.5) for 10-minutes and then rinsing the slides in xylene.

Figure 2.5 Sample deparaffinization in ThermoFisher Scientific Hi-Temp Vacuum Oven.

2.3.2 Tissue Rehydration and H&E Staining Sequence

The tissues were then rehydrated by following a series of graded ethanol washes: two rinses in 100% ethanol for 5-minutes, one rinse in 95% ethanol for 2-minutes, and one rinse in 70% ethanol for 2-minutes (Figure 2.6).

Figure 2.6 H&E staining assay sequence.
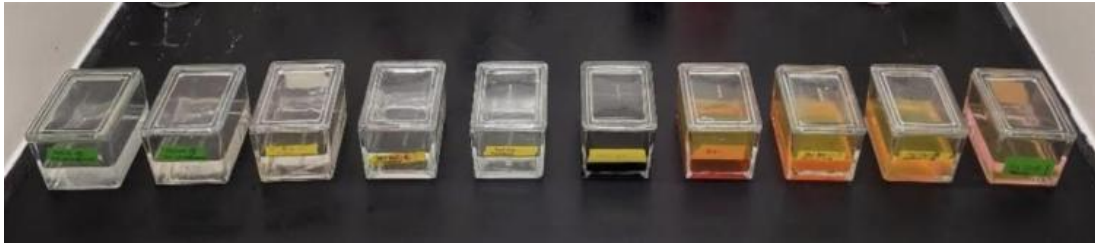
Following a rinse in Milli-Q water, the slides were immersed in hematoxylin (245656,

Protocol) for 2-minutes. After a thorough rinse with Milli-Q water, the slides were placed in

eosin (245658, Protocol) and then rinsed with Milli-Q water. After dipping the samples in 95%

ethanol three times and then rinsing in 100% ethanol, the samples were rinsed for 4-minutes in

xylene.

2.3.3 Mounting and Microscopy

Samples were covered with a glass coverslip (22 mm x 60 mm) using a mounting

solution, Permount (SP15100, Thermo Fisher Scientific, Figure 2.7). Imaging was completed

under brightfield using a Leica DM2000 microscope (Leica Microsystems), after drying the

stained slides.

Figure 2.7 Mounting slides with Permount solution and glass coverslip.
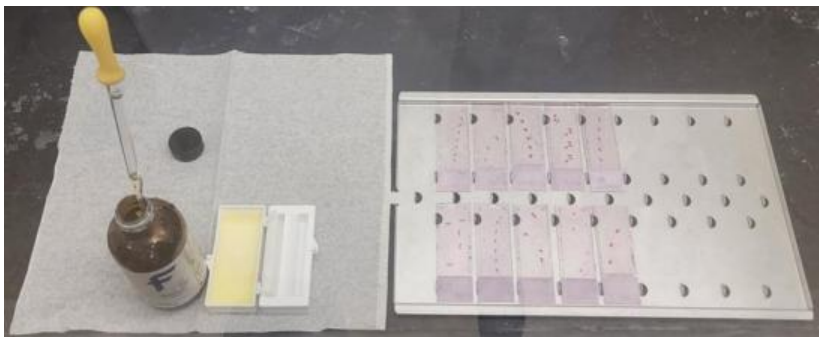
2.3.4 H&E qualitative and semi-quantitative inflammation analyses

Measurements and image characteristics were verified by two investigators

independently. Signs and relative quantity of inflammatory signs were assessed amongst

Healthy, P3C, and P4C samples. These signs included peri-vascular edema and red blood cells (RBC) presence within the connective tissue, an increase in inflammatory cells within the epithelium (e.g., polymorphonuclear, plasma, and lymphocytic cells), and increase in rete peg length. If present, peri-vascular edema was highlighted in blue and RBCs in red on the 4x image of each gingival sample. To compare and assign each gingival tissue type a severity level, the number of inflammatory cells in the 20x magnification were highlighted and counted by two separate observers. If there were less than 15 inflammatory cells, then the gingival sample was designated as having a slight number of inflammatory cells. A moderate number of inflammatory cells was designated to gingival samples with 15 but less than 30 inflammatory cells. Lastly, a severe number of inflammatory cells designation was reserved for gingival samples with 30 or more inflammatory cells. The length of rete pegs was calculated based on the average of three separate measurements, using a 20x image and Image J software (Figure 2.8 and 2.9).

Figure 2.8 Calibrating the pixel distance using a fixed reference scale. The Image J software ruler aligned with a fixed reference point on this 10x H&E stain to calibrate the distance.
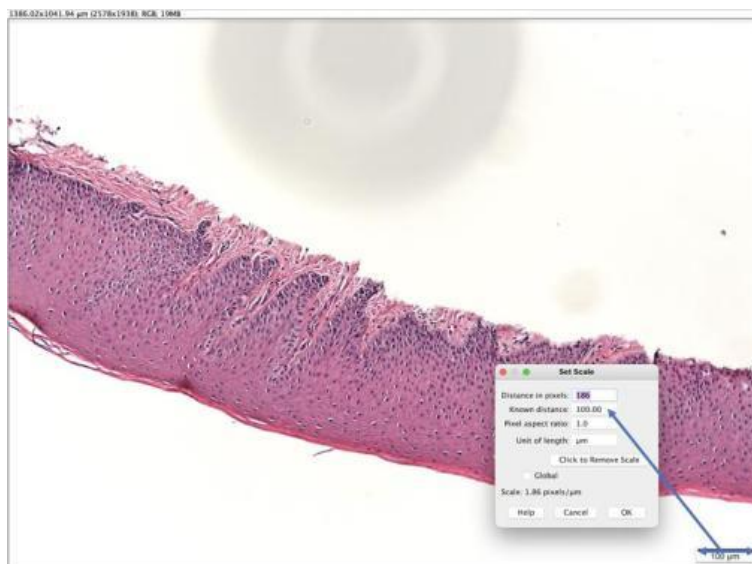
Figure 2.9 Measuring the length of rete pegs. After calibrating the Image J software ruler, three separate rete peg lengths were measured to determine an average length for each sample.
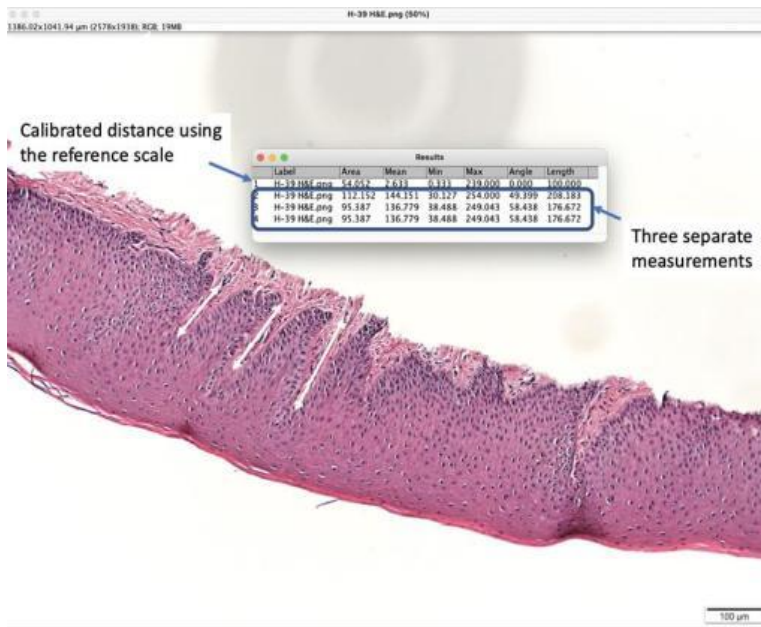
2.4 Immunofluorescence Antibody Staining

Samples were further histologically analysed via an adaption of the immunofluorescence protocol outlined in a study by Christodoulou et al (2019).

2.4.1 Sample deparaffinization and rehydration

Samples were deparaffinized in a Hi-Temp Vacuum Oven (3625A, ThermoFisher Scientific Hi-Temp Vacuum Oven, Figure 4) for 10-minutes at 65°C. Remaining paraffin was removed by completing a xylene wash (Figure 2.10). Tissues were re-hydrated through a graded series of ethanol rinses. The slides were immersed in two 100% ethanol rinses for 10-minutes each. This was followed by a rinse in 95% ethanol for 5-minutes. Lastly, the slides were immersed in 70% ethanol and then placed in Milli-Q water for 5-minutes.

Figure 2.10. Xylene and ethanol rinses to remove paraffin and rehydrate tissue samples.

2.4.2 Antigen optimization

Antigen optimization was completed by immersing the slides in slide mailers (22-363-900, Fisherbrand™ Polypropylene Slide Mailers) filled with antigen retrieval solution (0.006M citric acid, 0.01M trisodium citrate buffer, pH 6.0). The slide mailers (Figure 2.11) with the slides and antigen retrieval solution were heated to 90°C for 20 seconds and then allowed to cool for 30-minutes.

Figure 2.11 Slide Mailer used for completing antigen optimization.

Slides were washed three times for 5-minutes using PBS solution while shaking at 40 rpm on a lab rotator (Thermo Scientific 2314 Multi-Purpose Lab Rotator, Figure 2.12).

Figure 2.12 Multi-purpose lab rotator.
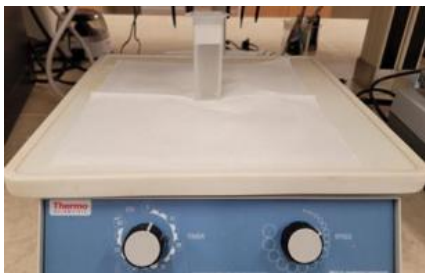
The slides were then dried by tapping horizontally on their sides and then removing any excess liquids using a Kimwipe (Kimberly-Clark Profession 34120) as to not contact the samples. The individual sections were encircled using an ImmunoPen™ (PAP Pen, 402176, Millipore) to create a hydrophobic barrier (Figure 2.13).

Figure 2.13 ImmunoPen™ tracing a hydrophobic barrier.
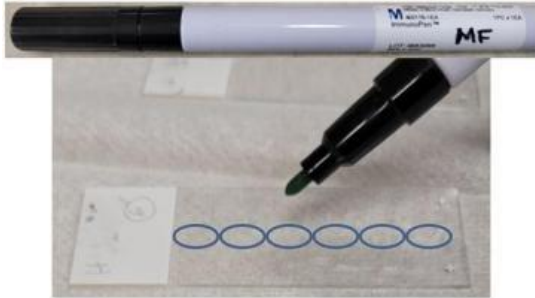
2.4.3 Primary antibody incubation

Prior to primary antibody incubation, non-specific antigen blocking was completed with goat serum (ab7481, Abcam). Tris-buffered saline (TBS, 0.05M Tris, pH 7.6; 0.015M sodium chloride) and 10% goat serum (100 µl of stock goat serum, 900 µl of bovine serum albumin (BSA) were added to each sample for 45-minutes in a humid chamber (Figure 2.14).

Figure 2.14 Samples incubating with blocking solution in a humid chamber.
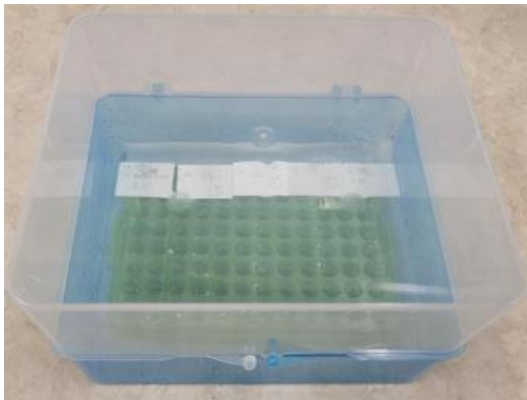
The blocking solution was then removed by tapping the slides on their side and gently blotting with a Kimtech wipe to remove any excess moisture. Immediately after, to avoid having

the tissue samples dry out, the primary antibodies (Table 1) were added onto designated sections of each slide, while reserving sections for two different types of negative controls (Figure 2.15).

Table 2.1 Primary antibodies implemented during immunofluorescence assay.

Antigen Target	Antibody Type	Host Source	BSA Dilution	Company	Catalogue
Loricrin	Polyclonal	Rabbit	1:100	Abcam	85679
CK1	Monoclonal	Rabbit	1:500	Abcam	185628
CK14	Monoclonal	Rabbit	1:500	Abcam	119695

Figure 2.15 Primary antibody and negative control schematic.
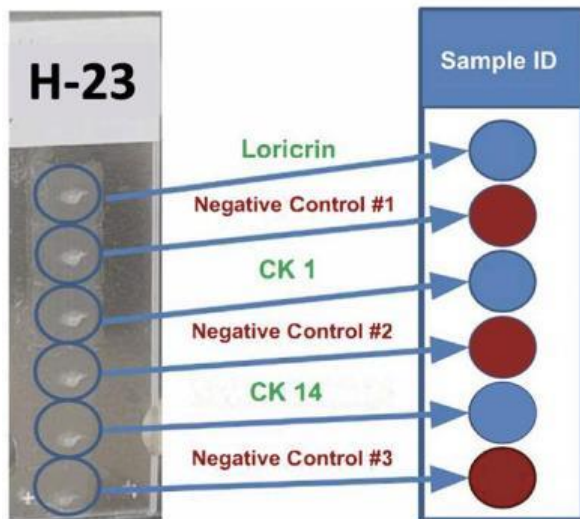
At the primary antibody incubation step, only PBS was added to the negative control sections. The slides were placed back into the humid chamber to incubate overnight at 4°C.

2.4.3 Secondary antibody incubation

The slides were then removed from the humid chamber following a 24-hour incubation period and placed in a slide mailer. PBS-Tween 1% was poured into the slide mailer; this was done three times for 5-minutes each, while shaking at 40 rpm. In the dark, the secondary antibody, conjugated with a fluorescent tag, was added to the samples and to negative controls #1 and 2 (Figure 2.16).

Figure 2.16 Secondary antibody and negative control schematic.
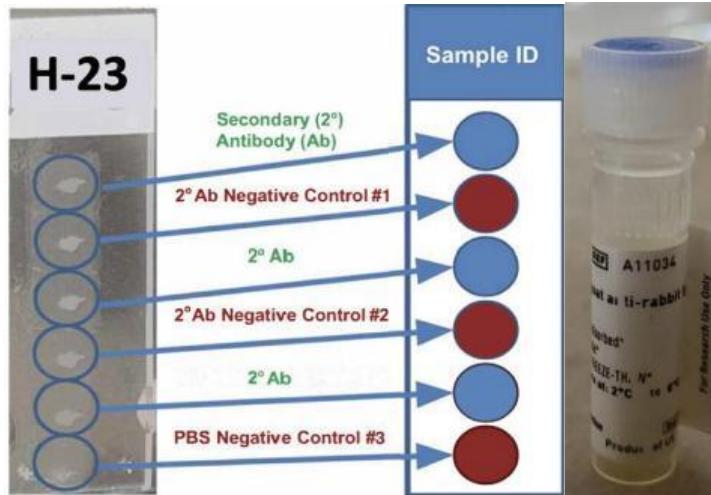
These negative controls were to gauge non-specific antigen-antibody binding. PBS was added to the negative control #3. For all antigens examined, DyLight 488 conjugated goat anti-rabbit (A11034, Thermo Fisher Scientific) was the secondary antibody utilised. The slides were placed in a humid chamber and allowed to incubate for 2-hours in the dark (Figure 2.17).

Figure 2.17 Incubating the secondary antibody in a humid chamber covered with tin foil.

Following the incubation period and a series of 3PBS washes for 5-minutes each, coverslips were mounted to each slide, in the dark, using SlowFade Gold Antifade Mountant 4', 6-diamidino-2-phenylindole (DAPI, S36938, Thermo Fisher Scientific) and then stored in a Pop-Up Slide Holder (Catalogue M6305, Allegiance) to reduce exposure until ready for microscopy (Figure 2.18).

Figure 2.18 DAPI mounting solution and light block-out slide holder storage.

The slides were visualised using an immunofluorescence microscope (Olympus Inverted

Microscope with X-Cite 120LED model IX73, LUMEN Dynamics and IX3 reflected

fluorescence system) in a low-lit room (Figure 2.19).

Figure 2.19 Immunofluorescence microscopy in a low-lit room.

2.4.4 Expression of loricrin, CK1, and CK14 qualitative analysis

The green IF signal represents the immunofluorescent tagged antibody bound to the

specific antigen being assessed (i.e., loricrin, CK1, or CK14). Further, a DAPI nuclear

counterstain (blue signal) was completed to orient the gingival sample. A qualitative analysis

was completed to assess the location and pattern of expression of each antigen. If the signal was observed to be a solid green line, then this was described as being uniform. In contrast, if the signal was not uniform appearing broken up then this was described as interrupted.

2.4.5 Expression of loricrin IF semi-quantitative analysis

Imaging was verified by two investigators independently. The width of the green immunofluorescence signal within the epithelium was measured using ImageJ software (National Institutes of Health (NIH), Bethesda, MD, USA). The ImageJ rule was calibrated using a fixed reference scale and then three separate width measurements of the green IF signal were completed to determine an average for each sample (Figure 2.20 and 2.21). These measurements were used as a semi-quantitative comparative analysis amongst the three tissue types.

Figure 2.20 Calibrating the pixel distance using a fixed reference scale. The Image J software ruler is aligned with a fixed reference point on this 20x IF stain for loricrin.
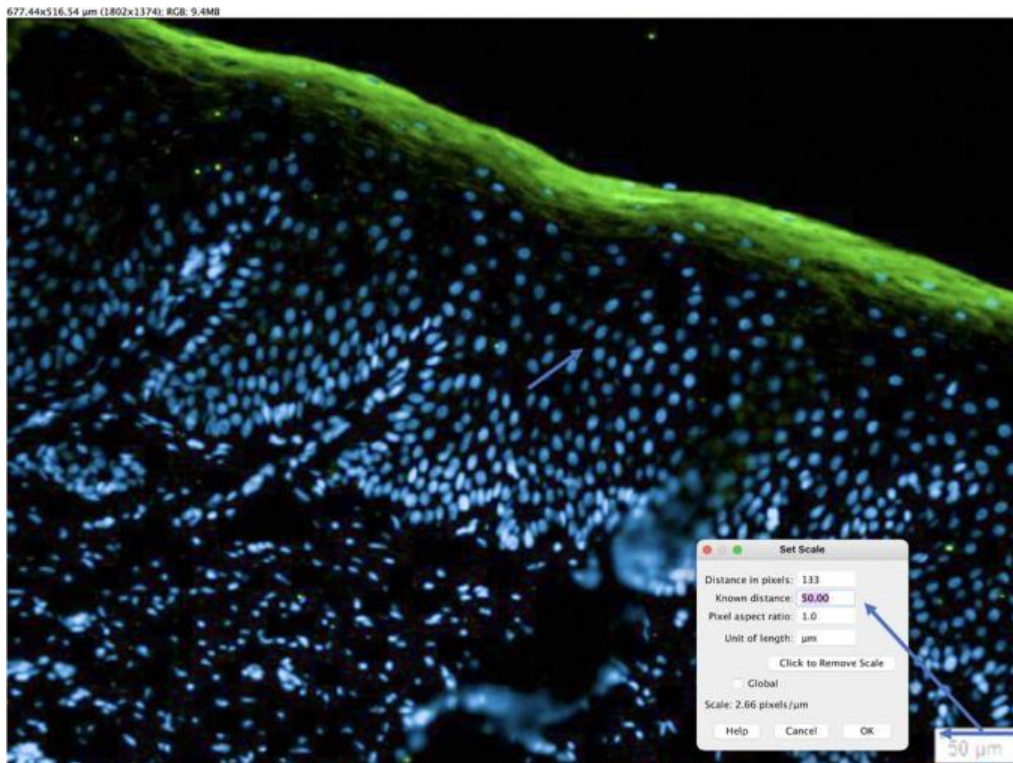
Figure 2.21 Measuring the width of loricrin. After calibrating the Image J software ruler, three separate width measurements of the green IF signal were completed to determine an average.
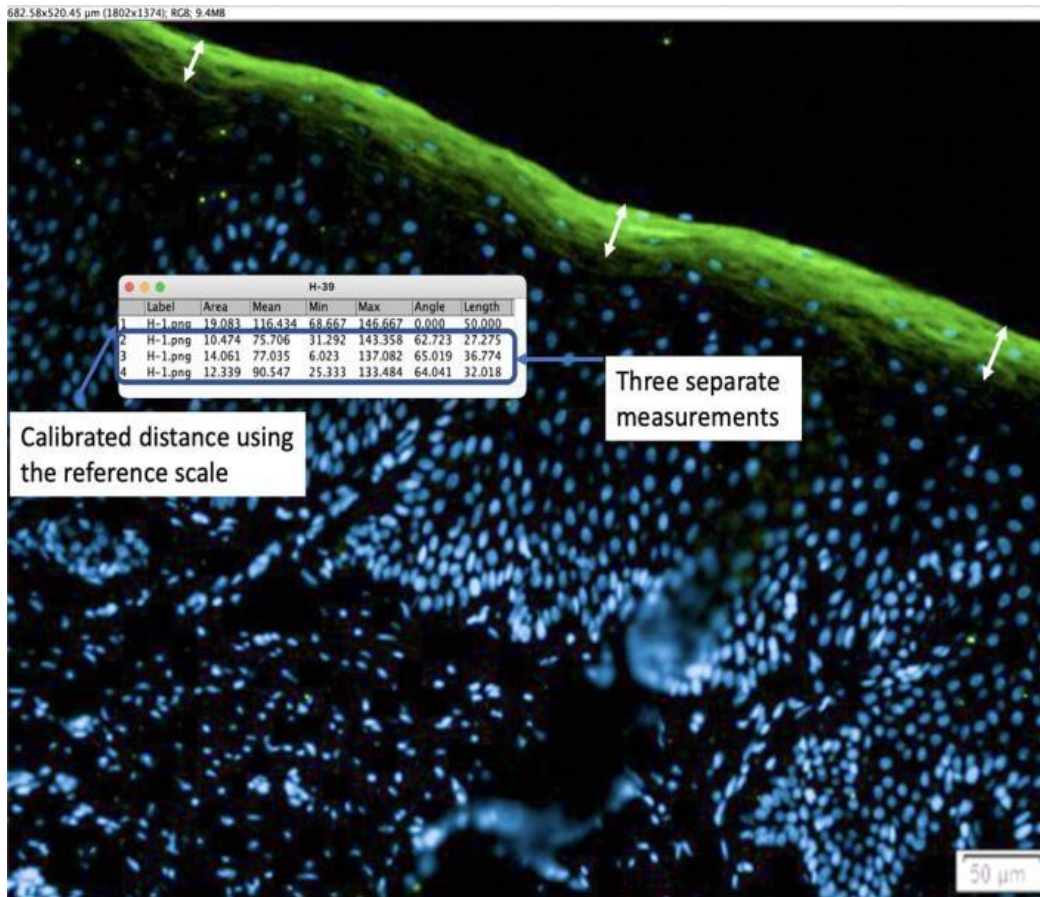
Chapter 3. Results

CHAPTER 3: Results

3.1 Patient demographics and diagnoses

A total of 15 gingival epithelium samples are evaluated in this thesis. The samples were derived from 5 patients with gingival health, 5 patients with generalized periodontitis stage III grade C, and 5 patients with generalized periodontitis IV grade C. Diagnoses were determined by the residents in the Periodontology Program using the 2017 American Academy of Periodontology Classification of Periodontal and Peri-Implant Diseases and Conditions (*2017 Classification of Periodontal and Peri-Implant Diseases and Conditions*, 2019). These patients underwent various periodontal procedures involving a gingival epithelium discard and were asked to participate in the research study by donating their tissue and gave informed consent (Annex 1).

The samples analyzed were derived from 8 male and 7 female patients ranging from 15 to 89 years of age with an average age of 61 (Figure 3.1).

Figure 3.1 Age demographics of participants.
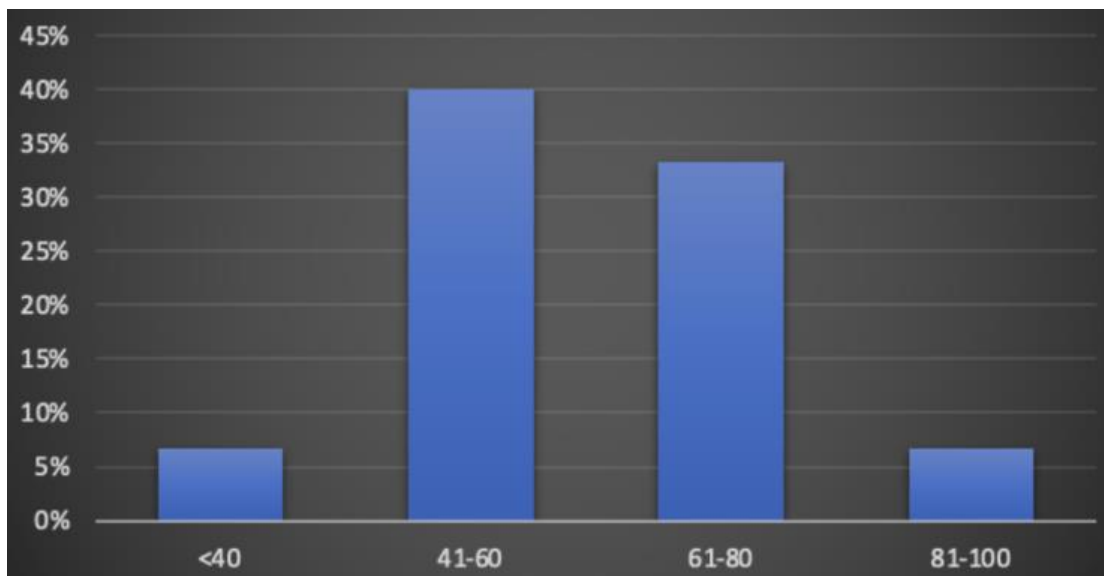
To reduce the potential of confounding variables, the majority of the participants were non-smokers and non-diabetics. Of note, two participants were identified as light smokers (Johnson & Hill, 2004), having smoked less than half-a-pack per day, while the remaining were non-smokers. Further, two non-smoker participants had type II diabetes. Both of these patients were assessed as having well controlled diabetes with recent Hemoglobin A1C measurements ranging from 6-6.9% (Punthakee et al, 2018).

The type of periodontal surgical procedures performed where gingival samples were collected included crown-lengthening, osseous resective procedures, open flap debridement, extractions, and orthodontic tooth exposures (Figure 3.2).

Figure 3.2 Periodontal procedures completed where gingival samples were collected.
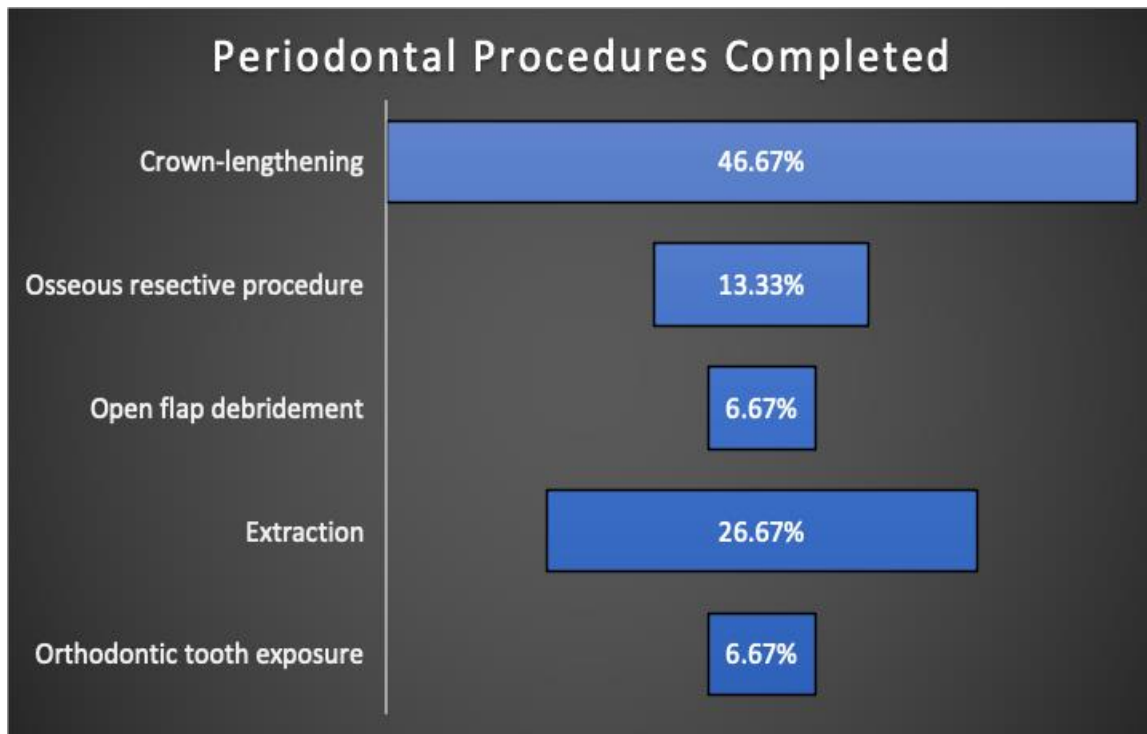
A crown lengthening procedure is often necessitated when a planned prosthodontic restorative treatment requires additional tooth structure above the gingiva. This elongates the

dimension of the tooth for additional mechanical retention of the future restoration (Figure 3.3).

Typically, the patient will have a healthy periodontium.

Figure 3.3 Crown lengthening procedure and gingival sample collection site.
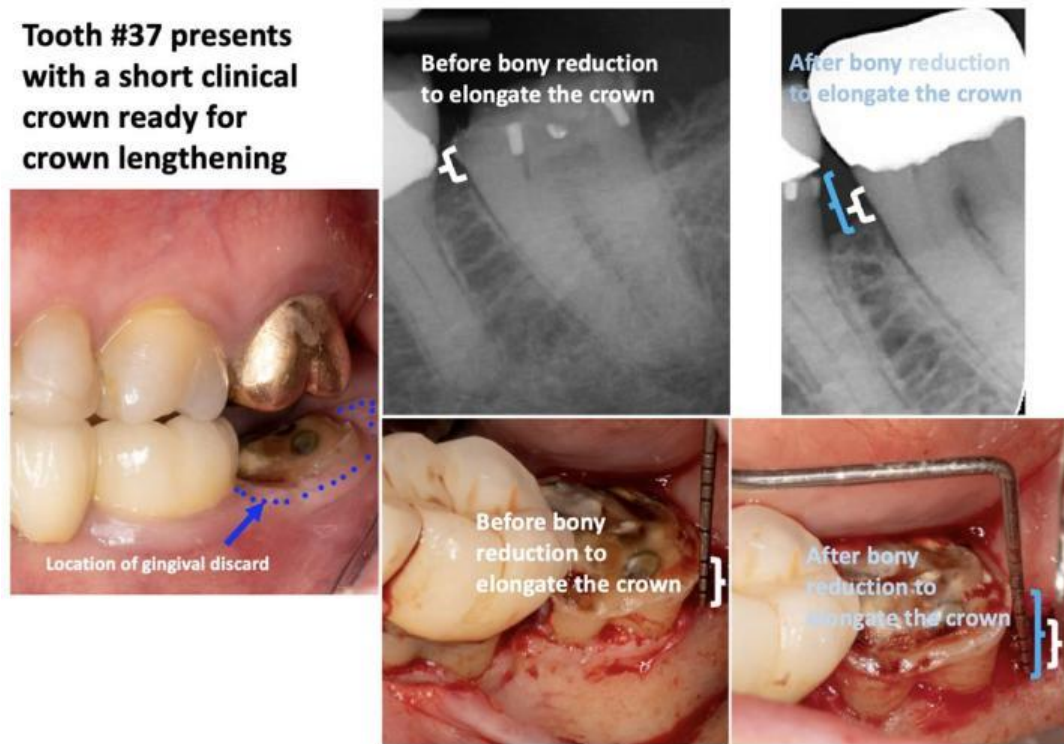
An osseous resective procedure follows similar surgical steps to a crown lengthening

procedure. Both treatment modalities involve a gingival discard and osseous reduction. The

objective of these procedures differs. The goal of an osseous resective procedure is to correct

gingival deep pocket probing depth (i.e., ≥ 5 mm) and underlying osseous anatomy defects to

improve overall periodontal architecture (Figure 3.4). In contrast and as aforementioned, crown

lengthening is performed in relation to a prosthodontic treatment plan to improve retention of a

future prosthesis.

Figure 3.4 Osseous resective procedure and gingival sample collection site.
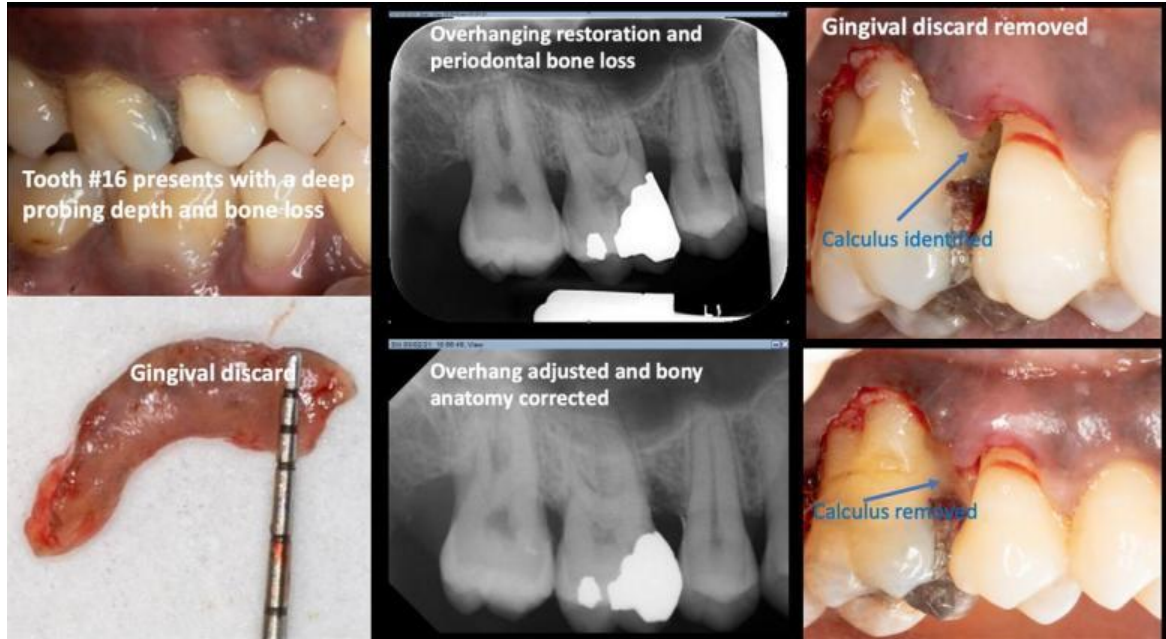
An open flap debridement is a surgical procedure that permits access to root anatomy at sites with deep probing depths. After completing initial scaling and root planing debridement, sites with persistent gingival inflammation and deep pocket probing depth may benefit from this procedure. A full thickness flap debridement may reveal subgingival calculus that is more accessible for removal. This procedure may also involve a gingival discard (Figure 3.5).

Figure 3.5. Open flap debridement and gingival sample collection site.
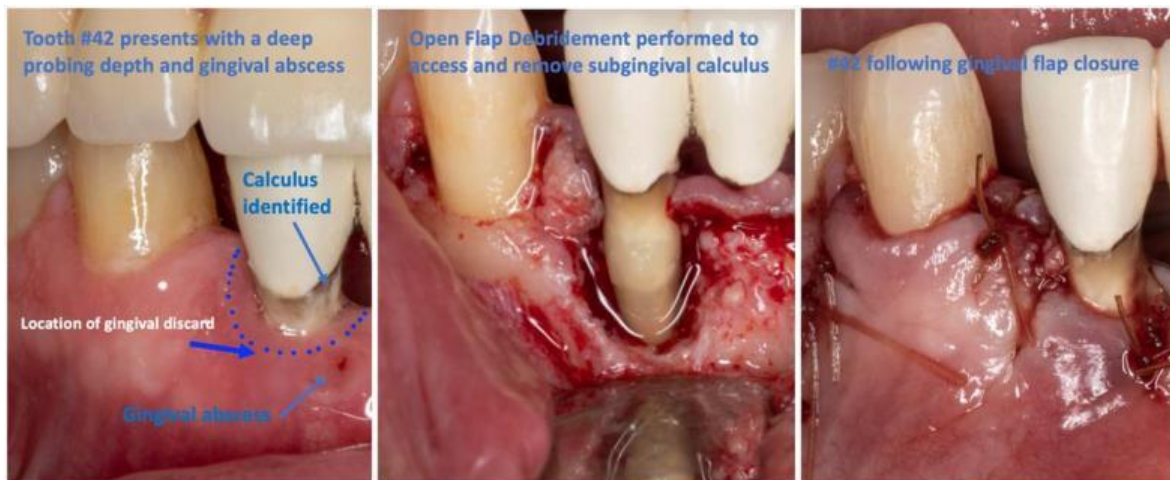
Periodontal therapy strives to preserve and restore periodontal health. If a tooth is deemed

to have a hopeless prognosis, then an extraction of said tooth is required. Reasons may include

restorative complexities, and persistent and/or recurring infections. Gingival discards at planned

extraction sites were collected on either the buccal or lingual gingival margins (Figure 3.6).

Figure 3.6 Lower molar extraction and gingival sample collection site.

An orthodontic tooth exposure may precede or be treatment planned during orthodontic

tooth movement. Patients with impacted dentition may be suitable for exposure of the underlying

tooth to be repositioned during the orthodontic tooth movement. In general, there are two types

of orthodontic tooth exposure treatment: closed and open approach. In the closed approach, a

gingival flap reveals the underlying tooth and eliminates any bony covering. Then the

orthodontic bracket is bonded, and the gingival flap is repositioned/closed. In the open approach,

a window of gingival epithelium is removed, the bony covering is removed, the orthodontic

bracket is bonded, and the site is left exposed (Figure 3.7).

Figure 3.7 Orthodontic tooth exposure and gingival sample collection site.
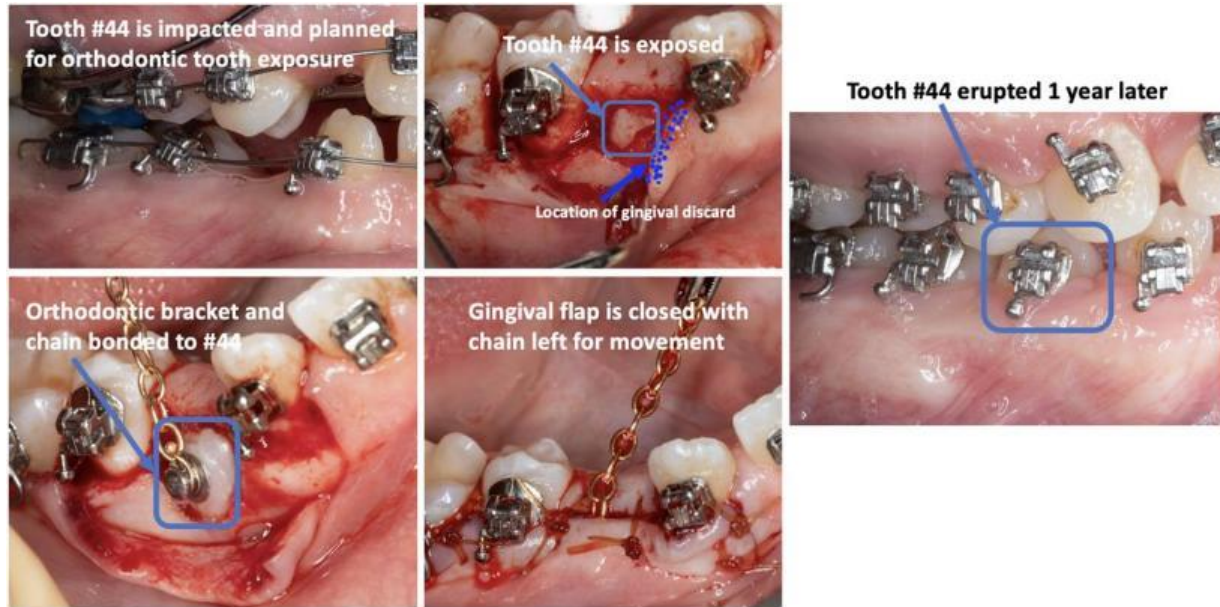
The demographic features of the patients and source of tissue collection are outlined in Table 3.1 below.

Table 3.1 Patient demographics and tissue collection source.

Tissue ID	Age	Sex	Smoker	Diabetic	Procedure
Periodontal Diagnosis: Healthy					
H-23	68	M	N	N	Crown Lengthening
H-26	89	F	N	N	Crown Lengthening
H-34	54	F	N	N	Crown Lengthening
H-39	15	M	N	N	Orthodontic Exposure
H-42	60	M	N	N	Crown Lengthening
Periodontal Diagnosis: P3C					
R4H	48	F	Y	N	Osseous Resective Surgery
H-6	66	M	Y	N	Crown Lengthening
H-12	74	M	N	N	Open Flap Debridement

H-14	66	M	N	N	Osseous Resective Surgery
H-44	78	F	N	N	Extraction
Periodontal Diagnosis: P4C					
R1H	58	M	N	N	Extraction
M1H	51	F	N	N	Extraction
H-19	47	F	N	Y (Type II)	Crown Lengthening
H-27	73	F	N	Y (Type II)	Crown Lengthening
H-48	69	M	N	N	Extraction

We hypothesized that histological and immunohistological differences exist in the epithelium of healthy versus severe periodontal disease patients; this may suggest a pathogen-mediated epithelial barrier breach due to loss of loricrin. The tissue samples collected from these procedures were used to test this hypothesis. H&E staining was performed to provide general morphological analysis of the epithelial patterns of the different groups. Further analyses involved immunohistological staining to investigate the distribution and expression of loricrin, CK1, and CK14 within each epithelium. The recent changes to the classification of periodontal diseases consolidated the former chronic and aggressive periodontitis under one heading: periodontitis. The reason for this was that the present etiological, pathophysiological, and histological evidence cannot distinguish between these two types of periodontal disease (Papapanou et al, 2018). This histological study strives to explore possible distinctions identified in severe periodontitis gingival tissues.

3.2 Hematoxylin and Eosin (H&E)

H&E staining of Healthy, P3C, and P4C samples were completed, and images captured at 4x, 20x, and 40x magnification. As one of the principal histological stains for evaluating tissue samples, H&E technique was employed to investigate any morphological differences between the tissue types, in particular, the type of keratinized epithelium and presence of inflammatory signs within each sample.

A summary of these findings for each tissue sample are captured in Table 3.2.

Table 3.2 Hematoxylin & Eosin (H&E) gingival sample features.

Tissue ID	Ortho / Para Keratinized	Inflammatory Cells	Edema Presence in CT	RBC Presence in CT	Avg Rete Peg Length (µm)
Periodontal Diagnosis: Healthy					
H-23	Parakeratinized	Slight	N	N	100.9
H-26	Parakeratinized	Slight	Y	N	80.2
H-34	Mixed	Moderate	Y	N	67.9
H-39	Orthokeratinized	Slight	Y	N	186.7
H-42	Parakeratinized	Slight	Y	N	302.0
Periodontal Diagnosis: P3C					
R4H	Orthokeratinized	Moderate	Y	Y	270.6
H-6	Parakeratinized	Severe	Y	Y	255.6
H-12	Parakeratinized	Moderate	Y	N	103.5
H-14	Parakeratinized	Severe	Y	Y	Indiscernible
H-44	Parakeratinized	Moderate	Y	Y	156.9
Periodontal Diagnosis: P4C					
R1H	Mixed	Severe	Y	N	Indiscernible
M1H	Parakeratinized	Severe	Y	Y	309.2

H-19	Orthokeratinized	Severe	Y	N	262.8
H-27	Parakeratinized	Severe	Y	Y	254.4
H-48	Parakeratinized	Moderate	Y	Y	Indiscernible

3.2.1 H-23 - Healthy gingival sample H&E descriptions

Gingival sample 23 was collected from the healthy periodontium of a 68-year-old male, non-smoker and non-diabetic, during a crown lengthening procedure. The orientation of the tissue sample was observed in the 4x, 20x and 40x images in Figure 3.8. The epithelium was parakeratinized and contained a slight number of inflammatory cells within the tissue. No edema nor RBCs were detected within the gingival sample. The average length of the rete pegs was 100.9 μm.

Figure 3.8 H-23 - Healthy gingival sample H&E. Representative images are depicted at 4x, 20x and 40x magnification. The green arrows in the 20x image identify inflammatory cells within the epithelium.
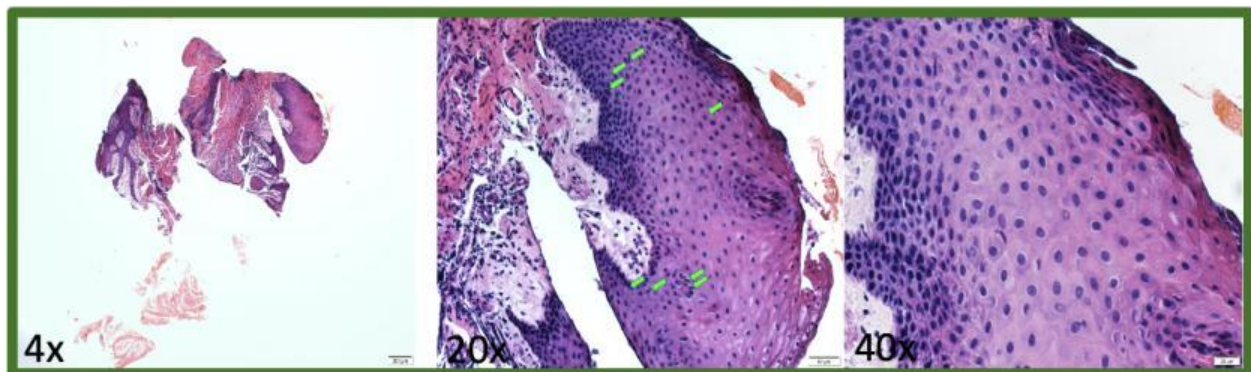
Back to Table 3.2 Features of gingival samples stained with H&E

3.2.2 H-26 - Healthy gingival sample H&E descriptions

Gingival sample 26 was collected from the healthy periodontium of an 89-year-old female, non-smoker and non-diabetic, during a crown lengthening procedure. The orientation of the sample was observed in the 4x, 20x and 40x images in Figure 3.9. The epithelium was parakeratinized, contained a slight number of inflammatory cells within the tissue, and edema in the connective tissue. RBCs were not detected within this gingival sample. The average length of the rete pegs was 80.2 μm.

Figure 3.9 H-26 - Healthy gingival sample H&E. Representative images are depicted at 4x, 20x and 40x magnification. The blue outlines the perivascular edema observed in the 4x image. The green arrows in the 20x image identify inflammatory cells within the epithelium.
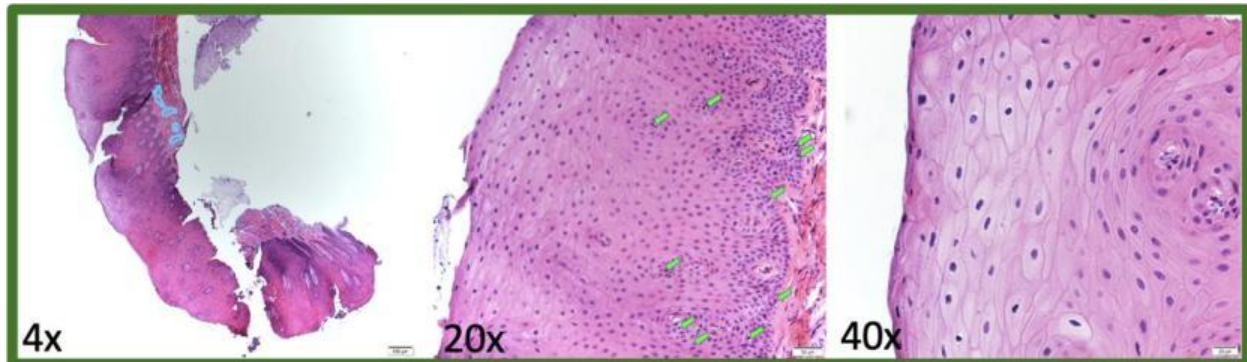
Back to Table 3.2 Features of gingival samples stained with H&E

3.2.3 H-34 - Healthy gingival sample H&E descriptions

Gingival sample 34 was collected from the healthy periodontium of a 54-year-old female, non-smoker and non-diabetic, during a crown lengthening procedure. The orientation of the sample was depicted in the 4x, 20x and 40x images presented in Figure 3.10. The epithelium was a mix of orthokeratinized and parakeratinized. There was a moderate number of inflammatory cells within the tissue, and edema observed in the connective tissue. RBCs were not detected within this gingival sample. The average length of the rete pegs was 67.9 μm.

Figure 3.10 H-34 - Healthy gingival sample H&E. Representative images are depicted at 4x, 20x and 40x magnification. The blue outlines the perivascular edema observed in the 4x image. The green arrows in the 20x image identify inflammatory cells within the epithelium.
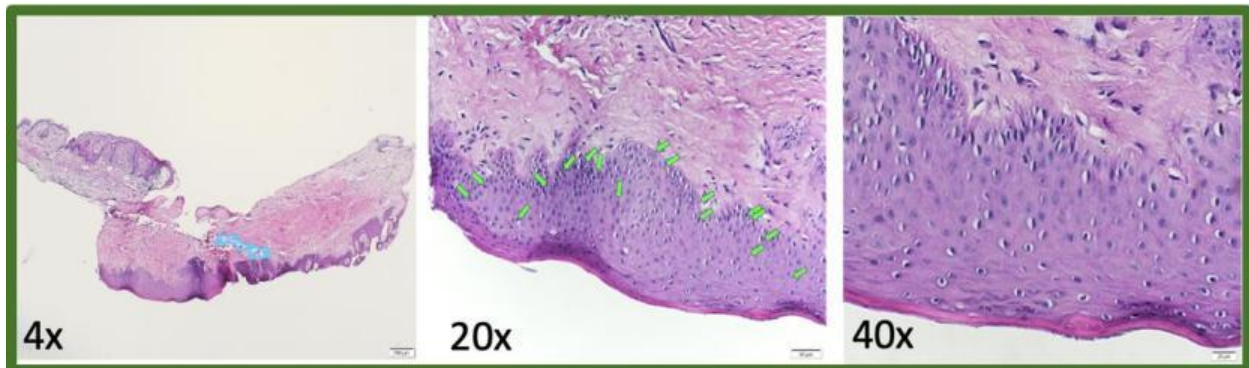
Back to Table 3.2 Features of gingival samples stained with H&E

3.2.4 H-39 - Healthy gingival sample H&E descriptions

Gingival sample 39 was collected from the healthy periodontium of a 15-year-old male, non-smoker and non-diabetic, during a crown lengthening procedure. The orientation of the sample was depicted in the 4x, 20x and 40x images presented in Figure 3.11. The epithelium was a mix of orthokeratinized and parakeratinized. There were a slight number of inflammatory cells within the tissue, and edema observed in the connective tissue. RBCs were not detected within this tissue sample. The average length of the rete pegs was 186.7 μm.

Figure 3.11 H-39 – Healthy gingival sample H&E. Representative images are depicted at 4x, 20x and 40x magnification. The blue outlines the perivascular edema observed in the 4x image. The green arrows in the 20x image identify inflammatory cells within the epithelium.
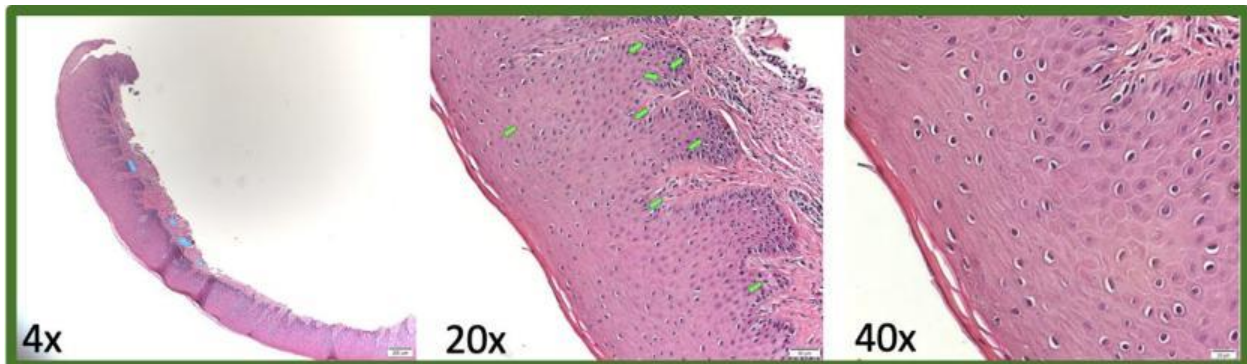
Back to Table 3.2 Features of gingival samples stained with H&E

3.2.5 H-42 - Healthy gingival sample H&E descriptions

Gingival sample 42 was collected from the healthy periodontium of a 60-year-old male, non-smoker and non-diabetic, during a crown lengthening procedure. The orientation of the sample was depicted in the 4x, 20x and 40x images presented in Figure 3.12. The epithelium was parakeratinized, contained a slight number of inflammatory cells within the tissue, and edema was present in the connective tissue. RBCs were not detected within the sample. The average length of the rete pegs was 302.0 μm.

Figure 3.12 H-42 - Healthy gingival sample H&E. Representative images are depicted at 4x, 20x and 40x magnification. The blue outlines the perivascular edema observed in the 4x image. The green arrows in the 20x image identify inflammatory cells within the epithelium.
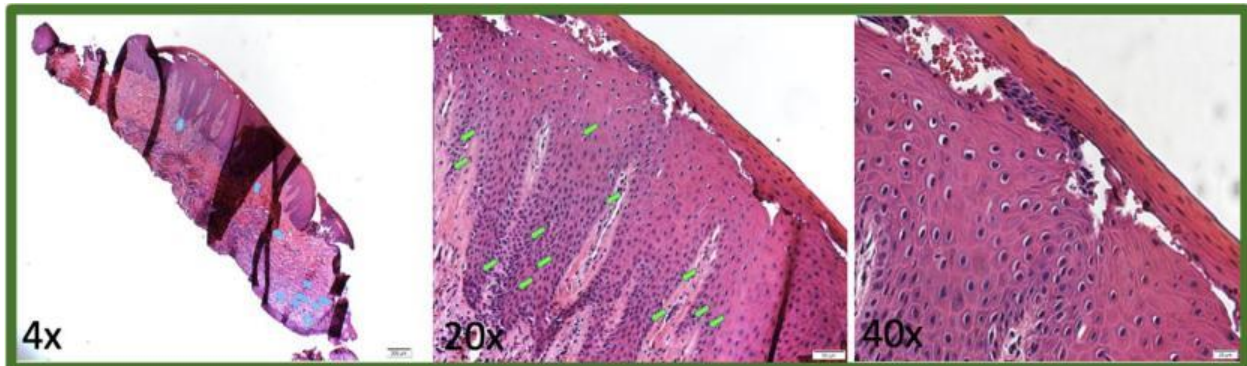
Back to Table 3.2 Features of gingival samples stained with H&E

3.2.6 R4H - P3C gingival sample H&E descriptions

Gingival sample R4H was collected during an osseous resective surgery procedure from a 48-year-old female smoker and non-diabetic with generalized stage III grade C periodontitis. Orientation of this tissue sample was observed at 4x, 20x and 40x magnification as shown in Figure 3.13. The epithelium was orthokeratinized and contained a moderate number of inflammatory cells. Edema and RBCs were detected within the gingival sample. The average length of the rete pegs was 270.6 μm.

Figure 3.13 R4H - P3C gingival sample H&E. Representative images are depicted at 4x, 20x and 40x magnification. The blue outlines the perivascular edema, and the red identifies the RBCs observed in the 4x image. The green arrows in the 20x image identify inflammatory cells within the epithelium.
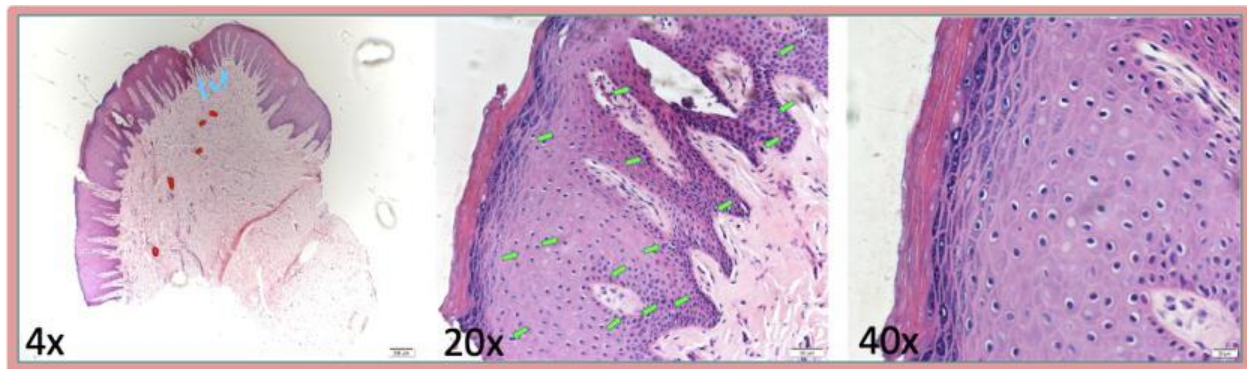
Back to Table 3.2 Features of gingival samples stained with H&E

3.2.7 H-6 - P3C gingival sample H&E descriptions

Gingival sample H6 was collected during a crown lengthening procedure from a 66-year-old male smoker and non-diabetic with generalized stage III grade C periodontitis. Orientation of this tissue sample was observed at 4x, 20x and 40x magnification as shown in Figure 3.14. The epithelium was parakeratinized and contained a severe number of inflammatory cells. Edema and RBCs were detected within the gingival sample. The average length of the rete pegs was 255.6 µm.

Figure 3.14 H-6 - P3C gingival sample H&E. Representative images are depicted at 4x, 20x and 40x magnification. The blue outlines the perivascular edema, and the red identifies the RBCs observed in the 4x image. The green arrows in the 20x image identify inflammatory cells within the epithelium.
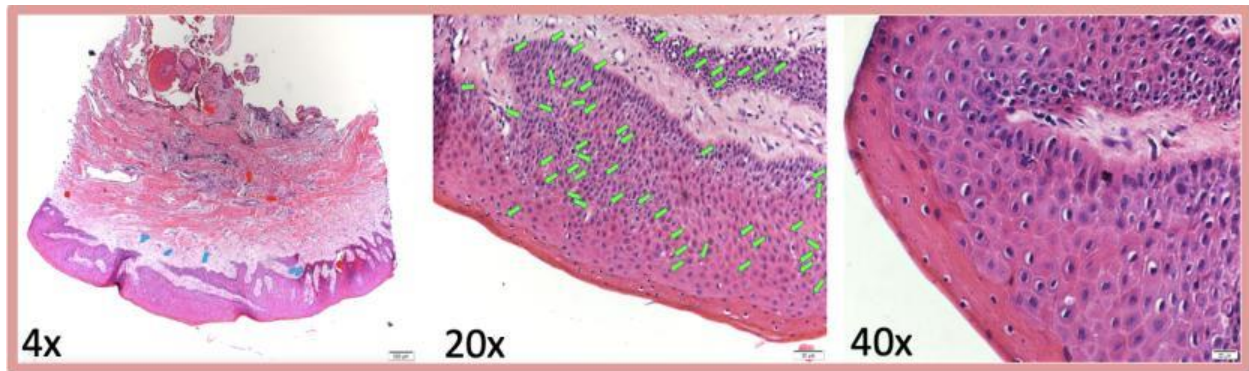
Back to Table 3.2 Features of gingival samples stained with H&E

3.2.8 H-12 - P3C gingival sample H&E descriptions

Gingival sample H-12 was collected during an open flap debridement procedure from a 74-year-old male non-smoker and non-diabetic with generalized stage III grade C periodontitis. Orientation of this tissue sample was observed at 4x, 20x and 40x magnification as shown in Figure 3.15. The epithelium was parakeratinized and contained a moderate number of inflammatory cells. Edema was observed, but RBCs were not detected within the sample. The average length of the rete pegs was 103.5 μm.

Figure 3.15 H-12 - P3C gingival sample H&E. Representative images are depicted at 4x, and two-20x magnification. The blue outlines the perivascular edema observed in the 4x image. The green arrows in the left 20x image identify inflammatory cells within the epithelium. The rete peg measurement was completed using the 20x image on the right.
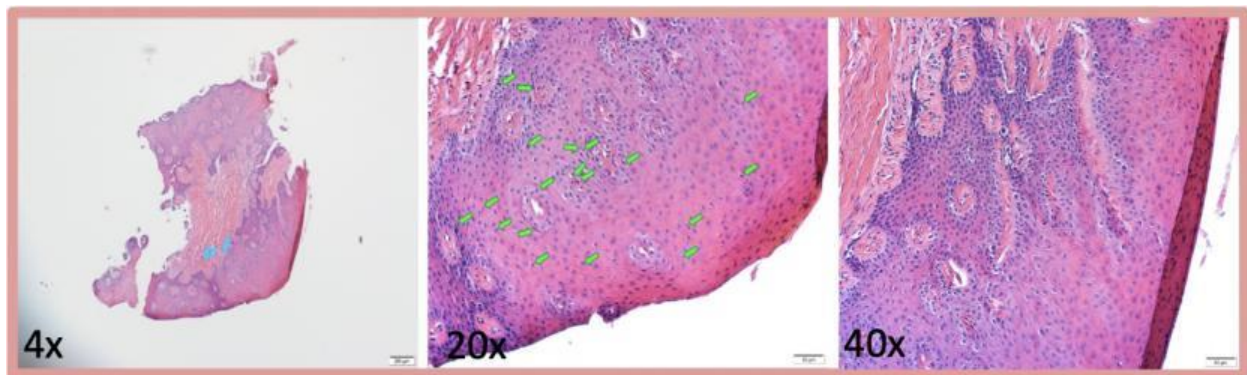
Back to Table 3.2 Features of gingival samples stained with H&E

3.2.9 H-14 - P3C gingival sample H&E descriptions

Gingival sample H-14 was collected during an osseous resective surgery procedure from a 48-year-old female smoker and non-diabetic with generalized stage III grade C periodontitis. Orientation of this tissue sample was observed at 4x, 20x and 40x magnification in Figure 3.16. The epithelium was parakeratinized and contained a severe number of inflammatory cells. Edema and RBCs were detected within the sample. Rete peg measurements could not be discerned due to the tangential orientation of this gingival sample.

Figure 3.16 H-14 - P3C gingival sample H&E. Representative images are depicted at 4x, 20x and 40x magnification. The blue outlines the perivascular edema, and the red identifies the RBCs in the 4x image. The green arrows in the 20x image identify inflammatory cells within the epithelium.
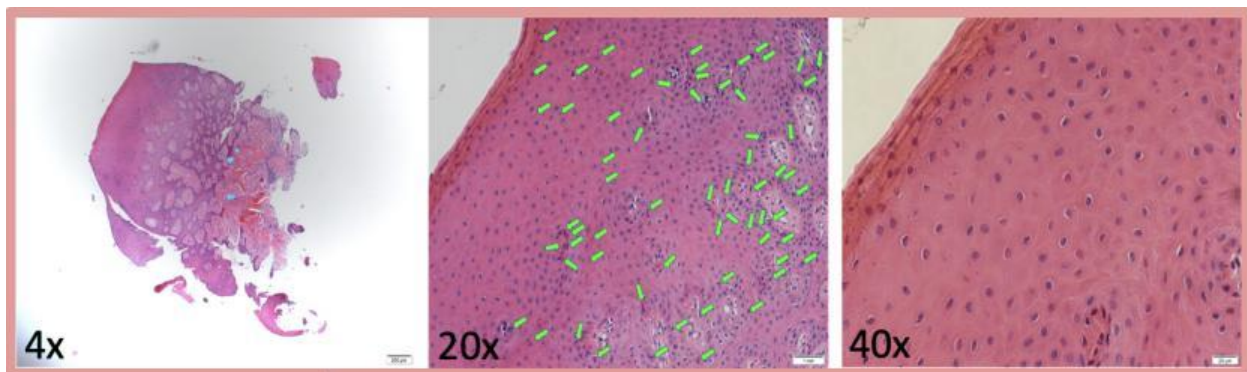
Back to Table 3.2 Features of gingival samples stained with H&E

3.2.10 H-44 - P3C gingival sample H&E descriptions

Gingival sample H-44 was collected during an extraction procedure from a 78-year-old female non-smoker and non-diabetic with generalized stage III grade C periodontitis. Orientation of this tissue sample was observed at 4x, 20x and 40x magnification as shown in Figure 3.17. The epithelium was parakeratinized and contained a moderate number of inflammatory cells. Edema and RBCs were detected within the sample. The average length of the rete pegs was 156.9 μm.

Figure 3.17 H-44 - P3C gingival sample H&E. Representative images are depicted at 4x, 20x and 40x magnification. The blue outlines the perivascular edema, and the red identifies the RBCs observed in the 4x image. The green arrows in the 20x image identify inflammatory cells within the epithelium.
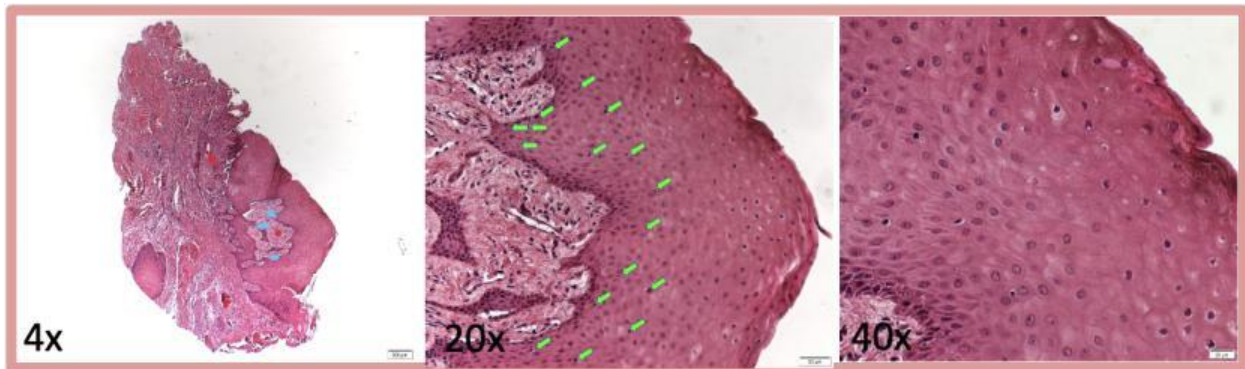
Back to Table 3.2 Features of gingival samples stained with H&E

3.2.11 R1H - P4C gingival sample H&E descriptions

Gingival sample R1H was collected during an extraction procedure from a 58-year-old male non-smoker and non-diabetic with generalized stage IV grade C periodontitis. Orientation of this tissue sample was observed at 4x, 20x and 40x magnification as shown in Figure 3.18. The epithelium was mixed keratinized and contained a severe number of inflammatory cells. Edema was observed, but RBCs could not be detected within the sample. Rete peg measurements could not be discerned due to the tangential orientation of this gingival sample.

Figure 3.18 R1H - P4C gingival sample H&E. Representative images are depicted at 4x, 20x and 40x magnification. The blue outlines the perivascular edema observed in the 4x image. The green arrows in the 20x image identify inflammatory cells within the epithelium.
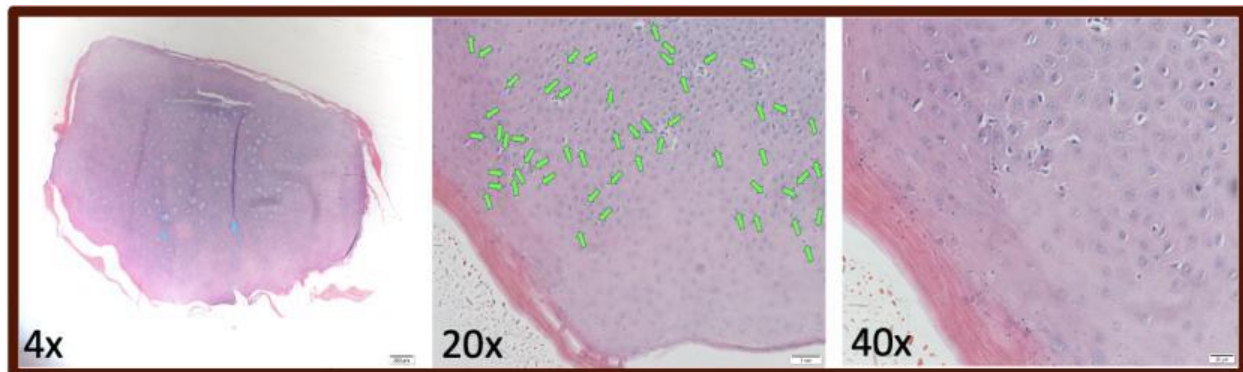
Back to Table 3.2 Features of gingival samples stained with H&E

3.2.12 M1H - P4C gingival sample H&E descriptions

Gingival sample M1H was collected during an extraction procedure from a 51-year-old female non-smoker and non-diabetic with generalized stage IV grade C periodontitis. Orientation of this tissue sample was observed at 4x, 20x and 40x magnification as shown in Figure 3.19 The epithelium was mixed parakeratinized and contained a severe number of inflammatory cells. Edema and RBCs were detected within the sample. The average length of the rete pegs was 309.2 μm.

Figure 3.19 M1H - P4C gingival sample H&E. Representative images are depicted at 4x, 20x and 40x magnification. The blue outlines the perivascular edema, and the red identifies the RBCs observed in the 4x image. The green arrows in the 20x image identify inflammatory cells within the epithelium.
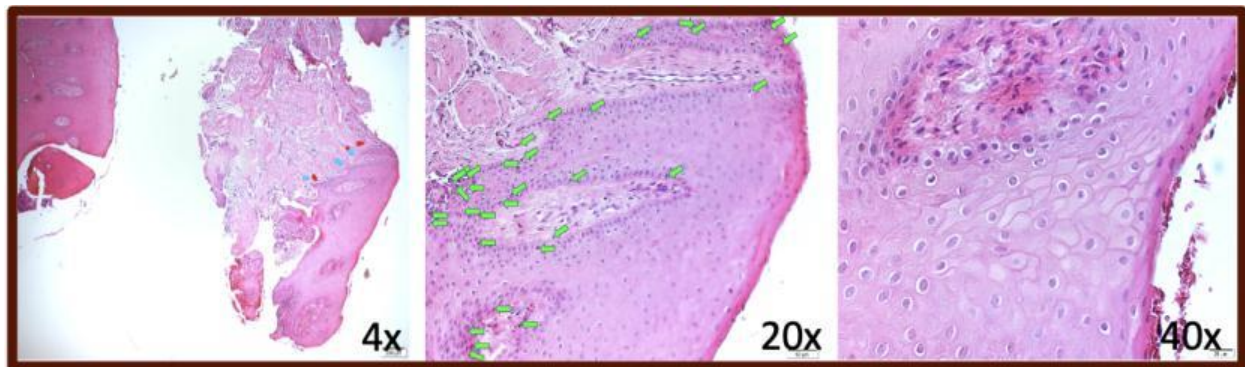
Back to Table 3.2 Features of gingival samples stained with H&E

3.2.13 H-19 - P4C gingival sample H&E descriptions

Gingival sample H-19 was collected during an extraction procedure from a 47-year-old

female non-smoker and type II diabetic with generalized stage IV grade C periodontitis.

Orientation of this tissue sample was observed at 4x, 20x and 40x magnification as shown in

Figure 3.20. The epithelium was orthokeratinized and contained a severe number of

inflammatory cells. Edema was observed, but RBCs were not detected within the sample. The

average length of the rete pegs was 262.8 μm.

Figure 3.20 H-19 - P4C gingival sample H&E. Representative images are depicted at 4x, 20x

and 40x magnification. The blue outlines the perivascular edema observed in the 4x image. The

green arrows in the 20x image identify inflammatory cells within the epithelium.
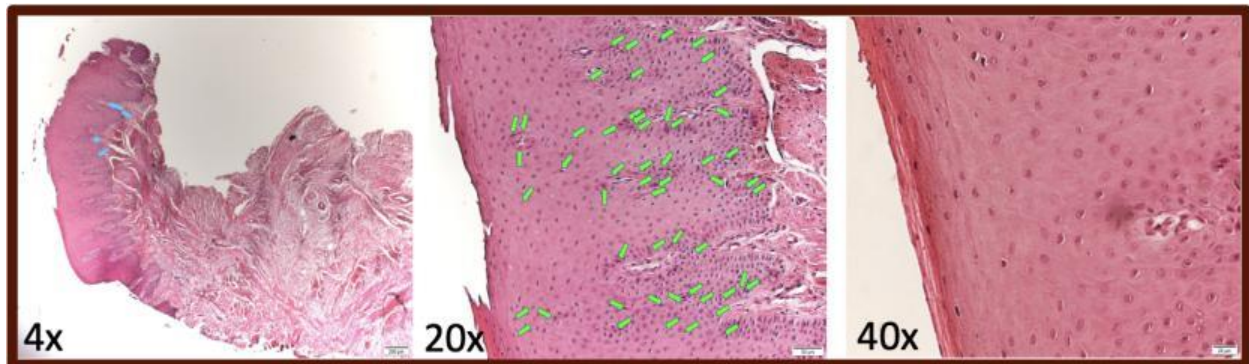
Back to Table 3.2 Features of gingival samples stained with H&E

3.2.14 H-27 - P4C gingival sample H&E descriptions

Gingival sample H-27 was collected during an extraction procedure from a 73-year-old female non-smoker and type II diabetic with generalized stage IV grade C periodontitis. Orientation of this tissue sample was observed at 4x, 20x and 40x magnification as shown in Figure 3.21. The epithelium was parakeratinized and contained a severe number of inflammatory cells. Edema and RBCs were detected within the sample. The average length of the rete pegs was 254.4 μm.

Figure 3.21 H-27 - P4C gingival sample H&E. Representative images are depicted at 4x, 20x and 40x magnification. The blue outlines the perivascular edema, and the red identifies the RBCs observed in the 4x image. The green arrows in the 20x image identify inflammatory cells within the epithelium.
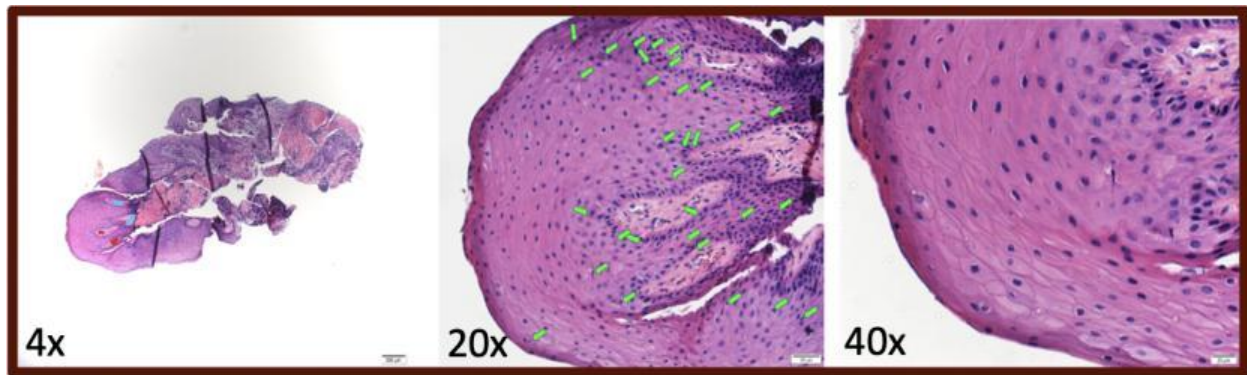
Back to Table 3.2 Features of gingival samples stained with H&E

3.2.15 H-48 - P4C gingival sample H&E descriptions

Gingival sample H-48 was collected during an extraction procedure from a 69-year-old male non-smoker and non-diabetic with generalized stage IV grade C periodontitis. Orientation of this tissue sample was observed at 4x, 20x and 40x magnification as shown in Figure 3.22. The epithelium was parakeratinized and contained a moderate number of inflammatory cells. Edema and RBCs were detected within the sample. Rete peg measurements could not be discerned due to the tangential orientation of this gingival sample.

Figure 3.22 H-48 - P4C gingival sample H&E. Representative images are depicted at 4x, 20x and 40x magnification. The blue outlines the perivascular edema, and the red identifies the RBCs observed in the 4x magnification. The green arrows in the 20x image identify inflammatory cells within the epithelium.
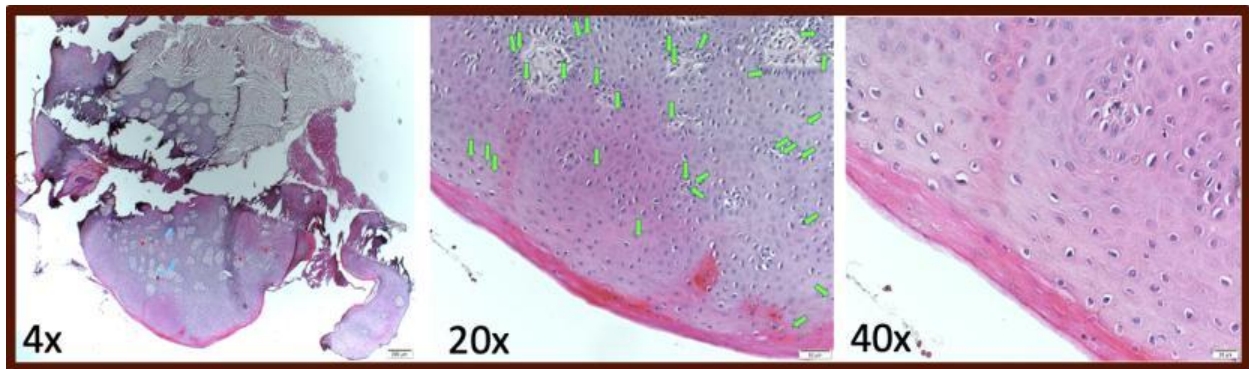
Back to Table 3.2 Features of gingival samples stained with H&E

3.3 Immunofluorescence (IF) Antibody Staining for Loricrin

IF staining for loricrin of healthy, P3C and P4C gingival samples was completed, and images captured at 4x, 10x, 20x, and 40x magnification. The green fluorescence represents the loricrin expression and the blue nuclei staining is a DAPI counterstain for orientation of the

sample. Qualitative features on the expression location and uniformity of the IF signaling are provided for each sample. The features of each sample are captured in Table 3.2.

Table 3.3 Loricrin Immunofluorescence (IF) gingival sample features.

Tissue ID	Expression	Uniformity	Width (μm)
Periodontal Diagnosis: Healthy			
H-23	Corneum and granulosum	Uniform	102.2
H-26	Corneum and granulosum	Uniform	84.0
H-34	Corneum, granulosum, and spinosum	Interrupted	41.3
H-39	Corneum	Uniform	26.1
H-42	Corneum and granulosum	Uniform	47.0
Periodontal Diagnosis: P3C			
R4H	Corneum	Interrupted	20.0
H-6	Corneum and granulosum	Interrupted	33.6
H-12	Corneum and granulosum	Interrupted	26.4
H-14	Corneum and granulosum	Interrupted	36.0
H-44	Corneum and granulosum	Interrupted	10.4
Periodontal Diagnosis: P4C			
R1H	Corneum	Interrupted	4.8
M1H	Corneum	Interrupted	8.9
H-19	Corneum and granulosum	Interrupted	7.2
H-27	Corneum, granulosum, and spinosum	Interrupted	9.4
H-48	Corneum and granulosum	Interrupted	8.5

3.3.1 H-23 - Healthy gingival sample IF Loricrin descriptions

IF staining of Healthy gingival sample - H-23 for loricrin was evaluated in 4x and 20x images depicted in Figure 3.23. The loricrin signal was expressed most strongly in the stratum corneum and granulosum. The fluorescence signal was uniform with an average width of 102.2 µm.

Figure 3.23 H-23 - Healthy gingival sample IF loricrin. Representative gingival samples are depicted at 4x, and 20x magnification.
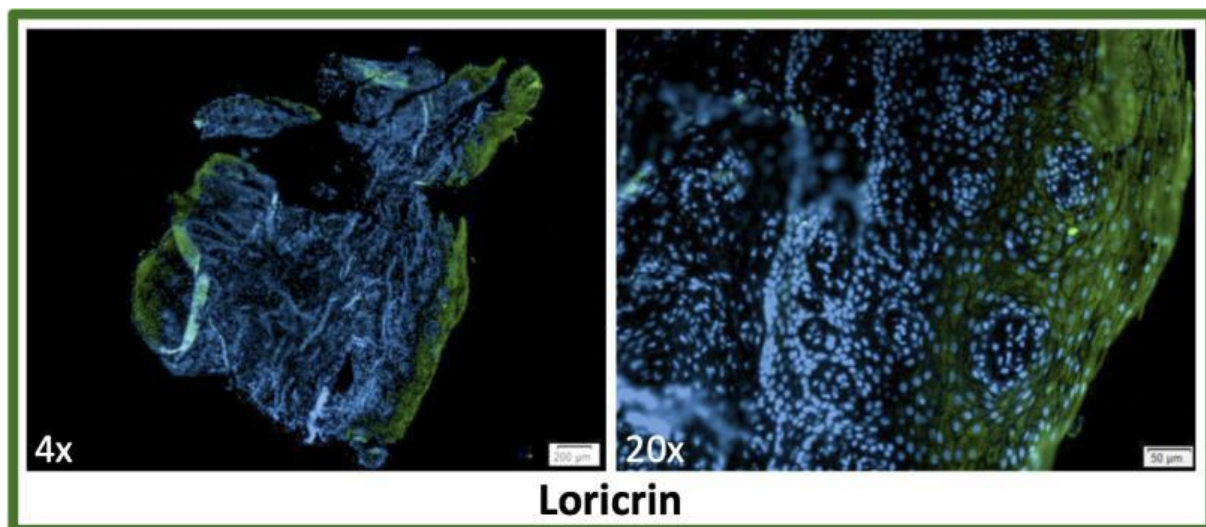
Back to Table 3.3 Features of IF Staining for Loricrin

3.3.2 H-26 - Healthy gingival sample IF Loricrin description

IF staining of Healthy gingival sample - H-26 for loricrin was evaluated in 10x and 20x images depicted in Figure 3.24. The loricrin signal was expressed most strongly in the stratum corneum and granulosum. The fluorescence signal was uniform with an average width of 84.0 μm.

Figure 3.24 H-26 - Healthy gingival sample IF Loricrin. Representative gingival samples are depicted at 10x, and 20x magnification.
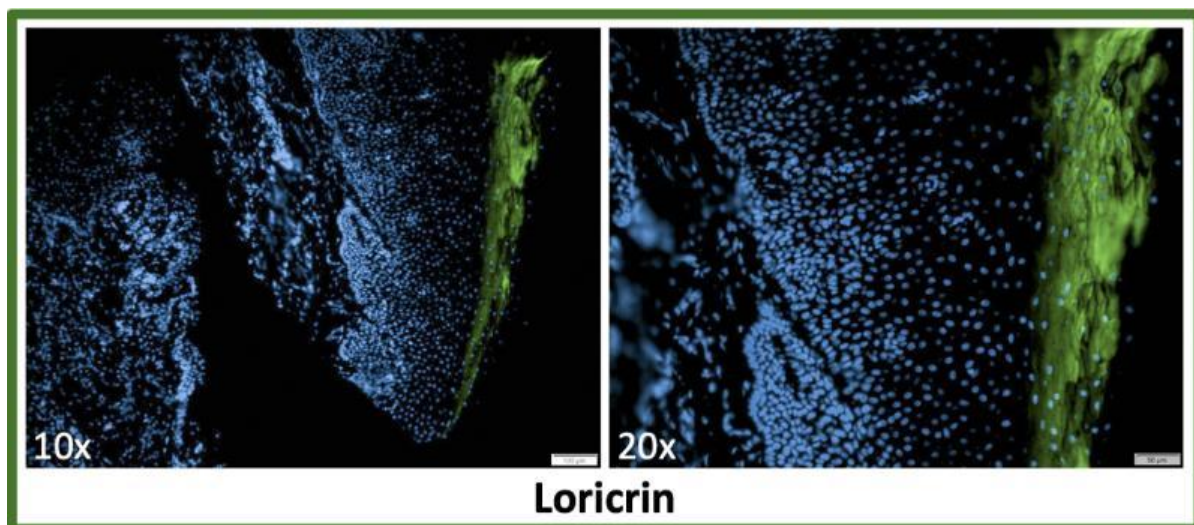
Loricrin

Back to Table 3.3 Features of IF Staining for Loricrin

3.3.3 H-34 - Healthy gingival sample IF Loricrin description

IF staining of Healthy gingival sample - H-34 for loricrin was evaluated in 10x and 20x images depicted in Figure 3.25. The loricrin signal was expressed most strongly in the stratum corneum, granulosum, and spinosum. The fluorescence signal appeared interrupted with an average width of 26.1 μm at its most uniform location.

Figure 3.25 H-34 - Healthy gingival sample IF Loricrin. Representative gingival samples are depicted at 10x, and 20x magnification.
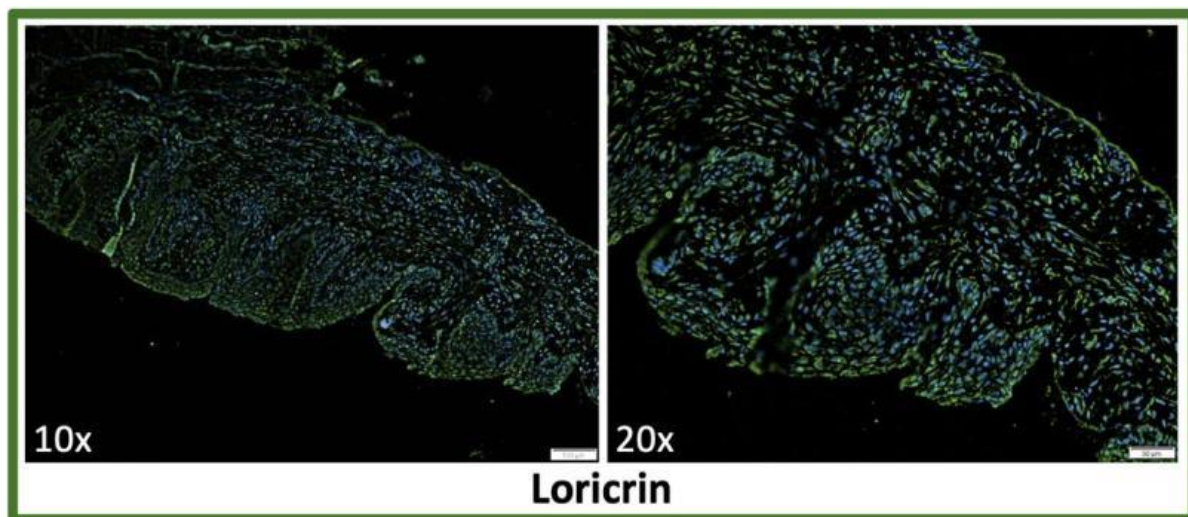
Back to Table 3.3 Features of IF Staining for Loricrin

3.3.4 H-39 - Healthy gingival sample IF Loricrin description

IF staining of Healthy gingival sample - H-39 for loricrin was evaluated in 10x and 20x images depicted in Figure 3.26. The loricrin signal was expressed most strongly in the stratum corneum. The fluorescence signal was uniform with an average width of 26.1 µm.

Figure 3.26 H-39 - Healthy gingival sample IF Loricrin. Representative gingival samples are depicted at 10x, and 20x magnification.
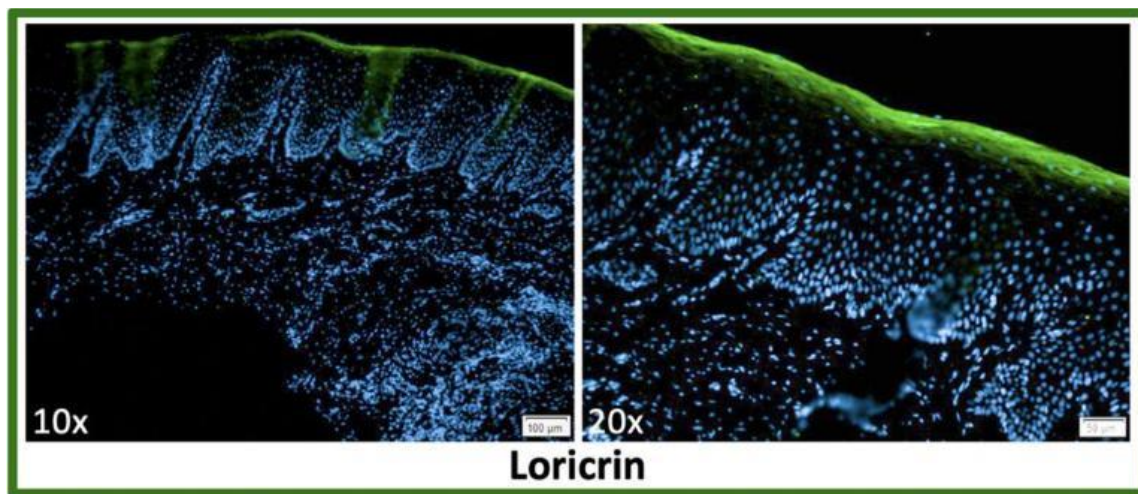
Back to Table 3.3 Features of IF Staining for Loricrin

3.3.5 H-42 - Healthy gingival sample IF Loricrin description

IF staining of Healthy gingival sample - H-42 for loricrin was evaluated in 20x and 40x images depicted in Figure 3.27. The loricrin signal was expressed most strongly in the stratum corneum and granulosum. The fluorescence signal was uniform with an average width of 47.0 μm.

Figure 3.27 H-42 - Healthy gingival sample IF Loricrin. Representative gingival samples are depicted at 20x, and 40x magnification.

20x   40x
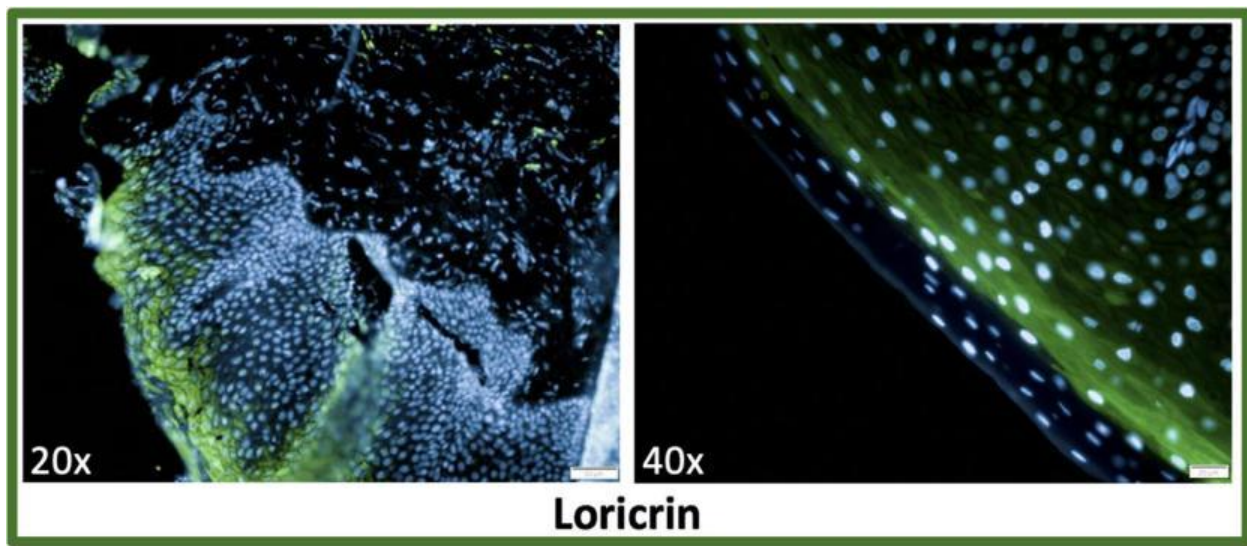
Loricrin

Back to Table 3.3 Features of IF Staining for Loricrin

3.3.6 R4H - P3C gingival sample IF Loricrin description

IF staining of P3C gingival sample - R4H for loricrin was evaluated in 20x and 40x images depicted in Figure 3.28. The loricrin signal was expressed most strongly in the stratum corneum. The fluorescence signal was interrupted with an average width of 20.0 μm.

Figure 3.28 R4H - P3C gingival sample IF Loricrin. Representative gingival samples are depicted at 20x, and 40x magnification.
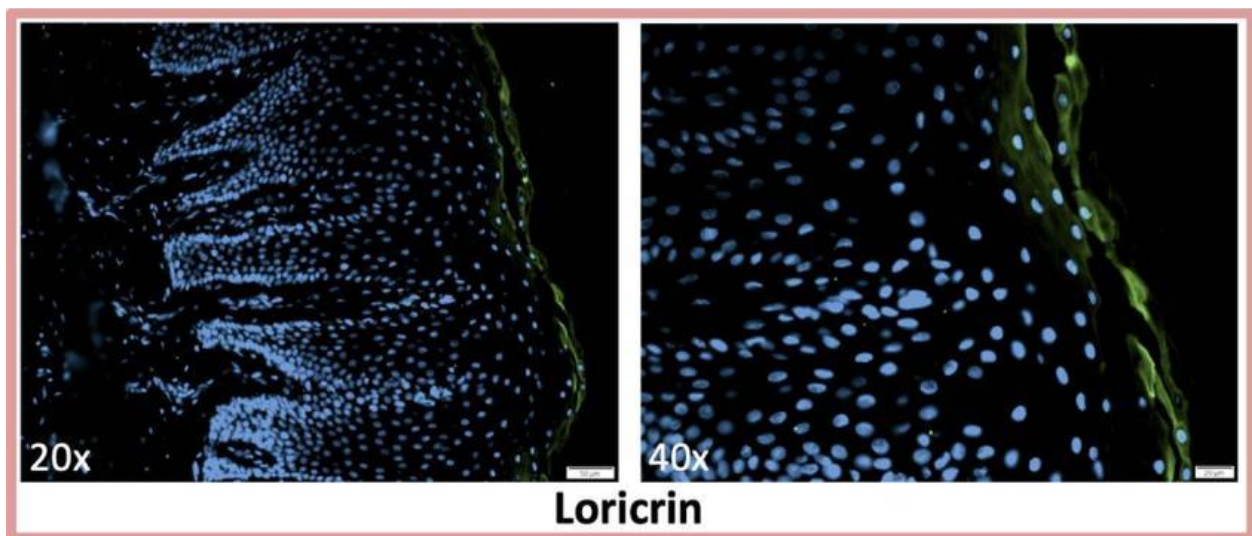
Back to Table 3.3 Features of IF Staining for Loricrin

3.3.7 H6 - P3C gingival sample IF Loricrin description

IF staining of P3C gingival sample - H6 for loricrin was evaluated in 20x and 40x images depicted in Figure 3.29. The loricrin signal was expressed most strongly in the stratum corneum and granulosum. The fluorescence signal was interrupted with an average width of 33.6 μm.

Figure 3.29 H6 - P3C gingival sample IF Loricrin. Representative gingival samples are depicted at 20x, and 40x magnification.

20x   40x
Loricrin
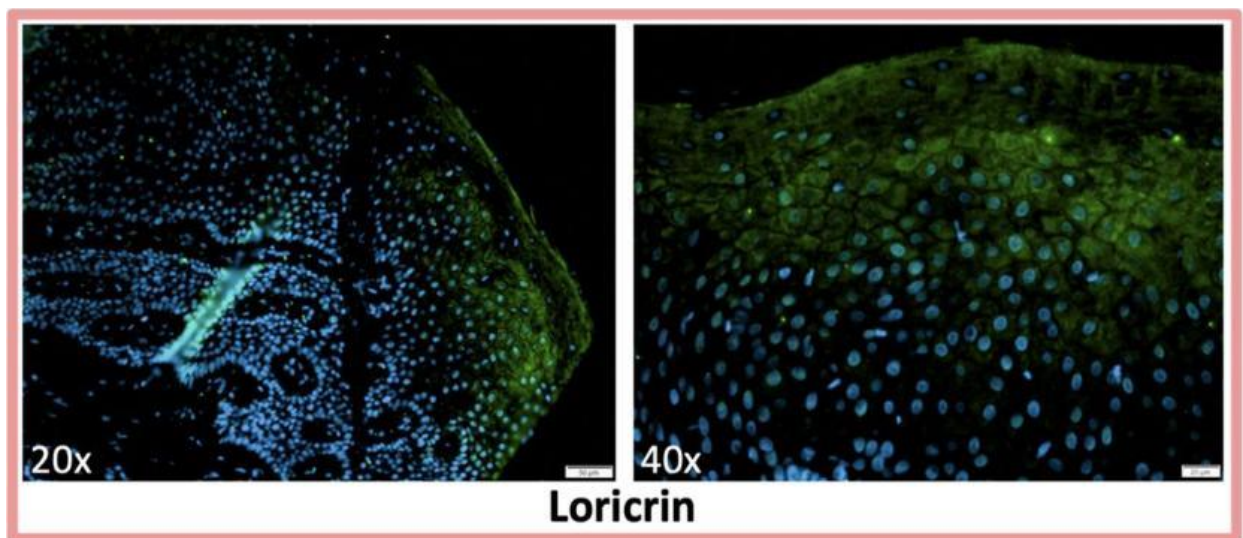
Back to Table 3.3 Features of IF Staining for Loricrin

3.3.8 H-12 - P3C gingival sample IF Loricrin description

IF staining of P3C gingival sample - H12 for loricrin was evaluated in 10x and 20x images depicted in Figure 3.30. The loricrin signal was expressed most strongly in the stratum corneum and granulosum. The fluorescence signal was interrupted with an average width of 26.4 μm.

Figure 3.30 H-12 - P3C gingival sample IF Loricrin. Representative gingival samples are depicted at 10x, and 20x magnification.
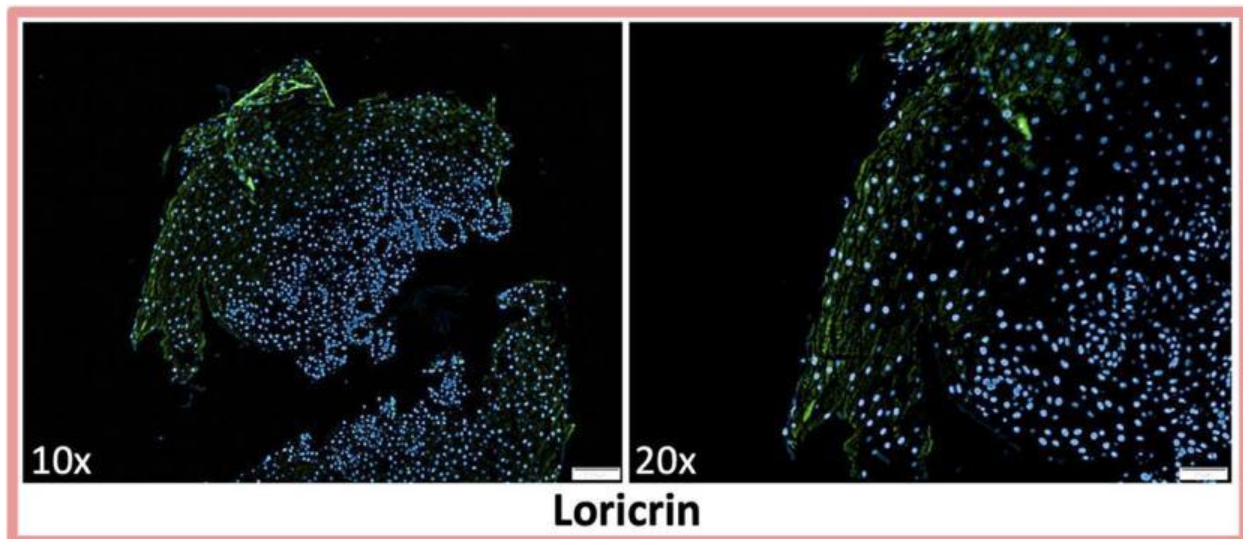
Back to Table 3.3 Features of IF Staining for Loricrin

3.3.9 H-14 - P3C gingival sample IF Loricrin description

IF staining of P3C gingival sample - H14 for loricrin was evaluated in 20x and 40x

images depicted in Figure 3.31. The loricrin signal was expressed most strongly in the stratum

corneum and granulosum. The fluorescence signal was interrupted with an average width of 36.0

μm.

Figure 3.31 H-14 - P3C gingival sample IF Loricrin. Representative gingival samples are
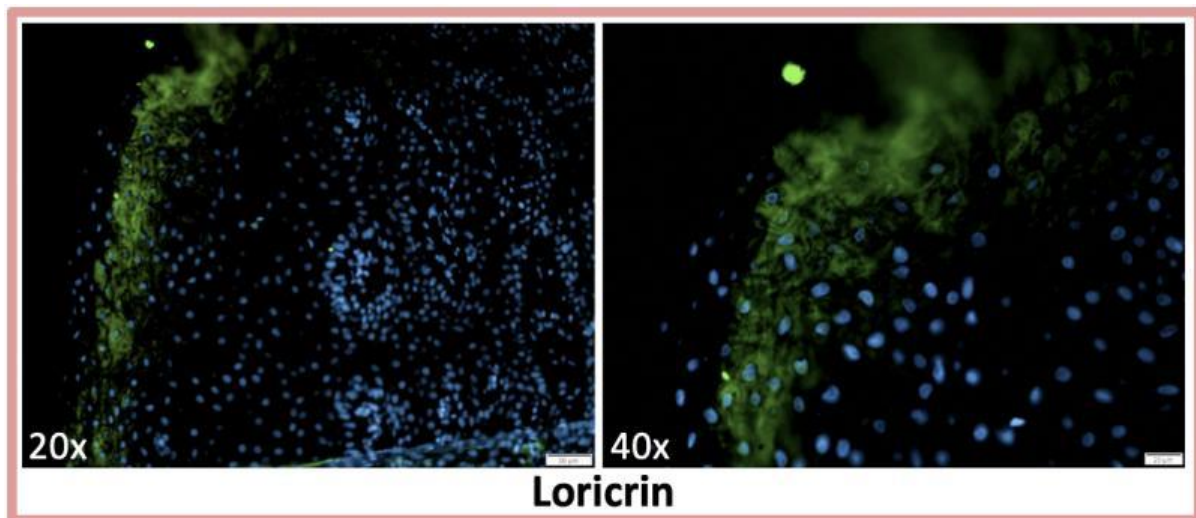
depicted at 20x, and 40x magnification.

3.3.10 H-44 - P3C gingival sample IF Loricrin description

IF staining of P3C gingival sample - H44 for loricrin was evaluated in 10x and 20x images depicted in Figure 3.32. The loricrin signal was expressed most strongly in the stratum corneum and granulosum. The fluorescence signal was interrupted with an average width of 10.4 µm.

Figure 3.32 H-44 - P3C gingival sample IF Loricrin. Representative gingival samples are depicted at 10x, and 20x magnification.
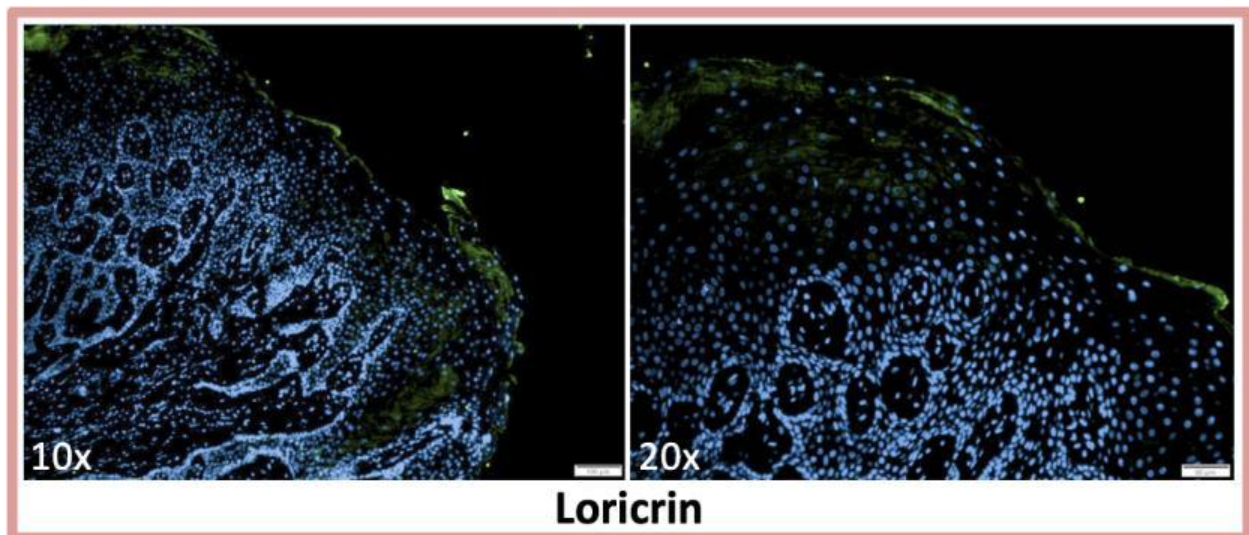
Back to Table 3.3 Features of IF Staining for Loricrin

3.3.11 R1H - P4C gingival sample IF Loricrin description

IF staining of P4C gingival sample - R1H for loricrin was evaluated in 10x and 20x images depicted in Figure 3.33. Although weakly expressed in this gingival sample, the loricrin signal was expressed most strongly in the stratum corneum. The fluorescence signal was interrupted with an average width of 4.8 μm.

Figure 3.33 R1H - P4C gingival sample IF Loricrin. Representative gingival samples are depicted at 10, and 20x magnification.

10x   20x
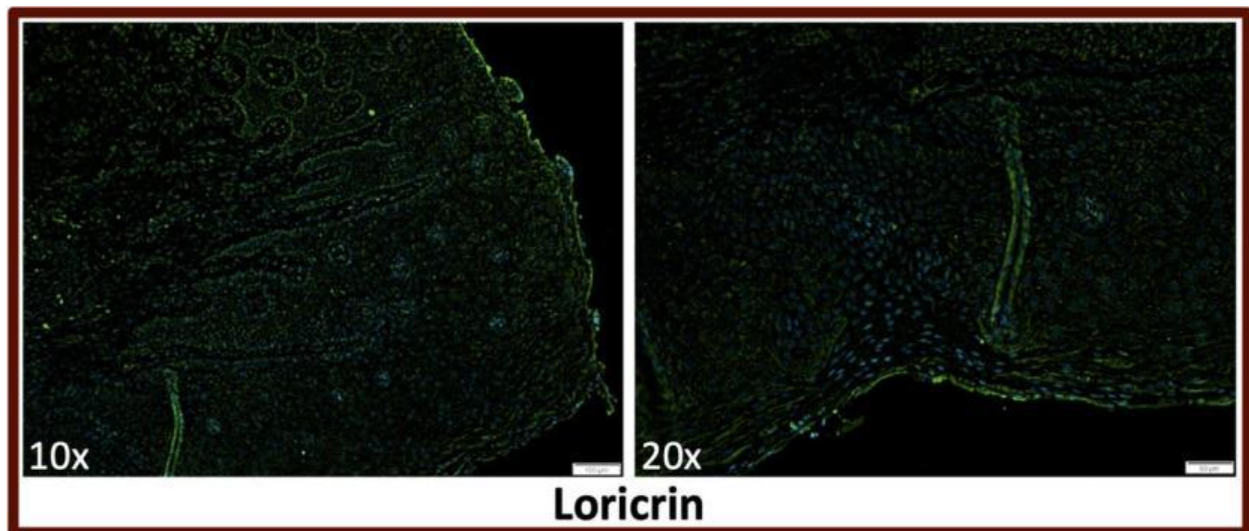
Loricrin

Back to Table 3.3 Features of IF Staining for Loricrin

3.3.12 M1H - P4C gingival sample IF Loricrin description

IF staining of P4C gingival sample - M1H for loricrin was evaluated in 10x and 20x images depicted in Figure 3.34. The loricrin signal was expressed most strongly in the stratum corneum. The fluorescence signal was interrupted with an average width of 8.9 μm.

Figure 3.34 M1H - P4C gingival sample IF Loricrin. Representative gingival samples are depicted at 10x, and 20x magnification.
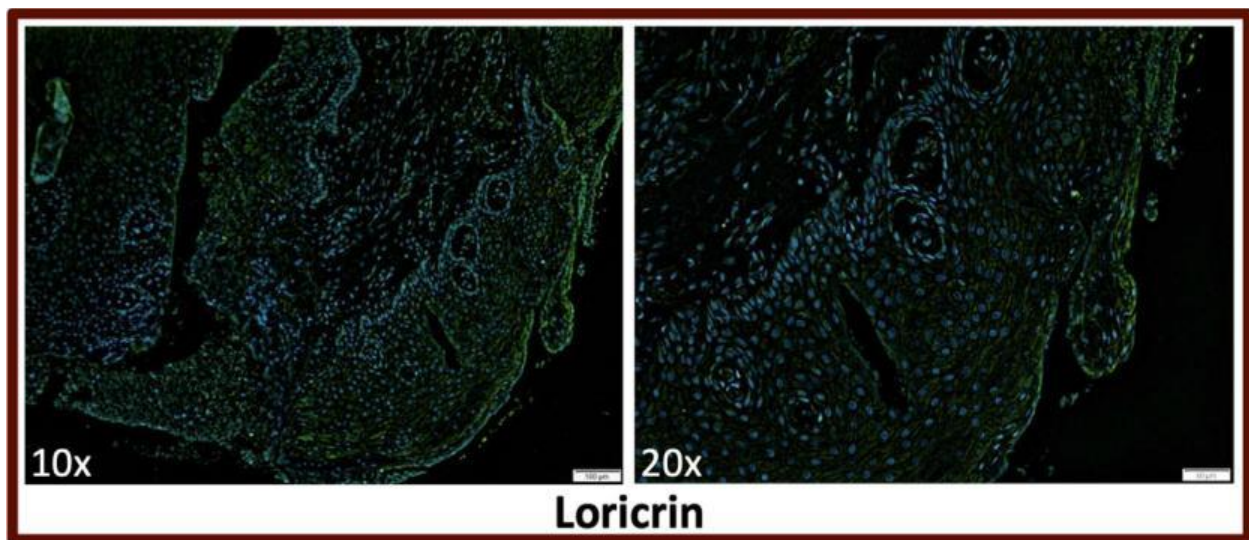
Back to Table 3.3 Features of IF Staining for Loricrin

3.3.13 H-19 - P4C gingival sample IF Loricrin descriptions

IF staining of P4C gingival sample - H-19 for loricrin was evaluated in 10x and 20x images depicted in Figure 3.35. The loricrin signal was expressed most strongly the stratum corneum and granulosum. The fluorescence signal was interrupted with an average width of 7.2 µm.

Figure 3.35 H-19 - P4C gingival sample IF Loricrin. Representative gingival samples are depicted at 10, and 20x magnification.

10x   20x
Loricrin
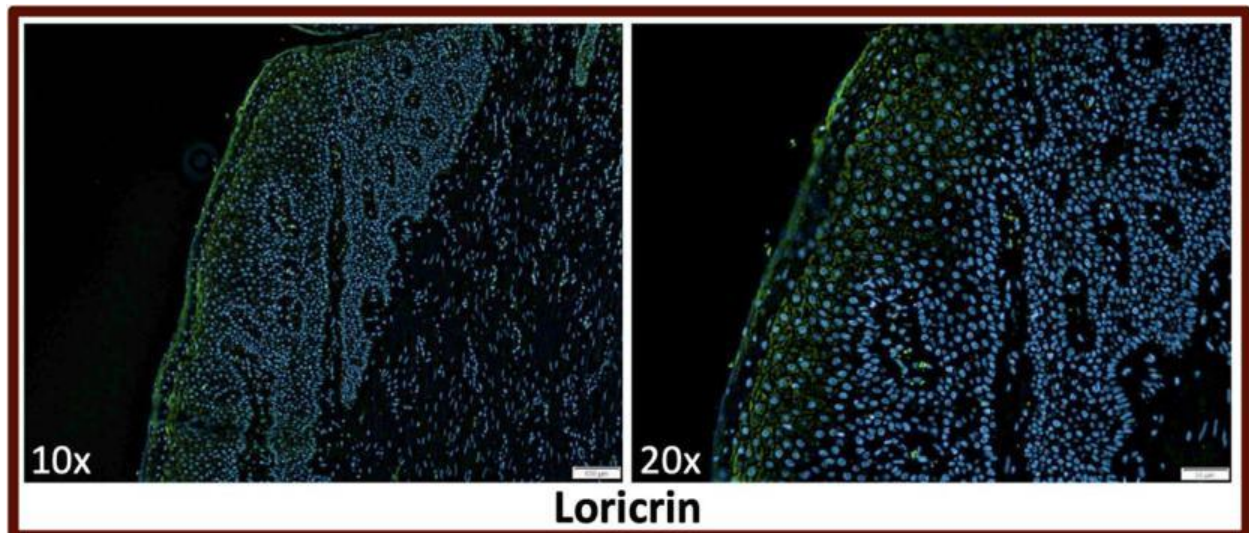
Back to Table 3.3 Features of IF Staining for Loricrin

3.3.14 H-27 - P4C gingival sample IF Loricrin descriptions

IF staining of P4C gingival sample - H-27 for loricrin was evaluated in 10x and 20x images depicted in Figure 3.36. The loricrin signal was expressed most strongly in the stratum corneum, granulosum, and spinosum. The fluorescence signal was interrupted with an average width of 9.4 μm.

Figure 3.36 H-27 - P4C gingival sample IF Loricrin. Representative gingival samples are depicted at 10x, and 20x magnification.
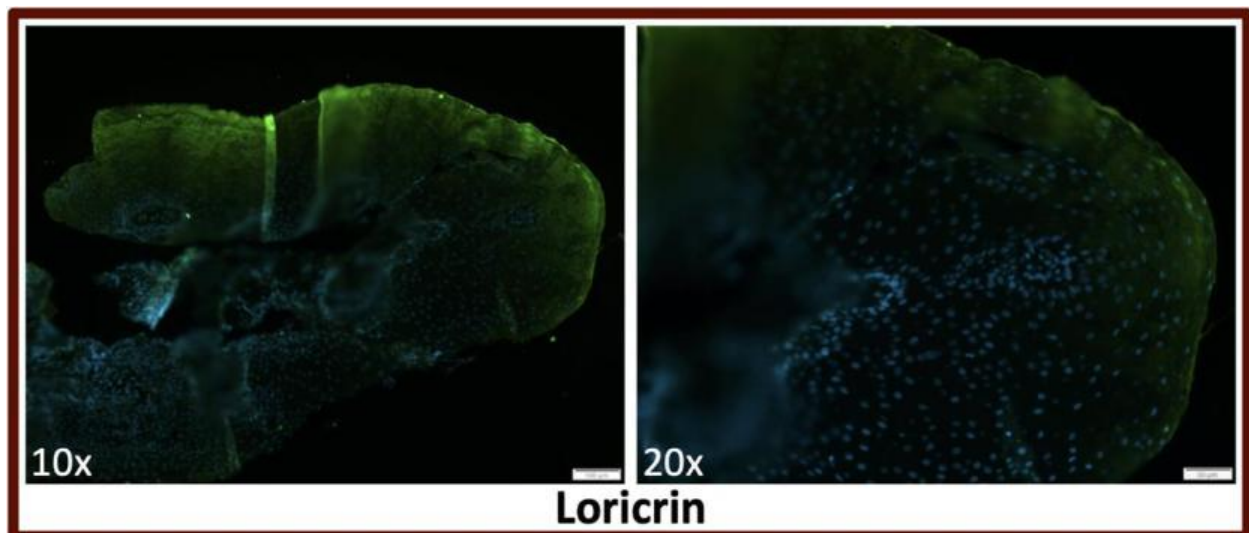
Back to Table 3.3 Features of IF Staining for Loricrin

3.3.15 H-48 - P4C gingival sample IF Loricrin descriptions

IF staining of P4C gingival sample - H-28 for loricrin was evaluated in 20x and 40x images depicted in Figure 3.37. The loricrin signal was expressed most strongly in the stratum corneum and granulosum. The fluorescence signal was interrupted with an average width of 8.5 µm.

Figure 3.37 H-48 - P4C gingival sample IF Loricrin. Representative gingival samples are depicted at 20x, and 40x magnification.
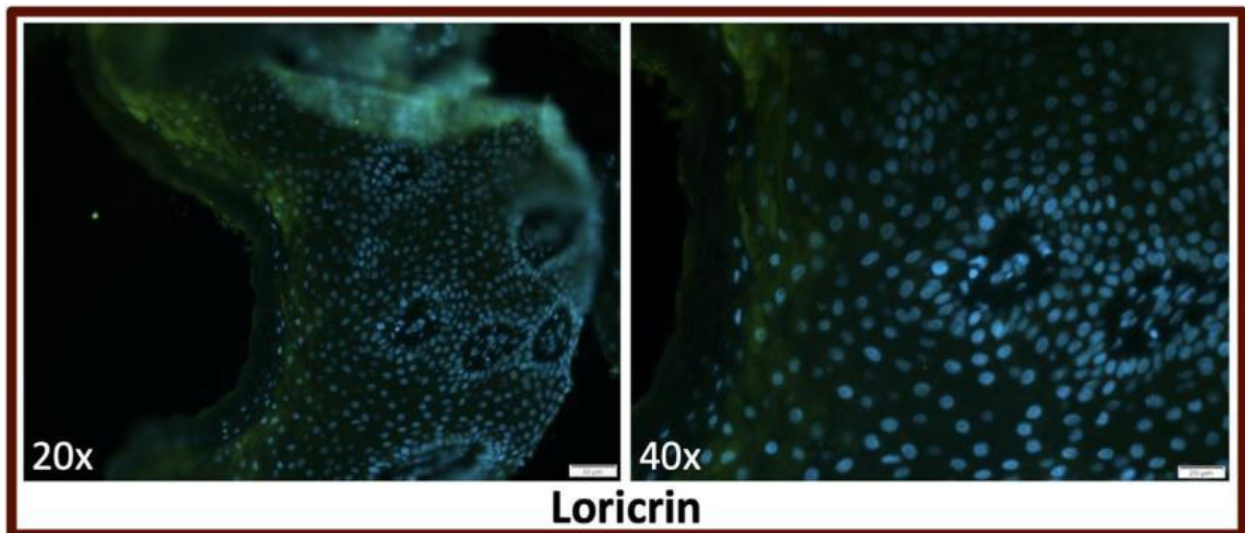
Back to Table 3.3 Features of IF Staining for Loricrin

3.4 Immunofluorescence (IF) Antibody Staining for Cytokeratin 1 (CK1)

IF staining for CK1 in Healthy, P3C and P4C samples was completed, and images captured at 10x, 20x, and 40x magnification. The green fluorescence represents the CK1 expression and the blue nuclei staining is a DAPI counterstain for orientation of the sample. Qualitative features on the expression location and uniformity of the IF signaling are provided for each sample. The features of each sample are described in Table 3.4.

Table 3.4 Cytokeratin 1 (CK1) Immunofluorescence (IF) gingival sample features.

Tissue ID	Expression	Uniformity
Periodontal Diagnosis: Healthy		
H-23	Granulosum and spinosum	Interrupted
H-26	Corneum, granulosum, and spinosum	Uniform
H-34	Granulosum, and spinosum	Uniform
H-39	Granulosum, and spinosum	Uniform
H-42	Granulosum, and spinosum	Uniform
Periodontal Diagnosis: P3C		
R4H	Granulosum, and spinosum	Interrupted
H-6	Corneum, and granulosum	Interrupted
H-12	Corneum, and granulosum	Interrupted
H-14	Corneum, and granulosum	Uniform
H-44	Spinosum, and basale	Interrupted
Periodontal Diagnosis: P4C		
R1H	Corneum, and granulosum	Interrupted
M1H	Corneum, granulosum, and spinosum	Interrupted
H-19	Granulosum, and spinosum	Interrupted
H-27	Granulosum, and spinosum	Uniform
H-48	Granulosum, and spinosum	Interrupted

3.4.1 H-23 - Healthy gingival sample IF CK1 description

IF staining of Healthy gingival sample - H-23 for CK1 was evaluated in 10x and 20x images depicted in Figure 3.38. The signal was expressed most strongly in the stratum granulosum and spinosum. This signal appeared interrupted within the strata.

Figure 3.38 H-23 - Healthy gingival sample IF CK1. Representative gingival samples are depicted at 10, and 20x magnification.

Cytokeratin 1
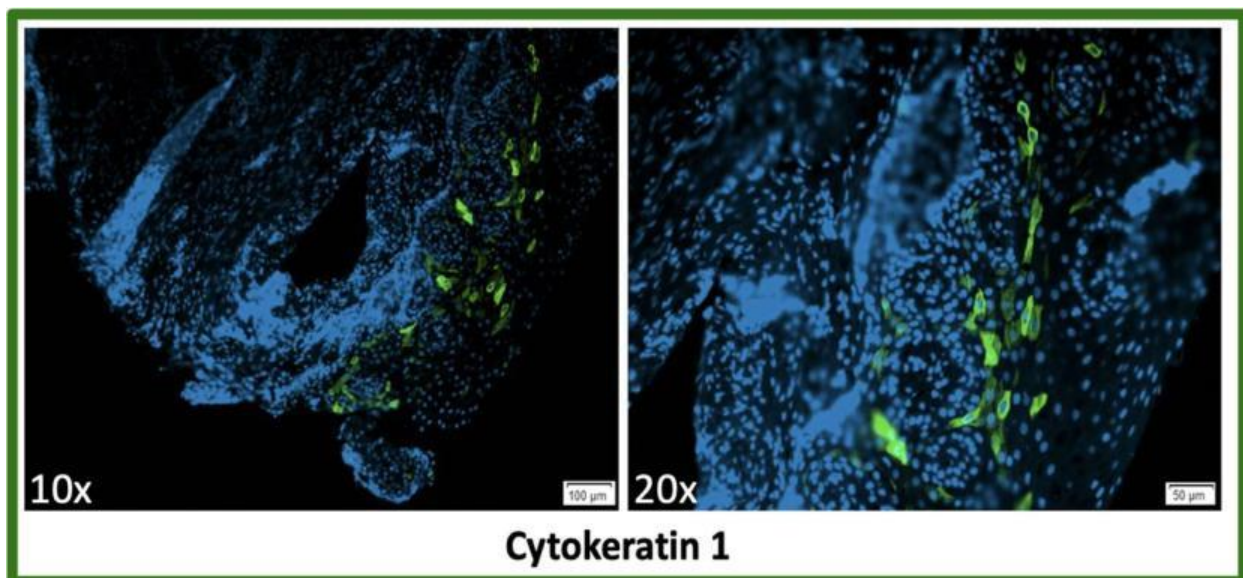
Back to Table 3.4 CK1 IF gingival sample features

3.4.2 H-26 - Healthy gingival sample IF CK1 description

IF staining of Healthy gingival sample - H-26 for CK1 was evaluated in 10x and 20x images depicted in Figure 3.39. The signal was expressed most strongly in the stratum corneum, granulosum, and spinosum. This signal appeared uniform within the strata.

Figure 3.39 H-26 - Healthy gingival sample IF CK1. Representative gingival samples are depicted at 10, and 20x magnification.

Cytokeratin 1
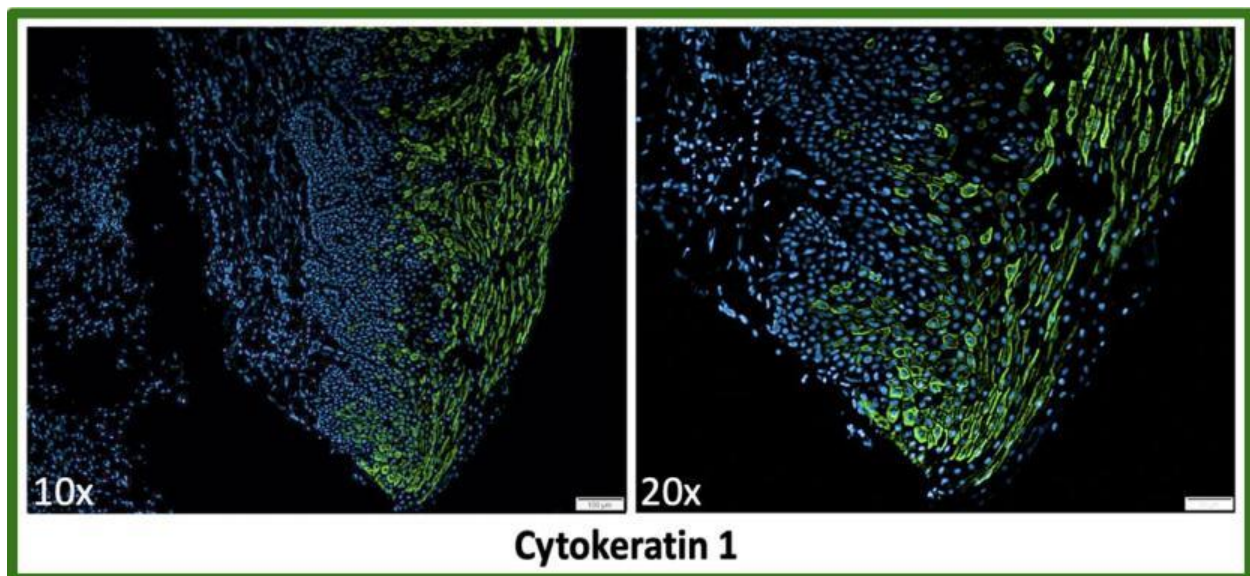
Back to Table 3.4 CK1 IF gingival sample features

3.4.3 H-34 - Healthy gingival sample IF CK1 description

IF stains of Healthy gingival sample - H-34 for CK1 was evaluated in 10x and 20x images depicted in Figure 3.40. The signal was expressed most strongly in the stratum granulosum and spinosum. This signal appears uniform within the strata.

Figure 3.40 H-34 - Healthy gingival sample IF CK1. Representative gingival samples are depicted at 10, and 20x magnification.

Cytokeratin 1
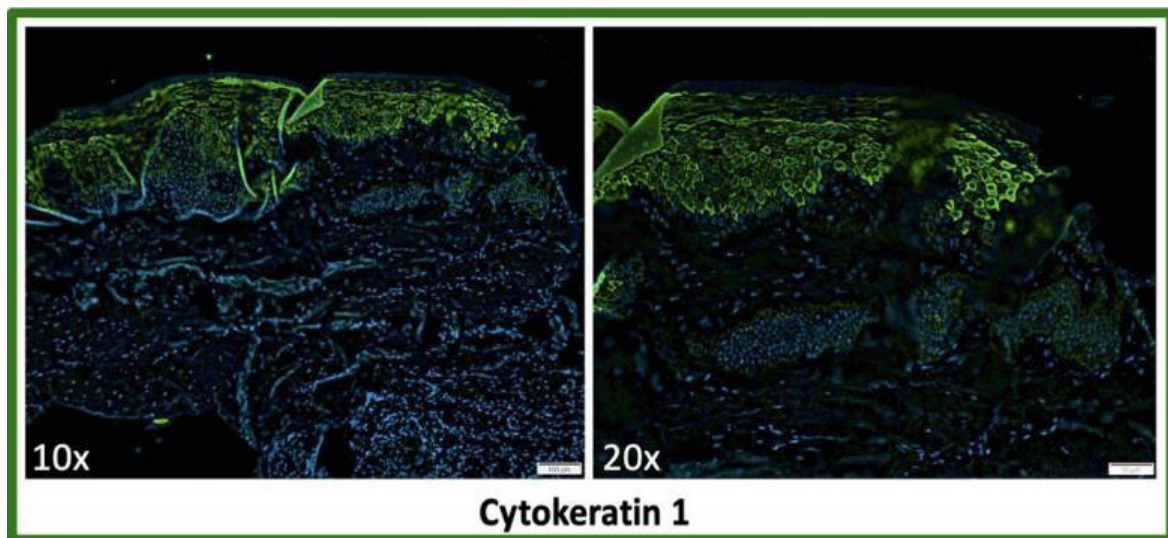
Back to Table 3.4 CK1 IF gingival sample features

3.4.4 H-39 - Healthy gingival sample IF CK1 description

IF staining of Healthy gingival sample - H-39 for CK1 was evaluated in 10x and 20x images depicted in Figure 3.41. The signal was expressed most strongly in the stratum granulosum and spinosum. This signal appeared uniform within the strata.

Figure 3.41 H-39 - Healthy gingival sample IF CK1. Representative gingival samples are depicted at 10, and 20x magnification.
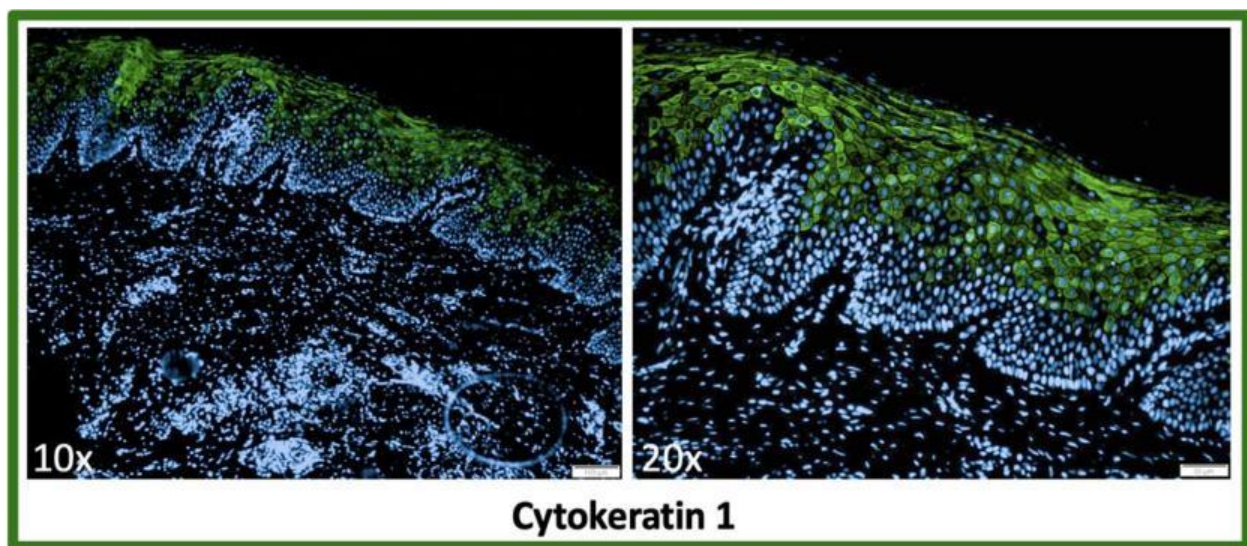
Back to Table 3.4 CK1 IF gingival sample features

3.4.5 H-42 - Healthy gingival sample IF CK1 description

IF staining of Healthy gingival sample - H-42 for CK1 was evaluated in 10x and 20x images depicted in Figure 3.42. The signal was expressed most strongly in the stratum granulosum and spinosum. This signal appeared uniform within the strata.

Figure 3.42 H-42 - Healthy gingival sample IF CK1. Representative gingival samples are depicted at 10, and 20x magnification.

Cytokeratin 1
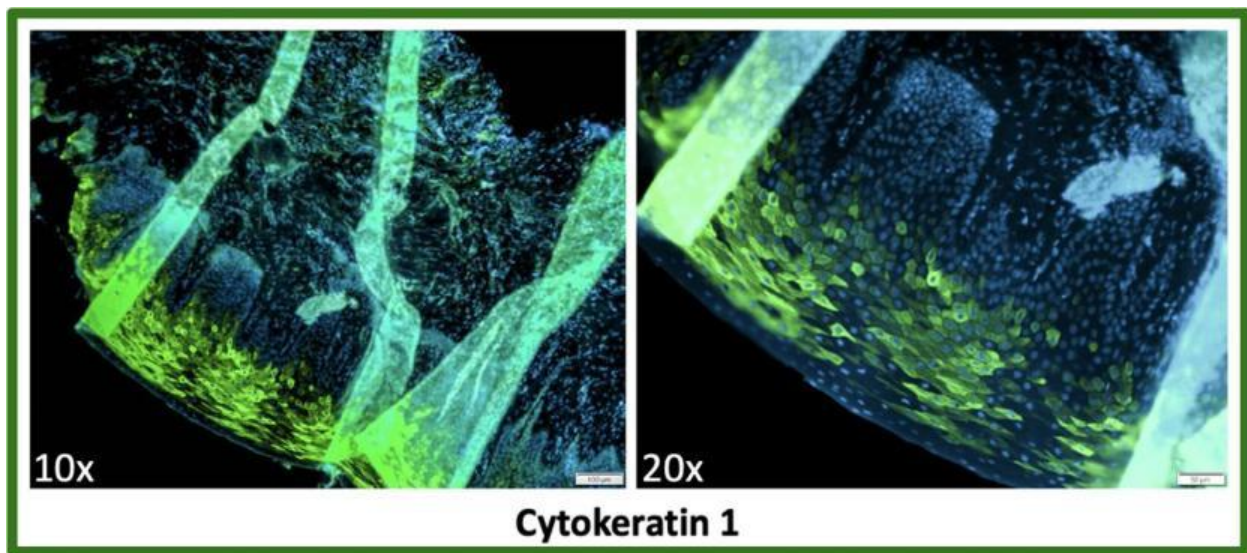
Back to Table 3.4 CK1 IF gingival sample features

3.4.6 R4H - P3C gingival sample IF CK1 description

IF staining of P3C gingival sample - R4H for CK1 was evaluated in 10x and 20x images depicted in Figure 3.43. The signal was expressed most strongly in the stratum granulosum and spinosum. This signal appeared interrupted with a distinct external signal.

Figure 3.43 R4H - P3C gingival sample IF CK1. Representative gingival samples are depicted at 10, and 20x magnification.
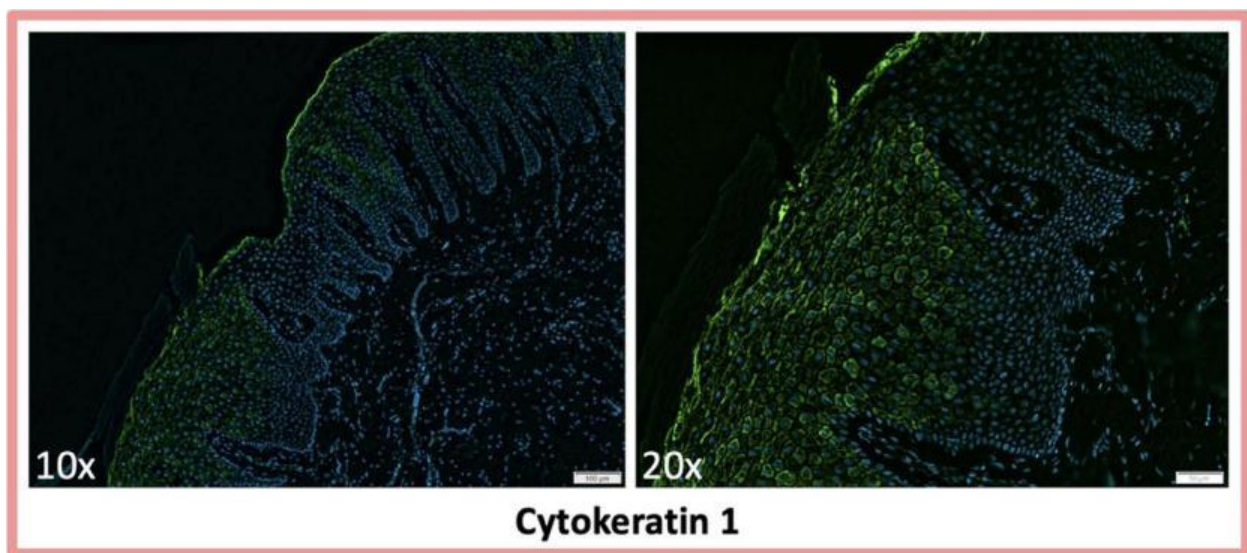
Back to Table 3.4 CK1 IF gingival sample features

3.4.7 H6 - P3C gingival sample IF CK1 description

IF staining of P3C gingival sample - H6 for CK1 was evaluated in 10x and 40x images depicted in Figure 3.44. The signal was expressed most strongly in the stratum corneum and granulosum. This signal appeared interrupted with a distinct external signal.

Figure 3.44 H6 - P3C gingival sample IF CK1. Representative gingival samples are depicted at 10, and 40x magnification.

Cytokeratin 1
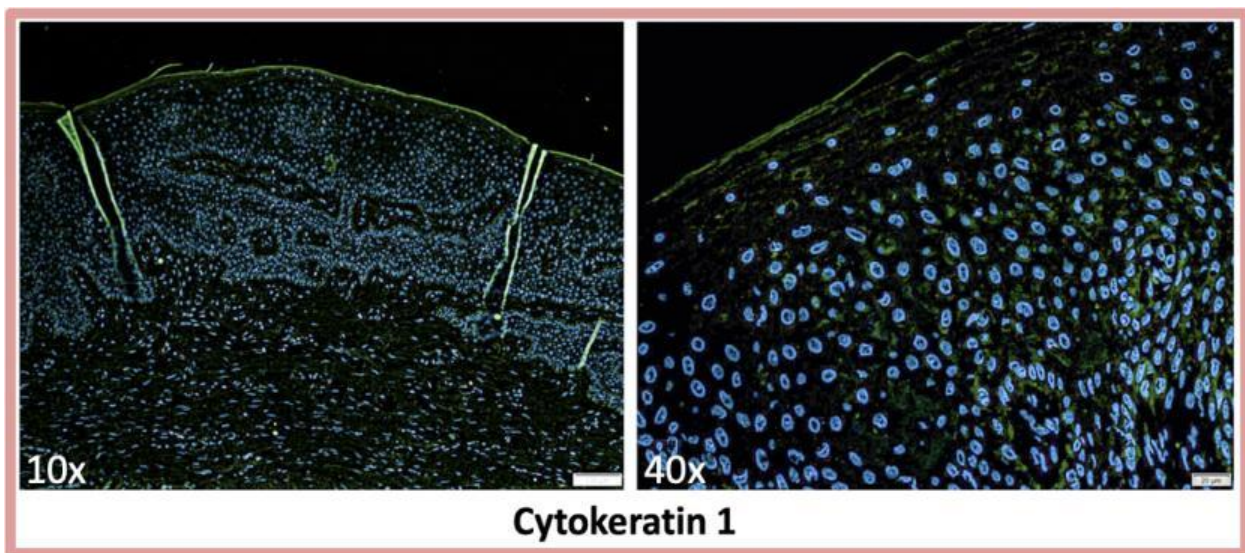
Back to Table 3.4 CK1 IF gingival sample features

3.4.8 H-12 - P3C gingival sample IF CK1 description

IF staining of P3C gingival sample - H-12 for CK1 was evaluated in 10x and 20x images depicted in Figure 3.45. The signal was expressed most strongly in the stratum corneum and granulosum. This signal appeared interrupted within the strata.

Figure 3.45 H-12 - P3C gingival sample IF CK1. Representative gingival samples are depicted at 10, and 20x magnification.
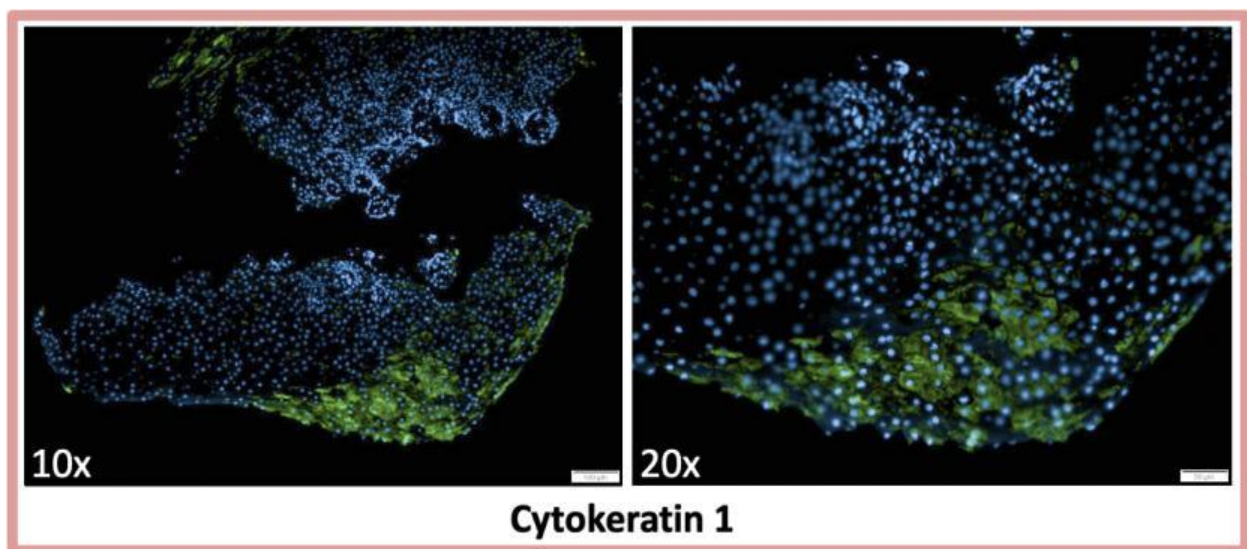
Back to Table 3.4 CK1 IF gingival sample features

3.4.9 H-14 - P3C gingival sample IF CK1 description

IF staining of P3C gingival sample - H-14 for CK1 was evaluated in 10x and 20x images depicted in Figure 3.46. The signal was expressed most strongly in the stratum corneum, and granulosum. This signal appeared uniform within the strata.

Figure 3.46 H-14 - P3C gingival sample IF CK1. Representative gingival samples are depicted at 10, and 20x magnification.
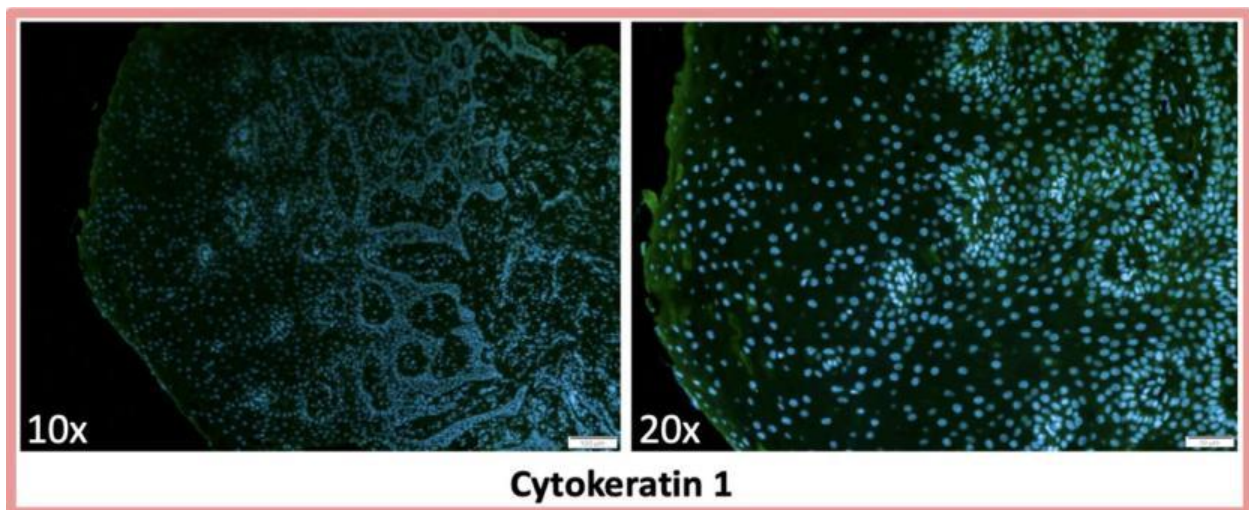
Back to Table 3.4 CK1 IF gingival sample features

3.4.10 H-44 - P3C gingival sample IF CK1 description

IF staining of P3C gingival sample - H-44 for CK1 was evaluated in 10x and 20x images depicted in Figure 3.47. The signal was expressed most strongly in the stratum spinosum, and basale. This signal appeared interrupted within the strata.

Figure 3.47 H-44 - P3C gingival sample IF CK1. Representative gingival samples are depicted at 10, and 20x magnification.

Cytokeratin 1
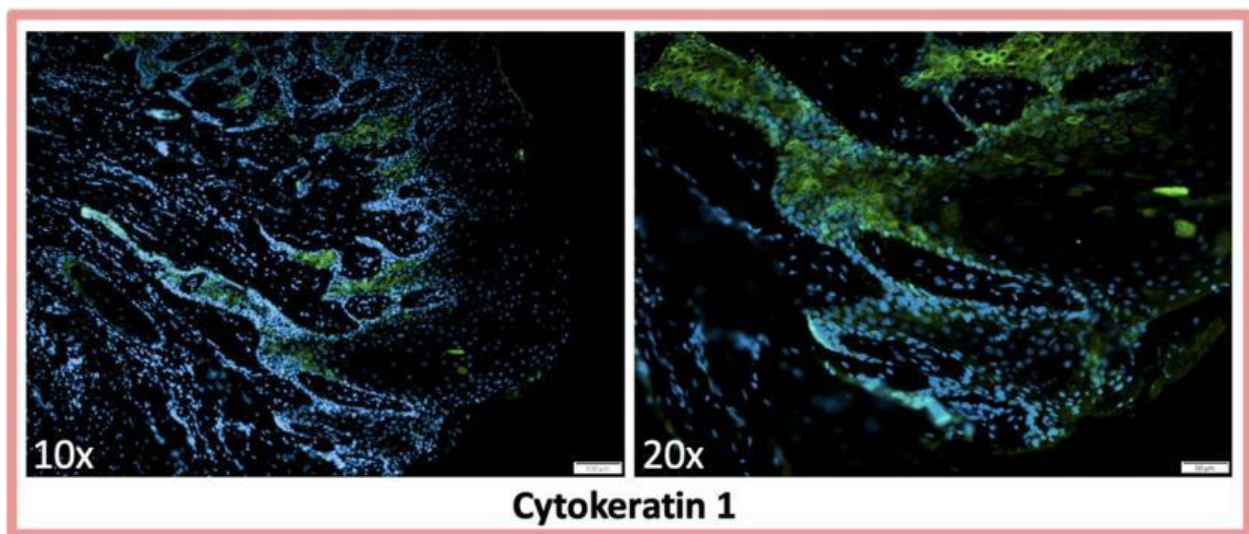
Back to Table 3.4 CK1 IF gingival sample features

3.4.11 R1H - P4C gingival sample IF CK1 description

IF staining of P4C gingival sample - R1H for CK1 was evaluated in 10x and 20x images depicted in Figure 3.48. The signal was expressed most strongly in the stratum corneum, and granulosum. This signal appeared interrupted within the strata.

Figure 3.48 R1H - P4C gingival sample IF CK1. Representative gingival samples are depicted at 10, and 20x magnification.

Cytokeratin 1
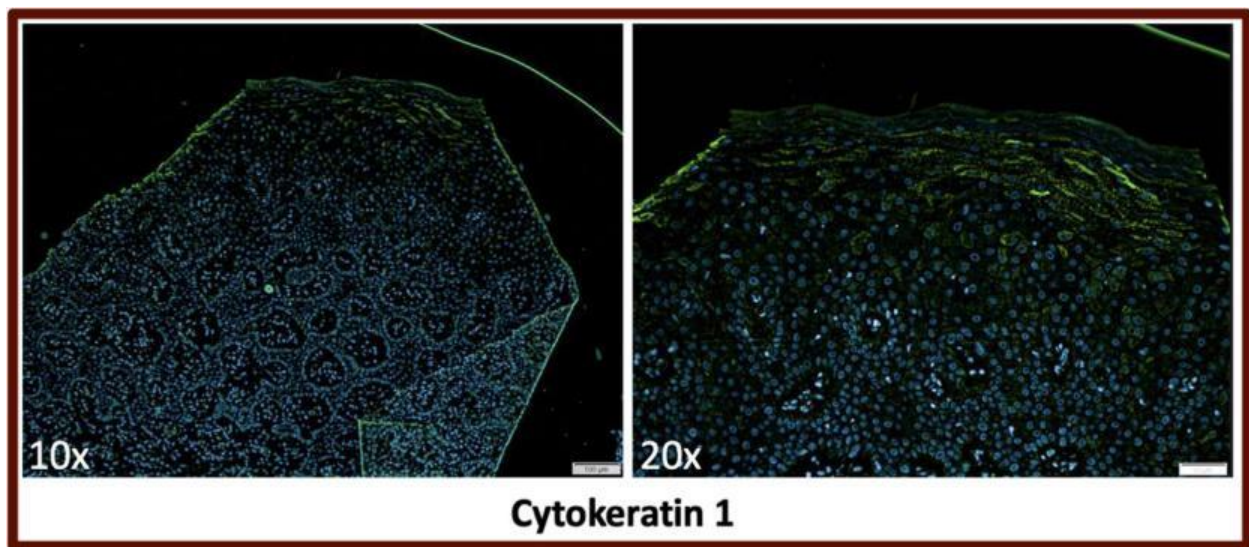
Back to Table 3.4 CK1 IF gingival sample features

3.4.12 M1H - P4C gingival sample IF CK1 description

IF staining of P4C gingival sample - M1H for CK1 was evaluated in 10x and 20x images depicted in Figure 3.49. The signal was expressed most strongly in the stratum corneum, granulosum, and spinosum. This signal appeared interrupted with a distinct external signal.

Figure 3.49 M1H - P4C gingival sample IF CK1. Representative gingival samples are depicted at 10, and 20x magnification.

Cytokeratin 1
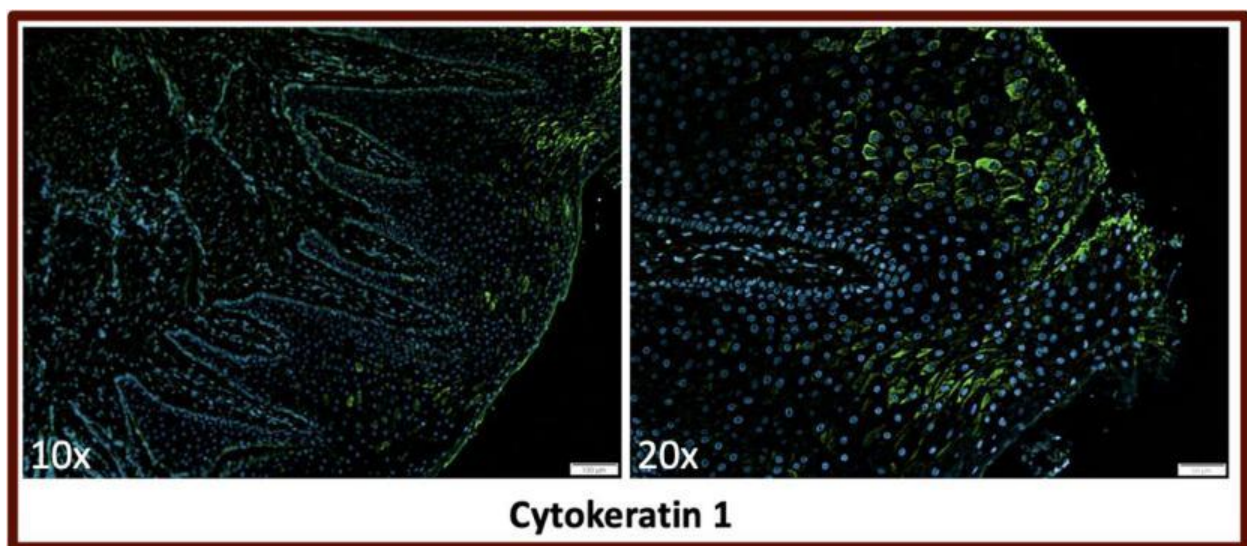
Back to Table 3.4 CK1 IF gingival sample features

3.4.13 H-19 - P4C gingival sample IF CK1 description

IF staining of P4C gingival sample - H-19 for CK1 was evaluated in 10x and 20x images depicted in Figure 3.50. The signal was expressed most strongly in the stratum granulosum, and spinosum. This signal appeared interrupted within the strata.

Figure 3.50 H-19 - P4C gingival sample IF CK1. Representative gingival samples are depicted at 10, and 20x magnification.
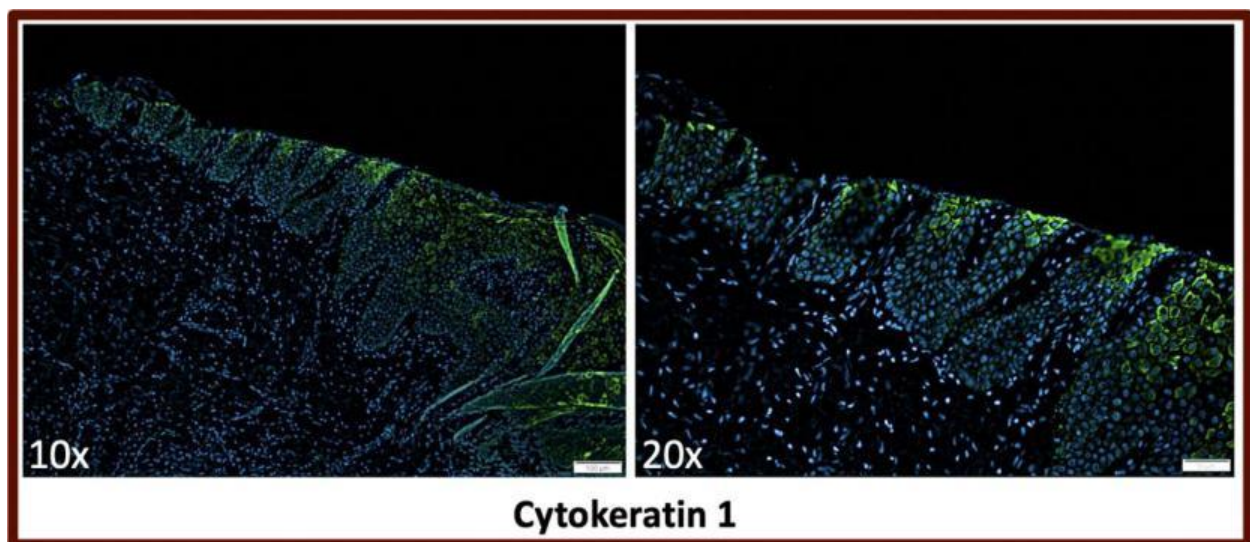
Back to Table 3.4 CK1 IF gingival sample features

3.4.14 H-27 - P4C gingival sample IF CK1 description

IF staining of P4C gingival sample - H-27 for CK1 was evaluated in 10x and 20x images depicted in Figure 3.51. The signal was expressed most strongly in the stratum granulosum, and spinosum. This signal appeared uniform within the strata.

Figure 3.51 H-27 - P4C gingival sample IF CK1. Representative gingival samples are depicted at 10, and 20x magnification.
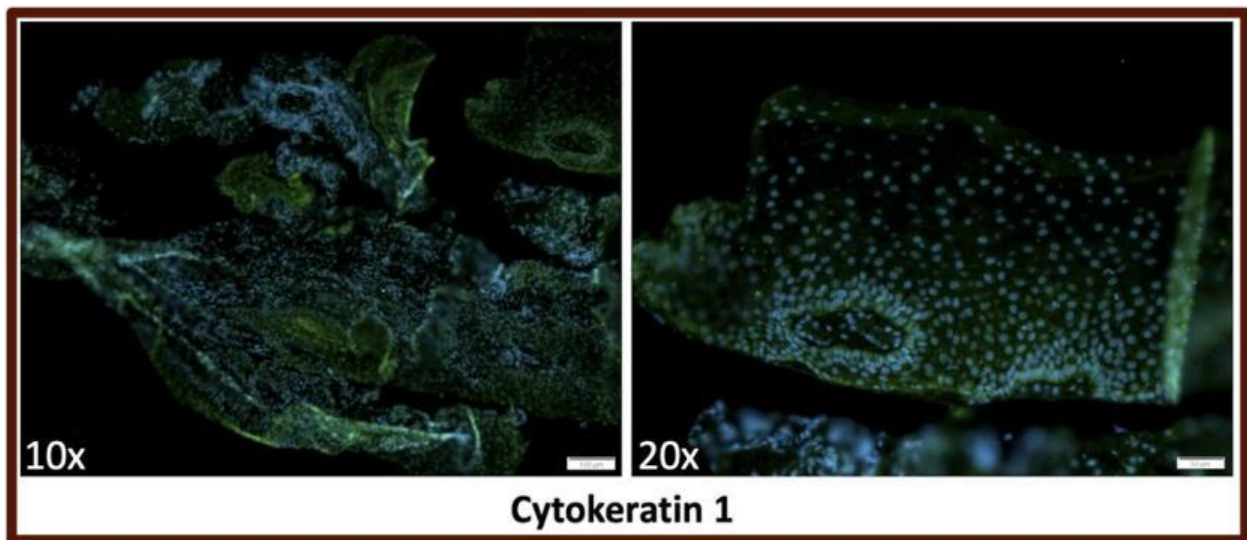
Back to Table 3.4 CK1 IF gingival sample features

3.4.15 H-48 - P4C gingival sample IF CK1 description

IF staining of P4C gingival sample - H-48 for CK1 was evaluated in 10x and 20x images depicted in Figure 3.52. The signal was expressed most strongly in the stratum granulosum, and spinosum. This signal appeared interrupted within the strata.

Figure 3.52 H-48 - P4C gingival sample IF CK1. Representative gingival samples are depicted at 10, and 20x magnification.
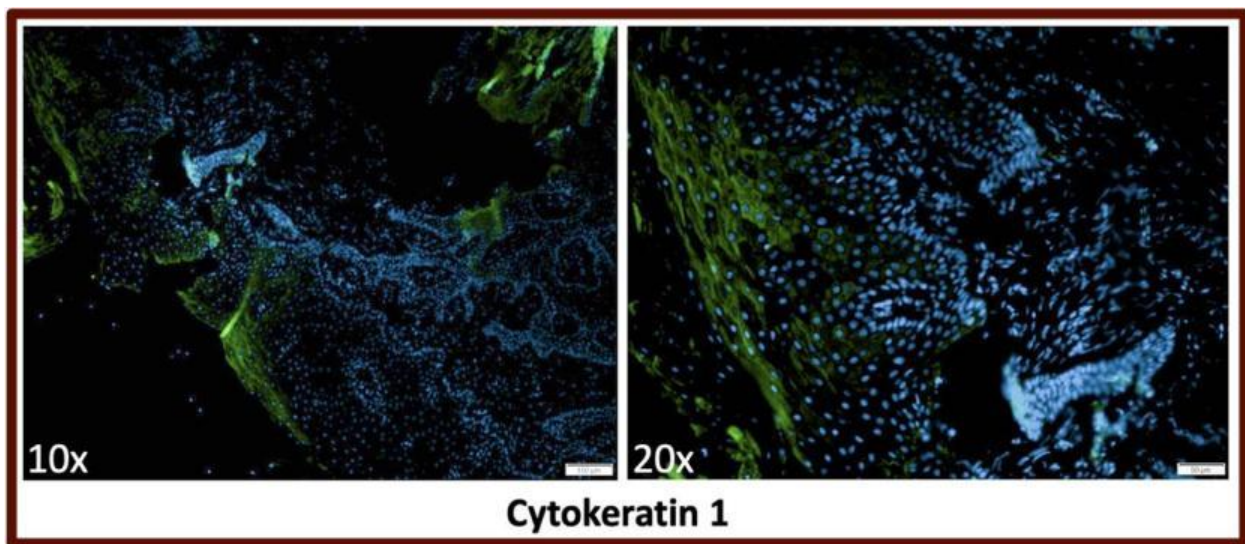
Cytokeratin 1

3.5 Immunofluorescence (IF) Antibody Staining for Cytokeratin 14 (CK14)

IF staining for CK14 in Healthy, P3C, and P4C samples was completed, and images captured at 10x, 20x and 40x magnification. The green fluorescence represents the CK14 expression, and the blue nuclei staining is a DAPI counterstain for orientation of the sample. Qualitative features on the expression location and uniformity of the IF signaling are provided for each sample. The features of each sample are captured in Table 3.5.

Table 3.5 Cytokeratin 14 (CK14) Immunofluorescence (IF) gingival sample features.

Tissue ID	Expression	Uniformity
Periodontal Diagnosis: Healthy		
H-23	Corneum and basale	Uniform
H-26	Basale	Uniform
H-34	Basale	Interrupted
H-39	Basale	Uniform
H-42	Spinosum and basale	Uniform
Periodontal Diagnosis: P3C		
R4H	Basale	Uniform
H-6	Basale	Interrupted
H-12	Basale	Uniform
H-14	Basale. Difficult to discern.	Uniform
H-44	Spinosum and basale	Uniform
Periodontal Diagnosis: P4C		
R1H	Corneum and basale	Interrupted
M1H	Corneum and basale	Interrupted
H-19	Basale	Uniform
H-27	All strata	Uniform
H-48	Basale	Uniform

3.5.1 H-23 - Healthy gingival sample IF CK14 description

      IF staining of Healthy gingival sample - H-23 for CK14 was evaluated in 10x and 20x images depicted in Figure 3.53. The signal was expressed most strongly in the stratum corneum and basale. This signal appeared uniform within the strata.

Figure 3.53 H-23 - Healthy gingival sample IF CK14. Representative gingival samples are depicted at 10, and 20x magnification.

Cytokeratin 14
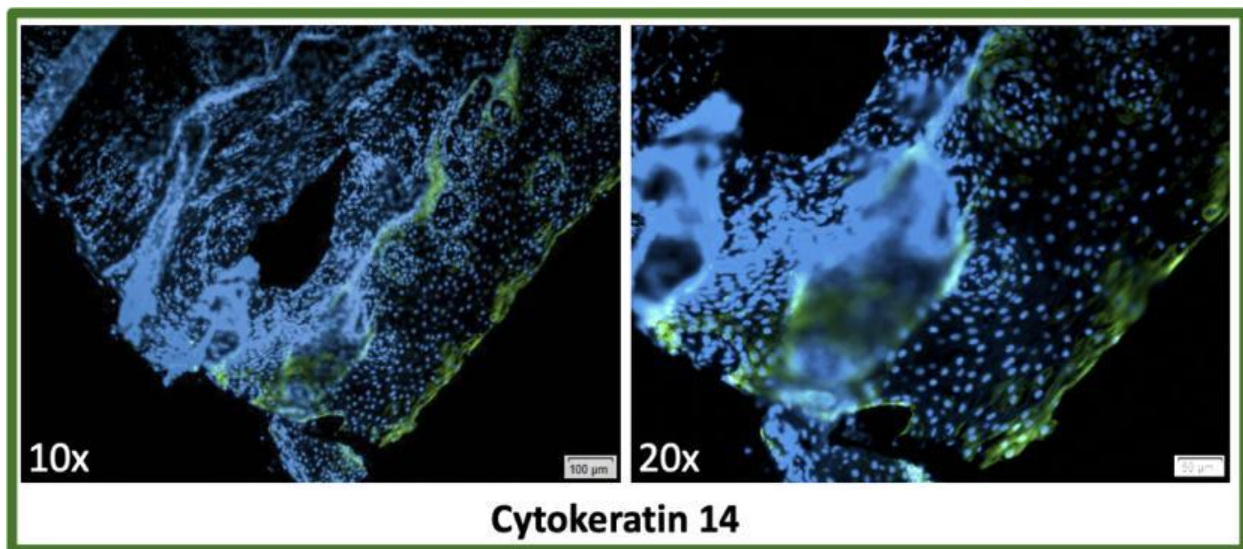
Back to Table 3.5 CK14 IF gingival sample features

3.5.2 H-26 - Healthy gingival sample IF CK14 description

IF staining of Healthy gingival sample - H-26 for CK14 was evaluated in 10x and 20x images depicted in Figure 3.54. The signal was expressed most strongly in the stratum basale. This signal appeared uniform within the strata.

Figure 3.54 H-26 - Healthy gingival sample IF CK14. Representative gingival samples are depicted at 10, and 20x magnification.
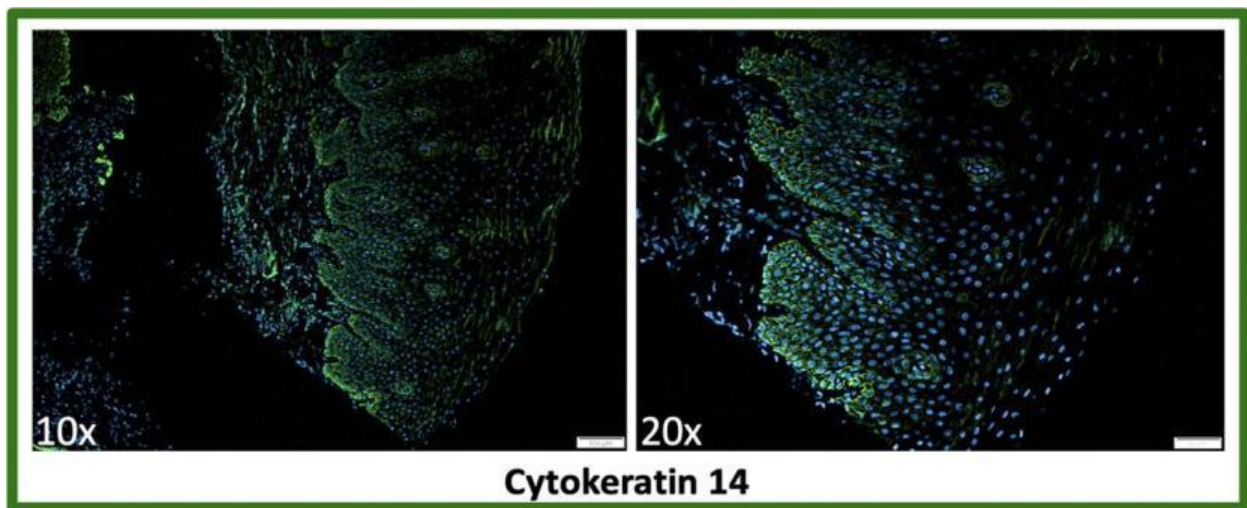
Back to Table 3.5 CK14 IF gingival sample features

3.5.3 H-34 - Healthy gingival sample IF CK14 description

IF staining of Healthy gingival sample - H-34 for CK14 was evaluated in 10x and 20x images depicted in Figure 3.55. The signal was expressed most strongly in the stratum basale. This signal appeared interrupted within the strata.

Figure 3.55 H-34 - Healthy gingival sample IF CK14. Representative gingival samples are depicted at 10, and 20x magnification.
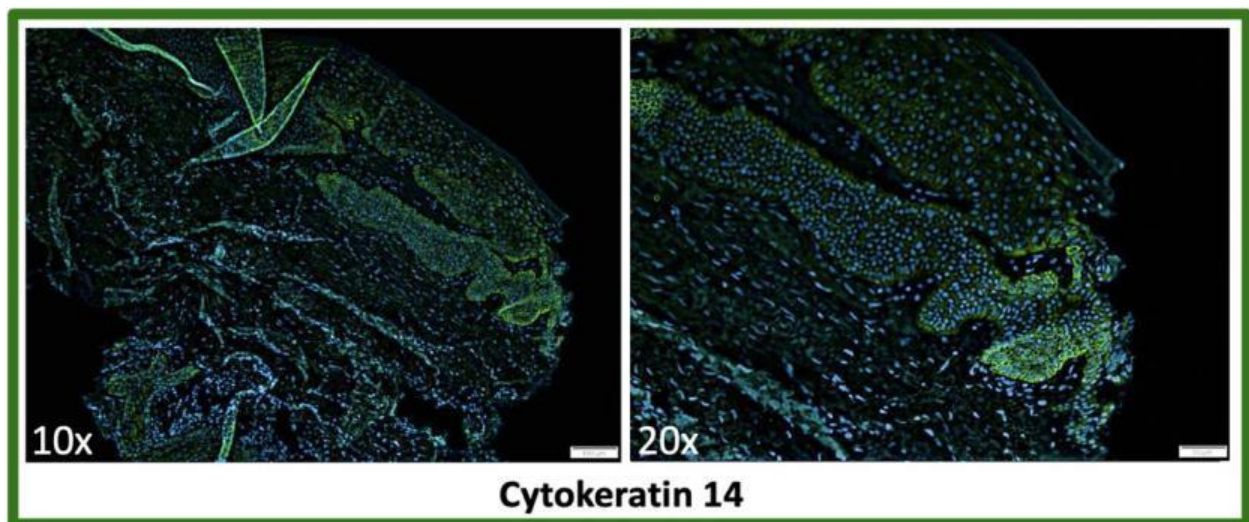
Back to Table 3.5 CK14 IF gingival sample features

3.5.4 H-39 - Healthy gingival sample IF CK14 description

IF staining of Healthy gingival sample - H-39 for CK14 was evaluated in 10x and 20x images depicted in Figure 3.56. The signal was expressed most strongly in the stratum basale. This signal appeared uniform within the strata.

Figure 3.56 H-39 - Healthy gingival sample IF CK14. Representative gingival samples are depicted at 10, and 20x magnification.
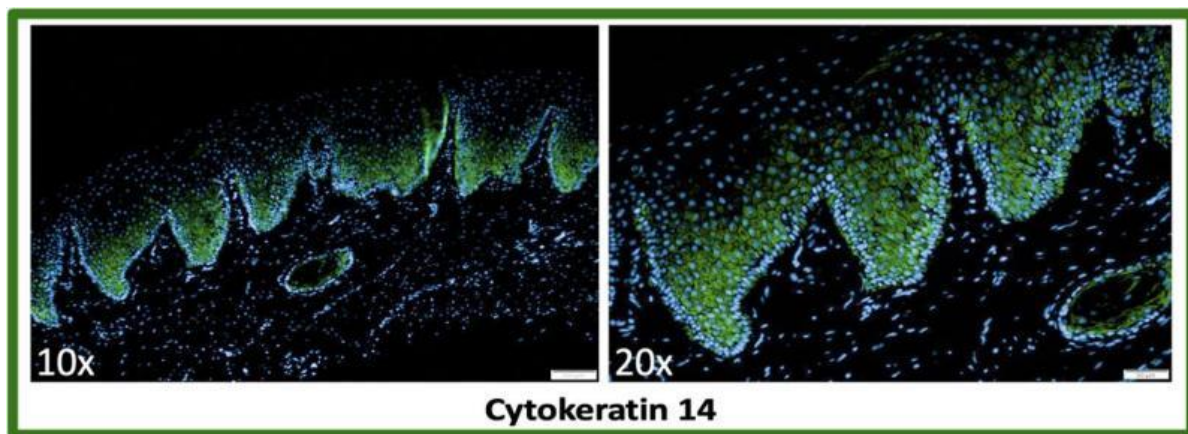
Back to Table 3.5 CK14 IF gingival sample features

3.5.5 H-42 - Healthy gingival sample IF CK14 description

IF staining of Healthy gingival sample - H-42 for CK14 was evaluated in 10x and 20x images depicted in Figure 3.57. The signal was expressed most strongly in the stratum spinosum and basale. This signal appeared uniform within the strata.

Figure 3.57 H-42 - Healthy gingival sample IF CK14. Representative gingival samples are depicted at 10, and 20x magnification.

Cytokeratin 14
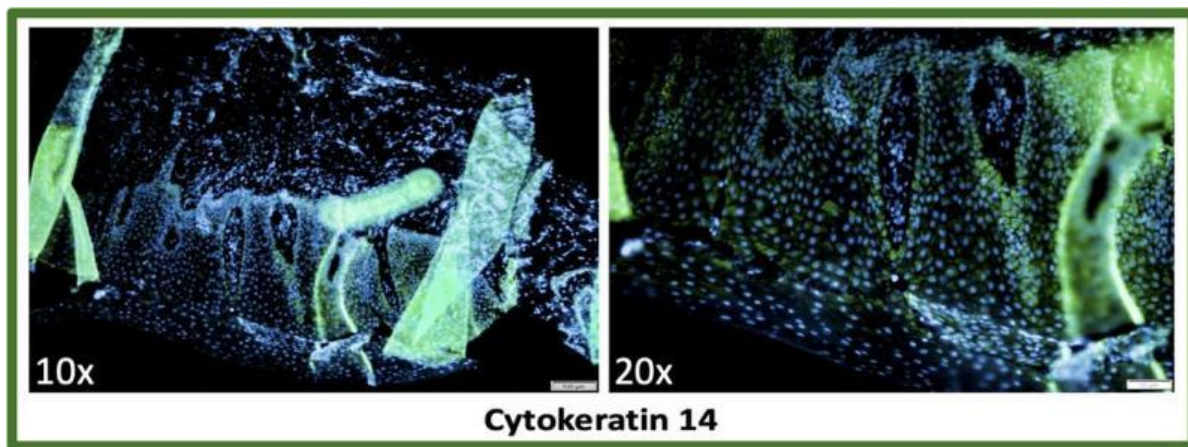
Back to Table 3.5 CK14 IF gingival sample features

3.5.6 R4H - P3C gingival sample IF CK14 description

IF staining of P3C gingival sample - R4H for CK14 was evaluated in 10x and 20x images depicted in Figure 3.58. The signal was expressed most strongly in the stratum basale. This signal appeared uniform within the strata.

Figure 3.58 R4H - P3C gingival sample IF CK14. Representative gingival samples are depicted at 10, and 20x magnification.

Cytokeratin 14
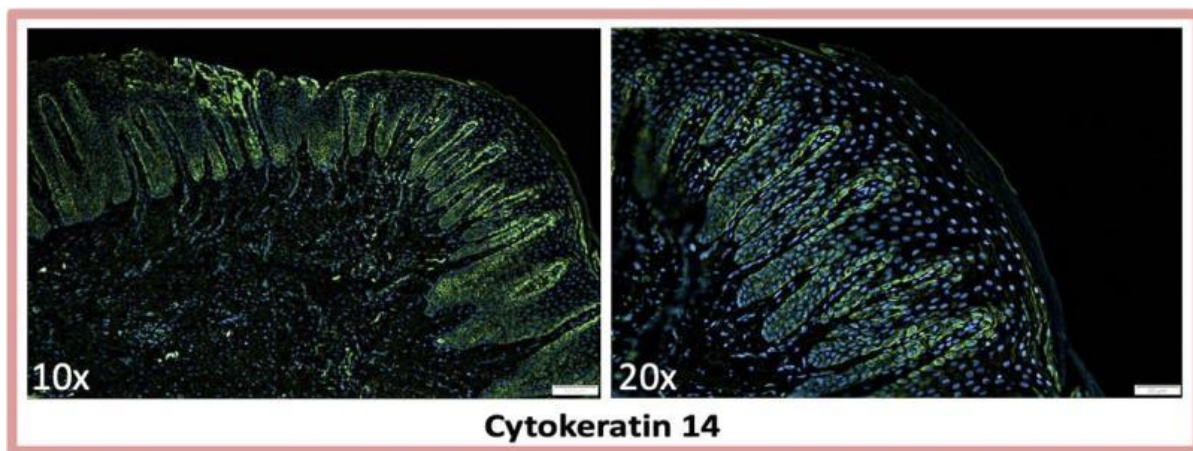
Back to Table 3.5 CK14 IF gingival sample features

3.5.7 H-6 - P3C gingival sample IF CK14 description

IF staining of P3C gingival sample - H-6 for CK14 was evaluated in 10x and 20x images depicted in Figure 3.59. The signal was expressed most strongly in the stratum basale. This signal appeared interrupted within the strata.

Figure 3.59 H-6 - P3C gingival sample IF CK14. Representative gingival samples are depicted at 10, and 20x magnification.

Cytokeratin 14
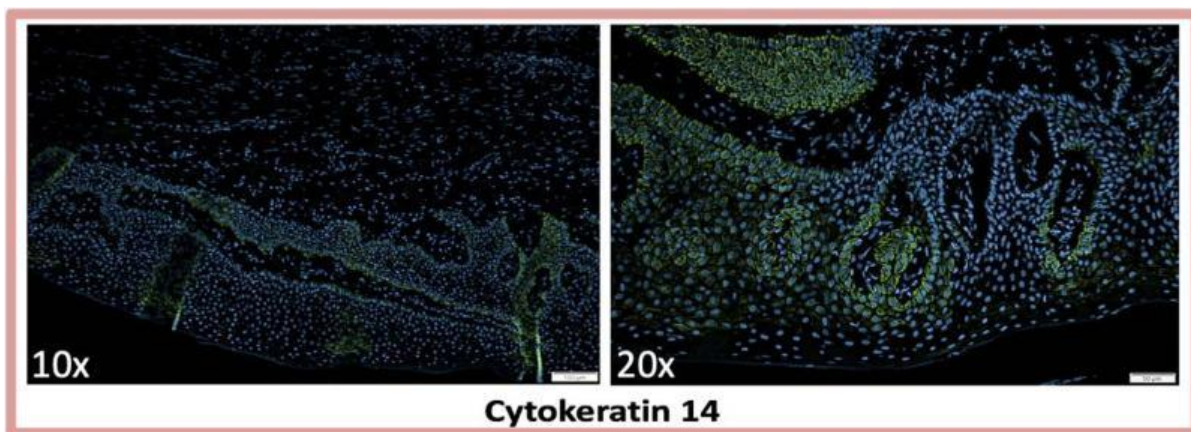
Back to Table 3.5 CK14 IF gingival sample features

3.5.8 H-12 - P3C gingival sample IF CK14 description

IF staining of P3C gingival sample - H-12 for CK14 was evaluated in 10x and 20x images depicted in Figure 3.60. The signal was expressed most strongly in the stratum basale. This signal appeared uniform within the strata.

Figure 3.60 H-12 - P3C gingival sample IF CK14. Representative gingival samples are depicted at 10, and 20x magnification.

Cytokeratin 14
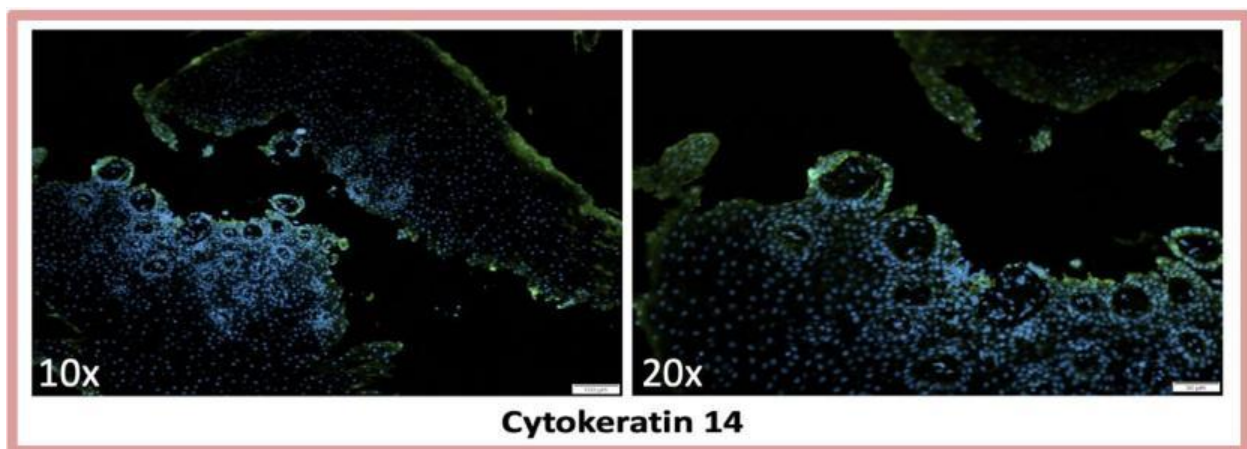
Back to Table 3.5 CK14 IF gingival sample features

3.5.9 H-14 - P3C gingival sample IF CK14 description

IF staining of P3C gingival sample - H-14 for CK14 was evaluated in 10x and 40x images depicted in Figure 3.61. The signal was expressed most strongly in the stratum basale. However, it was difficult to discern the exact signal position and width due to this being more of a tangential tissue section.

Figure 3.61 H-14 - P3C gingival sample IF CK14. Representative gingival samples are depicted at 10, and 40x magnification.

Cytokeratin 14
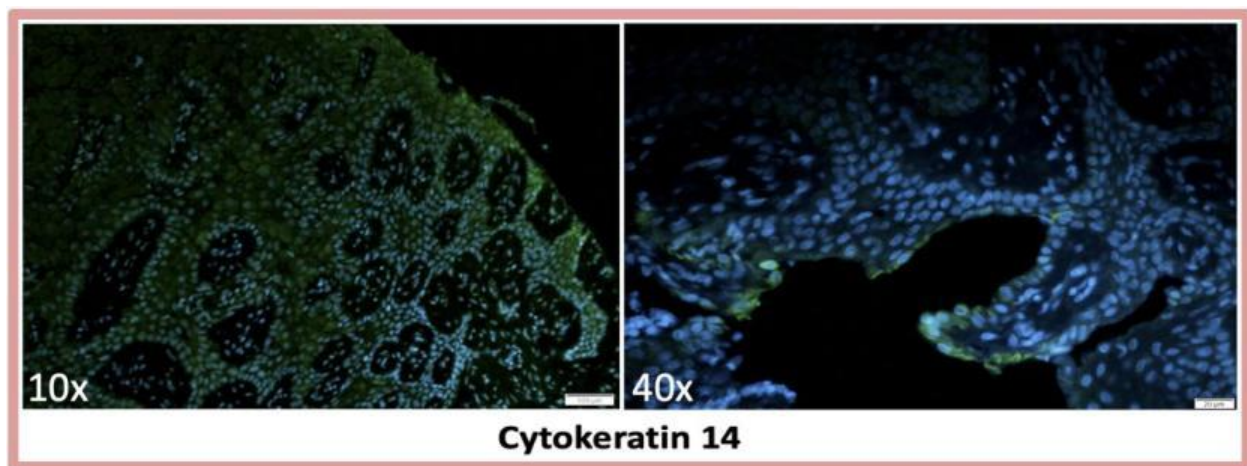
Back to Table 3.5 CK14 IF gingival sample features

3.5.10 H-44 - P3C gingival sample IF CK14 description

IF staining of P3C gingival sample - H-44 for CK14 was evaluated in 10x and 20x images depicted in Figure 3.62. The signal was expressed most strongly in the stratum spinosum and basale. This signal appeared uniform within the strata.

Figure 3.62 H-44 - P3C gingival sample IF CK14. Representative gingival samples are depicted at 10, and 20x magnification.

Cytokeratin 14
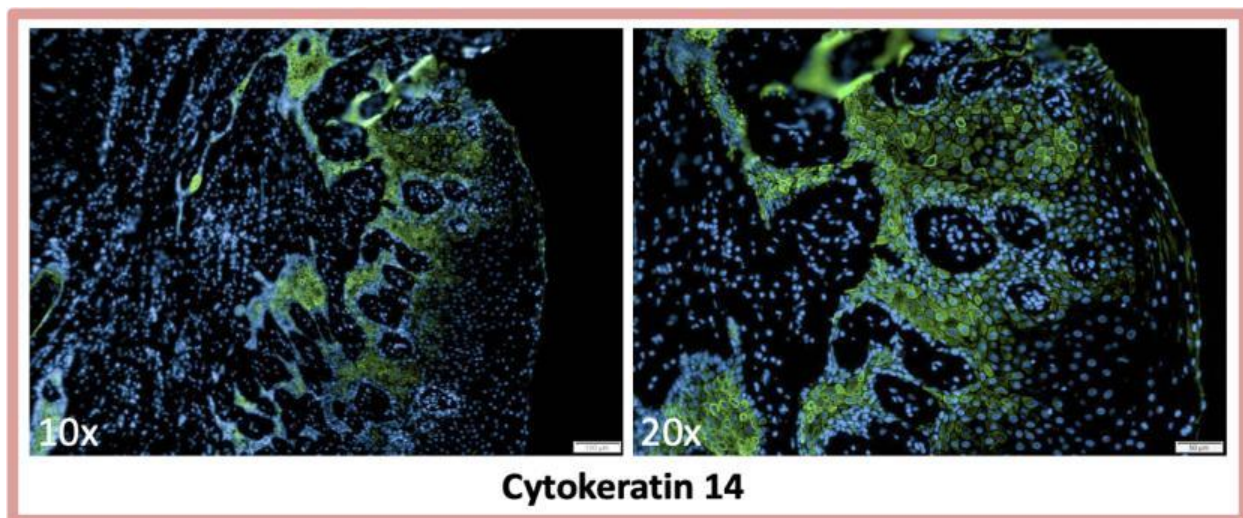
Back to Table 3.5 CK14 IF gingival sample features

3.5.11 R1H - P4C gingival sample IF CK14 description

IF staining of P4C gingival sample - R1H for CK14 was evaluated in 10x and 20x images depicted in Figure 3.63. The signal was expressed most strongly in the stratum corneum, and basale. This signal appeared interrupted within the strata.

Figure 3.63 R1H - P4C gingival sample IF CK14. Representative gingival samples are depicted at 10, and 20x magnification.
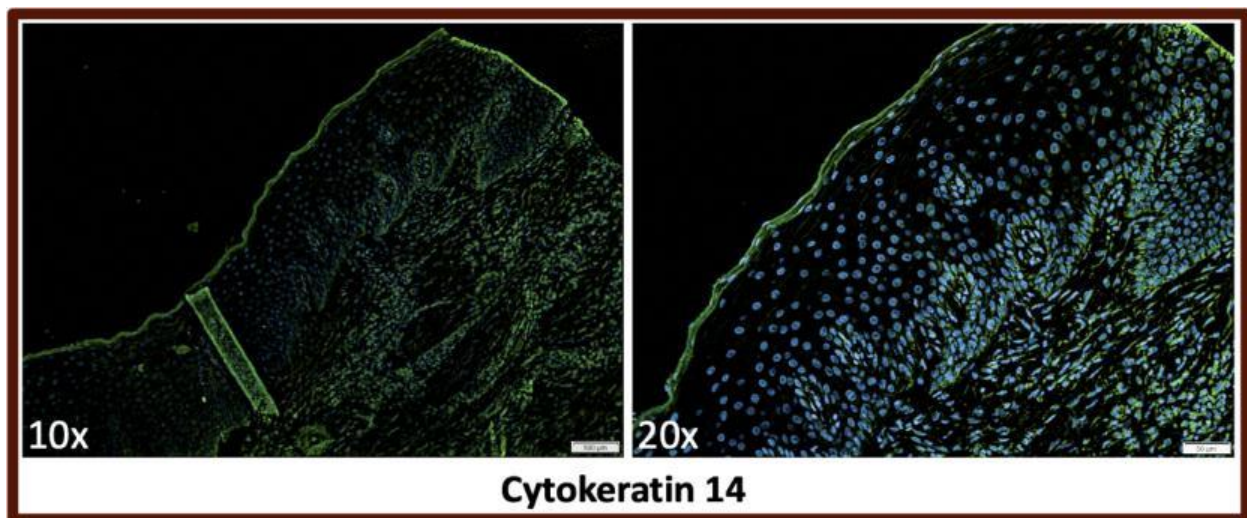
Back to Table 3.5 CK14 IF gingival sample features

3.5.12 M1H - P4C gingival sample IF CK14 description

IF staining of P4C gingival sample - M1H for CK14 was evaluated in 10x and 20x images depicted in Figure 3.64. The signal was expressed most strongly in the stratum corneum, and basale. This signal appeared interrupted within the strata.

Figure 3.64 M1H - P4C gingival sample IF CK14. Representative gingival samples are depicted at 10, and 20x magnification.

Cytokeratin 14
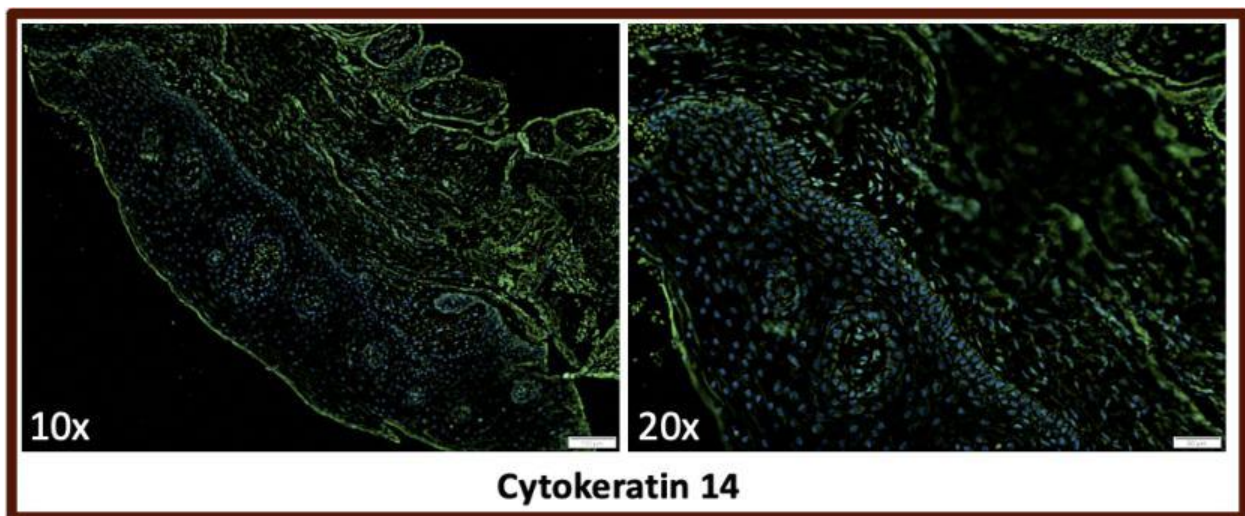
Back to Table 3.5 CK14 IF gingival sample features

3.5.13 H-19 - P4C gingival sample IF CK14 description

IF staining of P4C gingival sample - H-19 for CK14 was evaluated in 10x and 20x images depicted in Figure 3.65. The signal was expressed most strongly in the stratum basale. This signal appeared uniform within the strata.

Figure 3.65 H-19 - P4C gingival sample IF CK14. Representative gingival samples are depicted at 10, and 20x magnification.
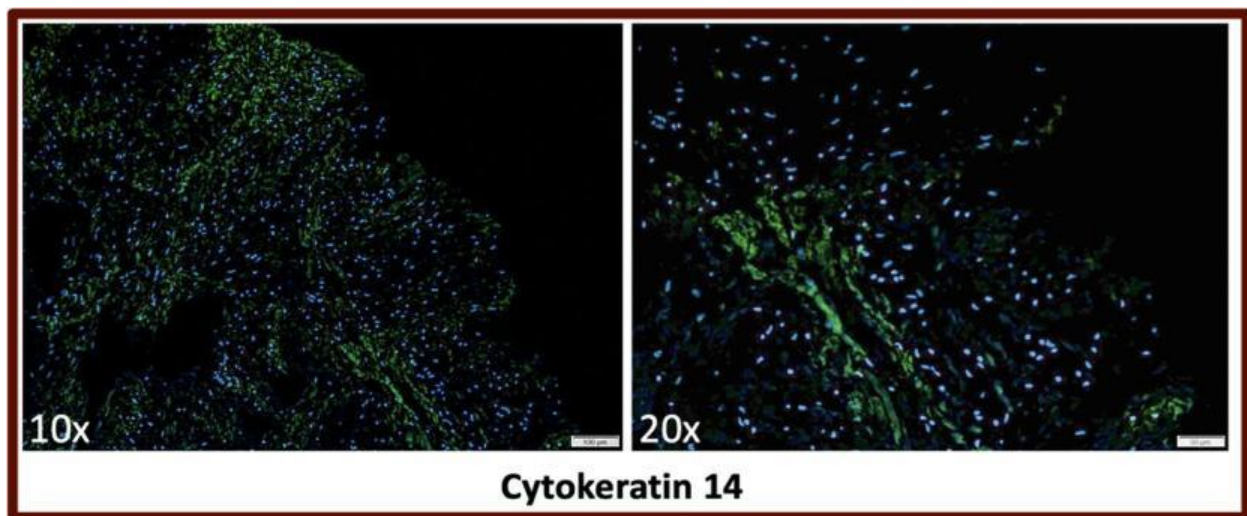
Back to Table 3.5 CK14 IF gingival sample features

3.5.14 H-27 - P4C gingival sample IF CK14 description

IF staining of P4C gingival sample - H-27 for CK14 was evaluated in 10x and 20x images depicted in Figure 3.66. The signal was expressed throughout the entire epithelium (i.e., all stratum). This signal appeared uniform within the strata.

Figure 3.66 H-27 - P4C gingival sample IF CK14. Representative gingival samples are depicted at 10, and 20x magnification.

Cytokeratin 14
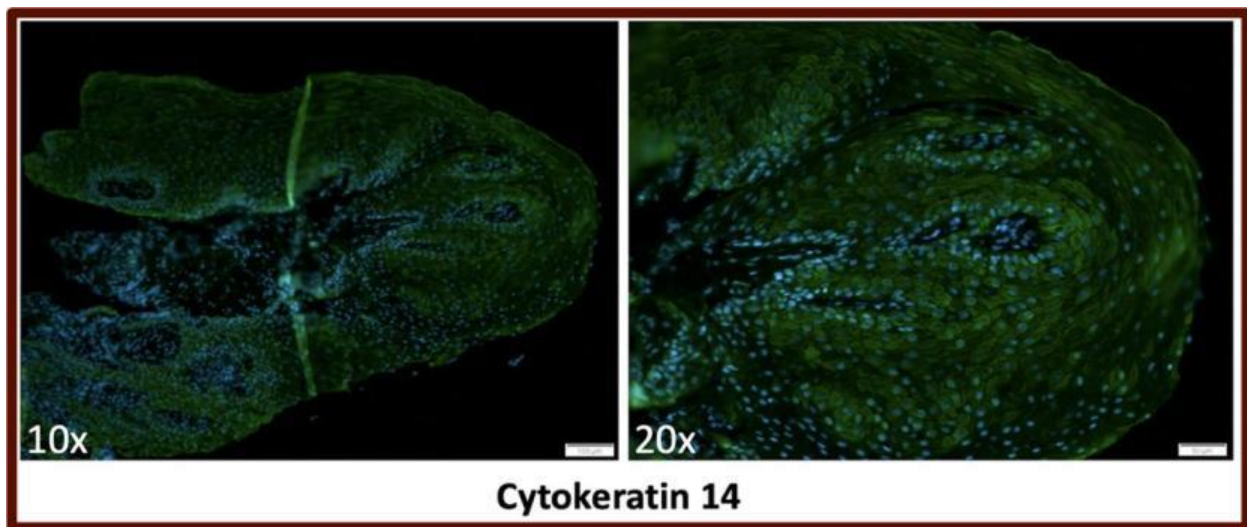
Back to Table 3.5 CK14 IF gingival sample features

3.5.15 H-48 - P4C gingival sample IF CK14 description

IF staining of P4C gingival sample - H-48 for CK14 was evaluated in 10x and 20x images depicted in Figure 3.67. The signal was expressed most strongly in the stratum basale. This signal appeared uniform within the strata.

Figure 3.67 H-48 - P4C gingival sample IF CK14. Representative gingival samples are depicted at 10, and 20x magnification.

10x   20x

Cytokeratin 14
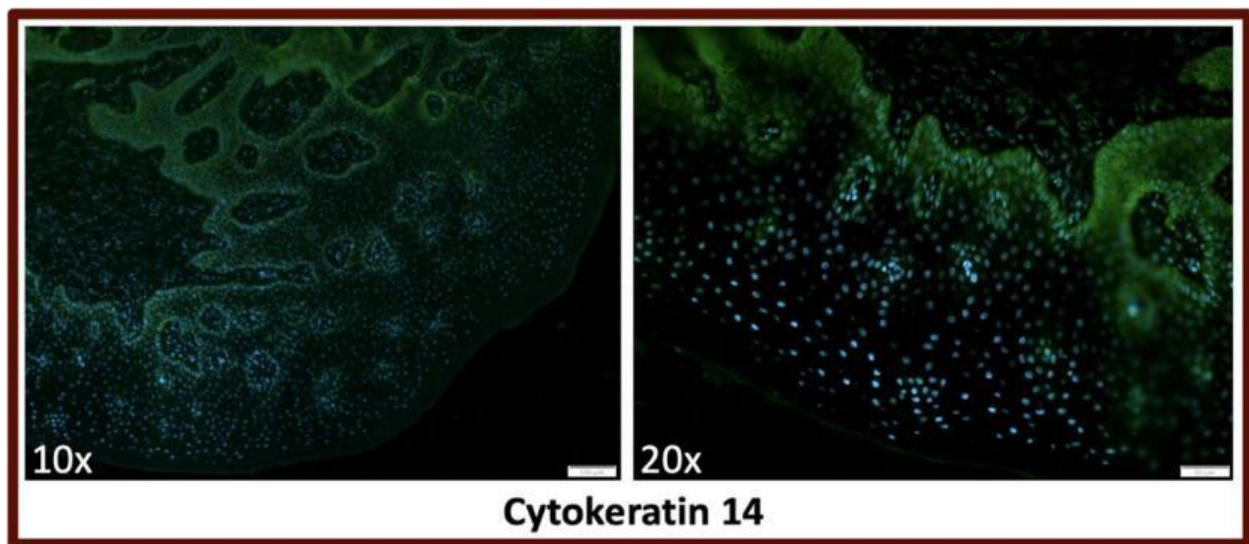
Back to Table 3.5 CK14 IF gingival sample features

3.6 Overview of All Histological Stains

A side-by-side compilation of H&E and IF images for each sample is presented in the figures below.

Figure 3.68 H-23 - Healthy gingival sample combined histological stains.
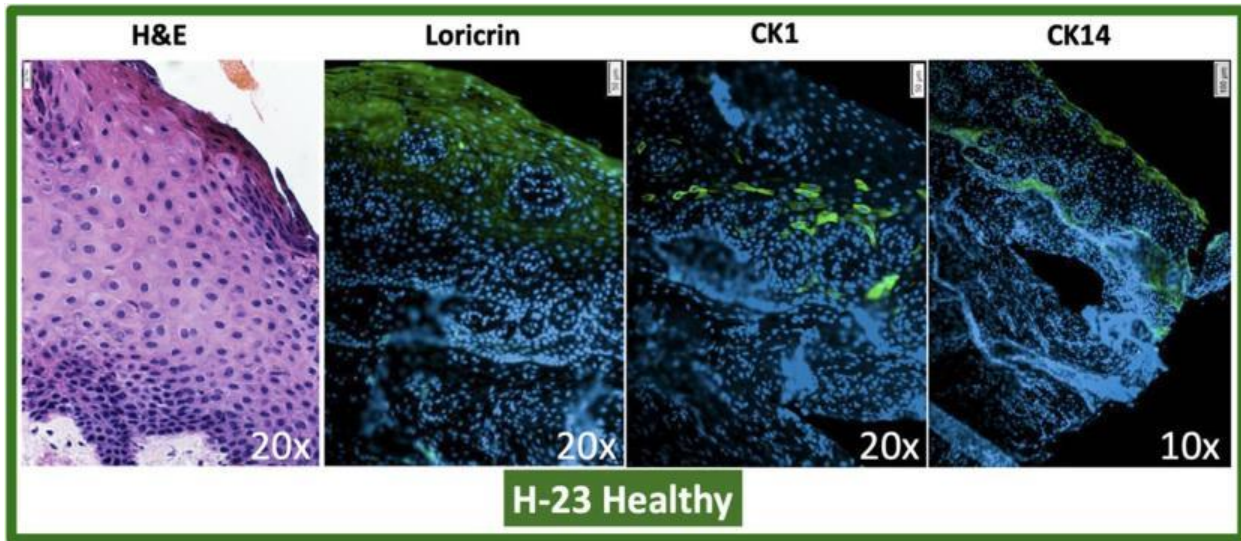
Figure 3.69 H-26 - Healthy gingival sample combined histological stains.
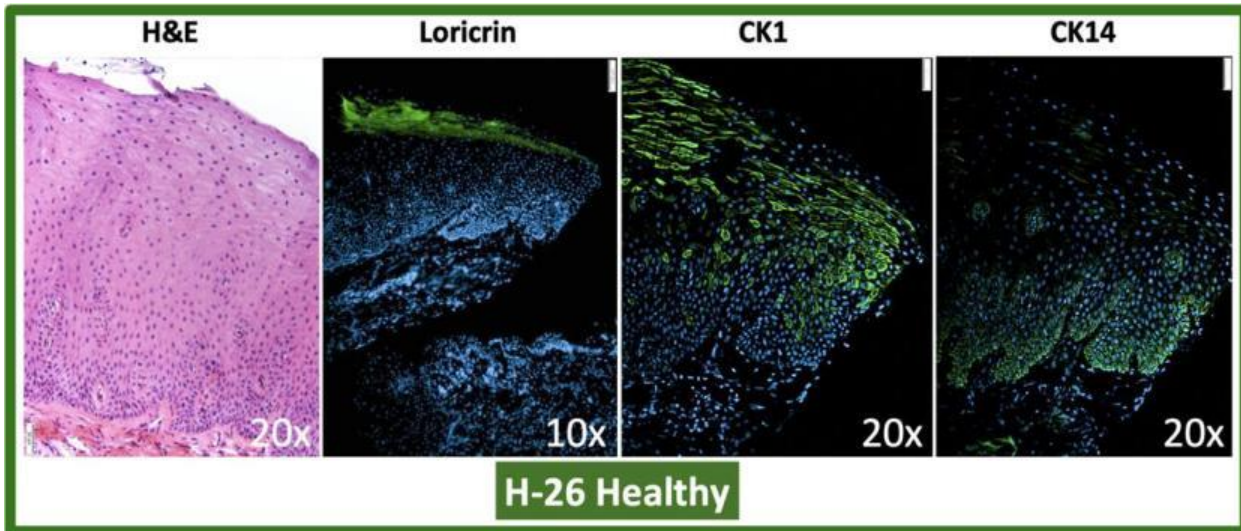
Figure 3.70 H-34 - Healthy gingival sample combined histological stains.
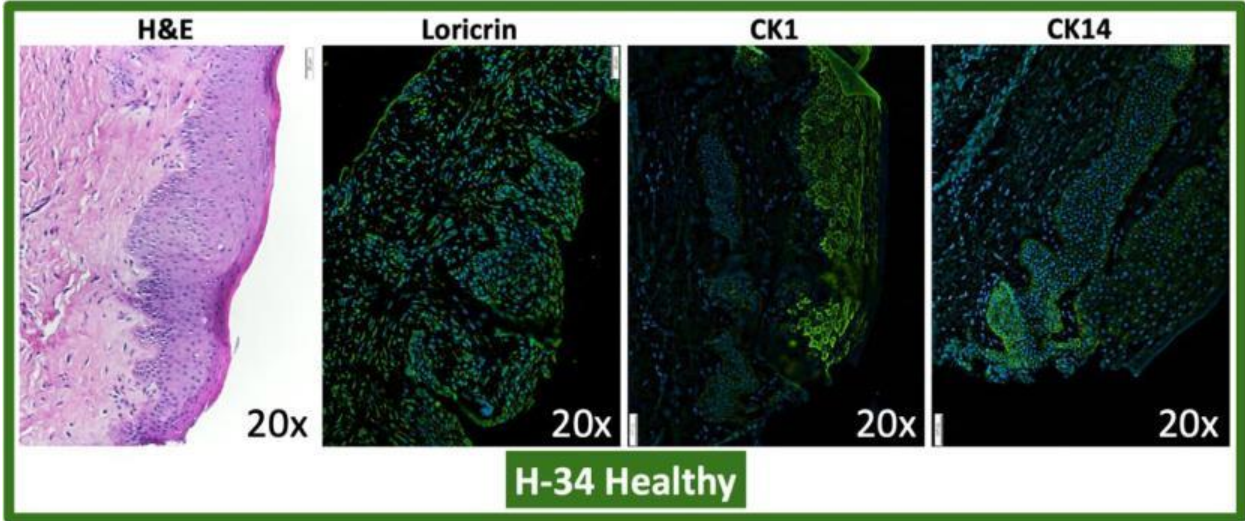
Figure 3.71 H-39 - Healthy gingival sample combined histological stains.
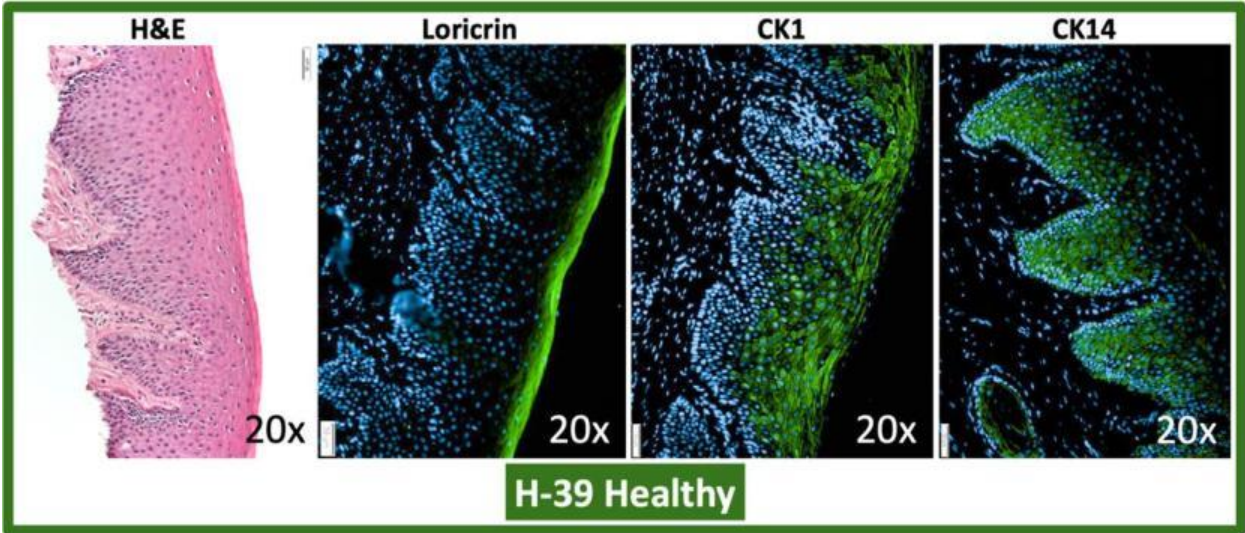
Figure 3.72 H-42 - Healthy gingival sample combined histological stains.
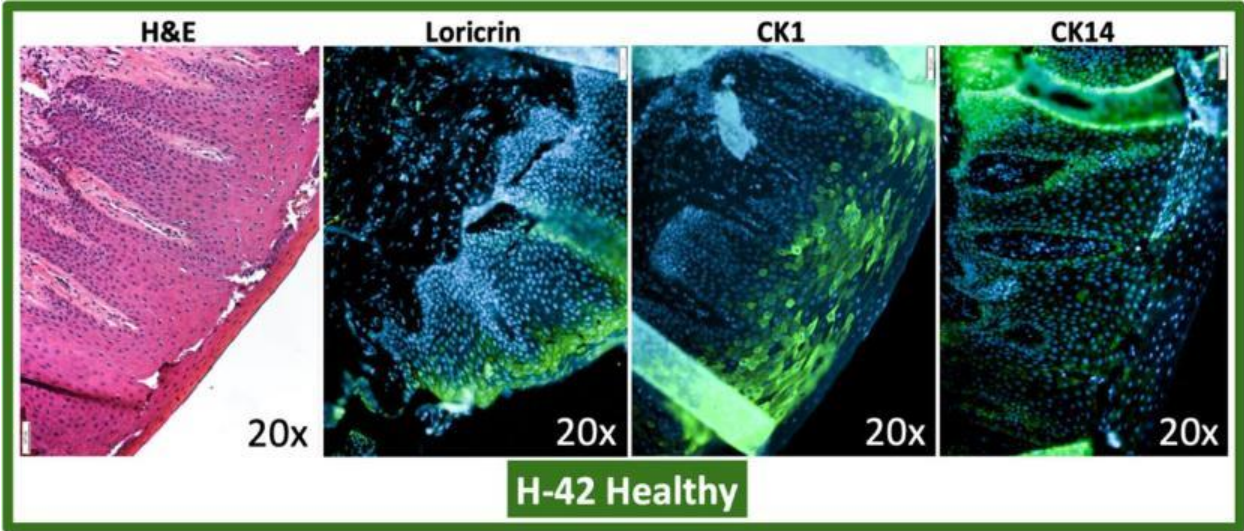
Figure 3.73 R4H - P3C gingival sample combined histological stains.
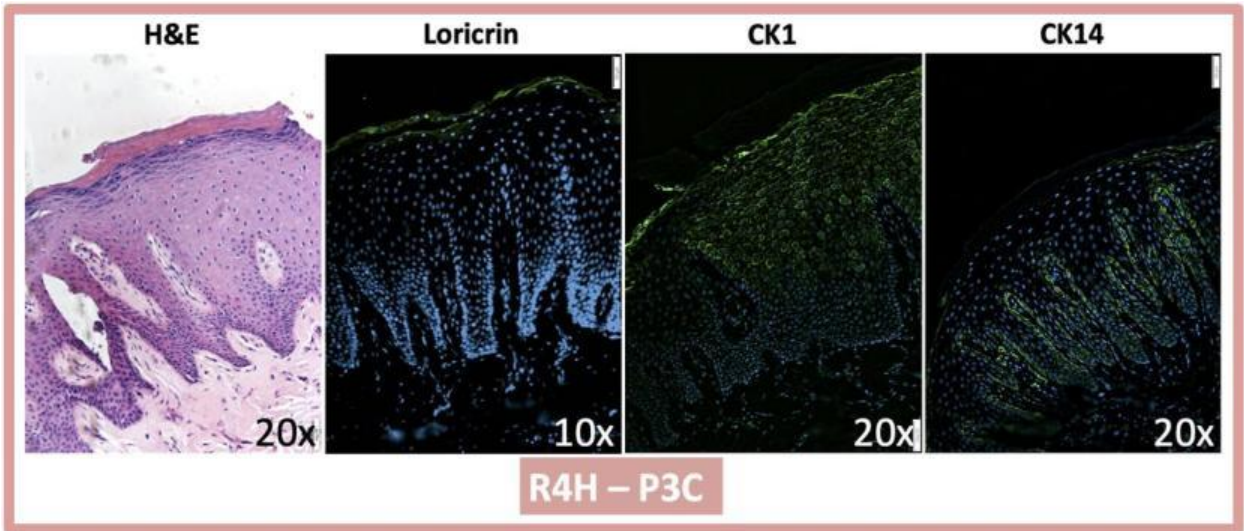
Figure 3.74 H-6 - P3C gingival sample combined histological stains.
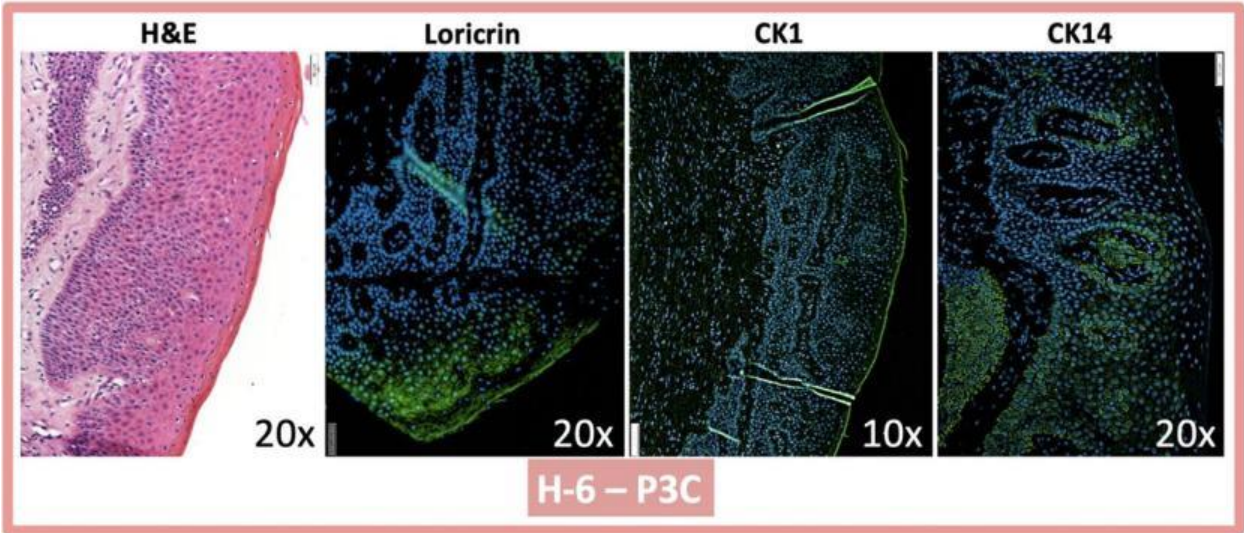
Figure 3.75 H-12 - P3C gingival sample combined histological stains.
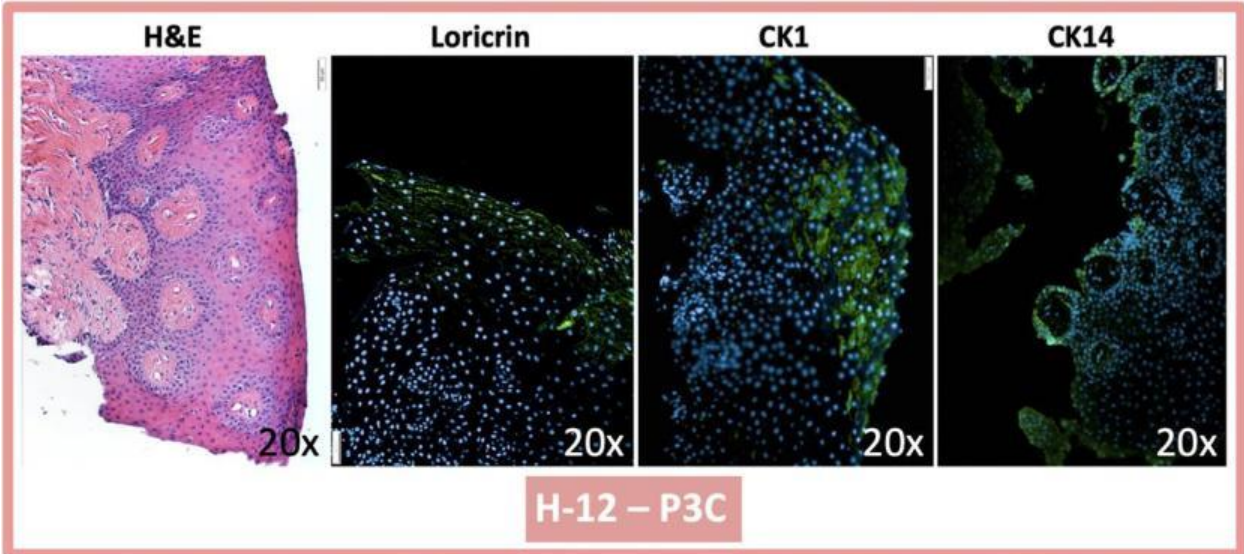
Figure 3.76 H-14 - P3C gingival sample combined histological stains.
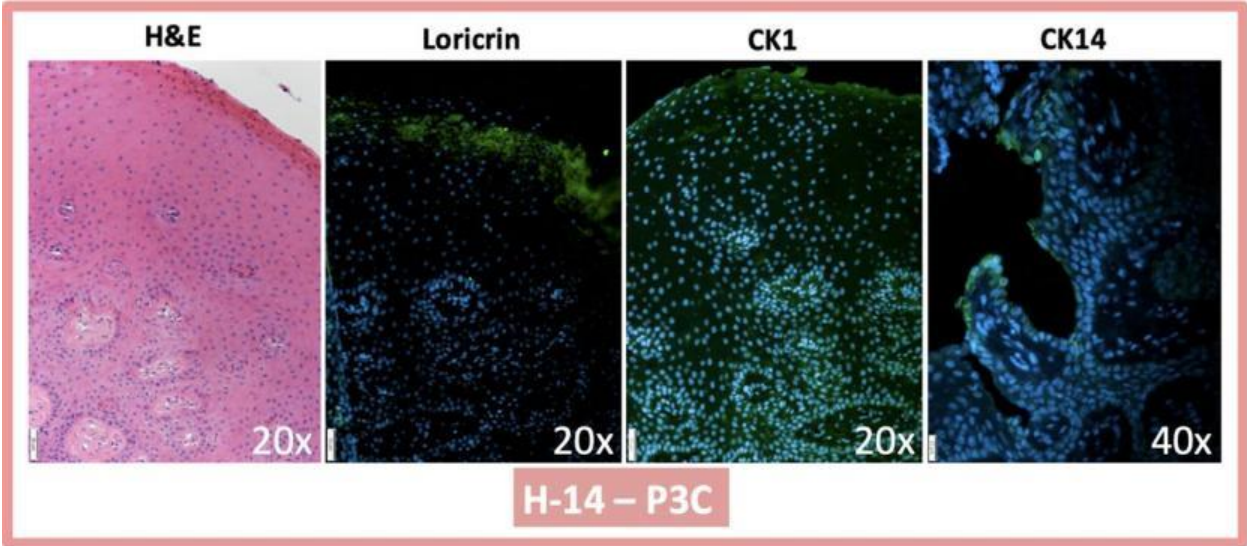
Figure 3.77 H-44 - P3C gingival sample combined histological stains.
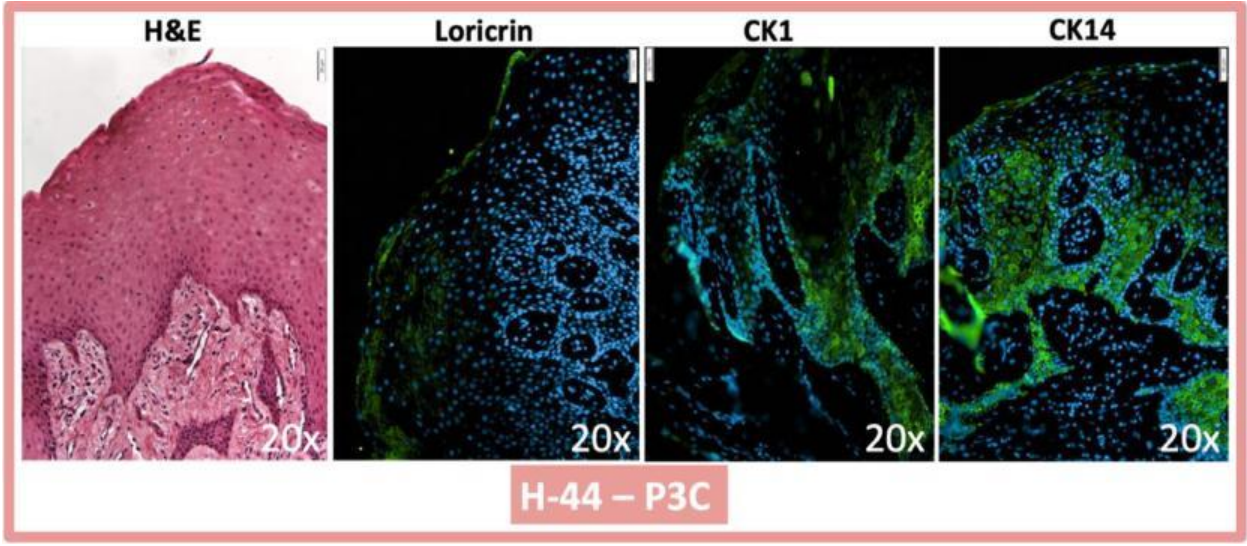
Figure 3.78 R1H - P4C gingival sample combined histological stains.
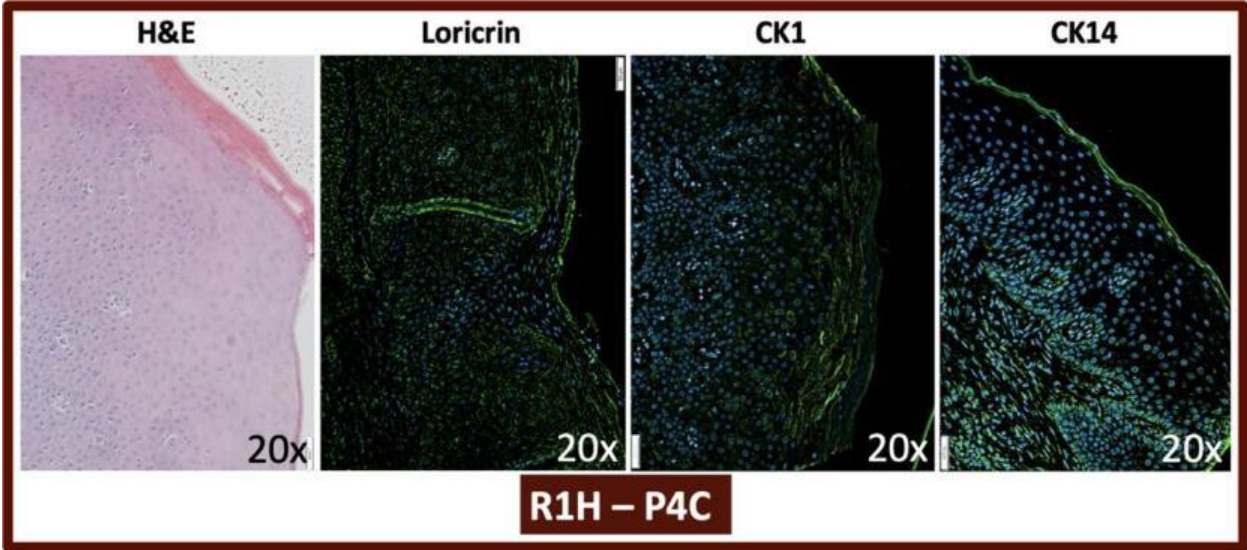
Figure 3.79 M1H - P4C gingival sample combined histological stains.
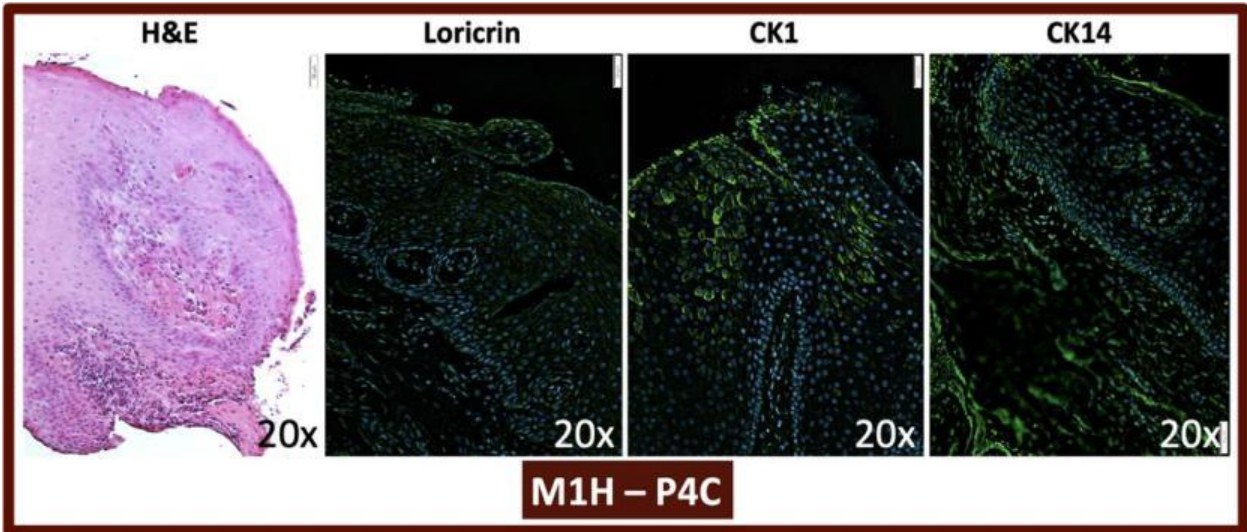
Figure 3.80 H-19 - P4C gingival sample combined histological stains.
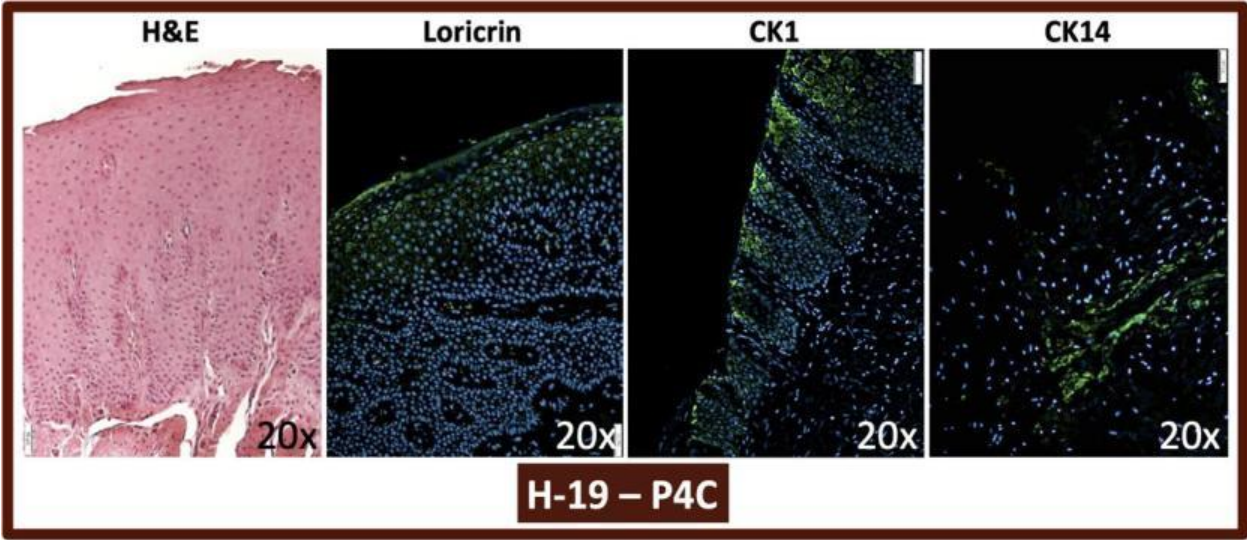
Figure 3.81 H-27 - P4C gingival sample combined histological stains.
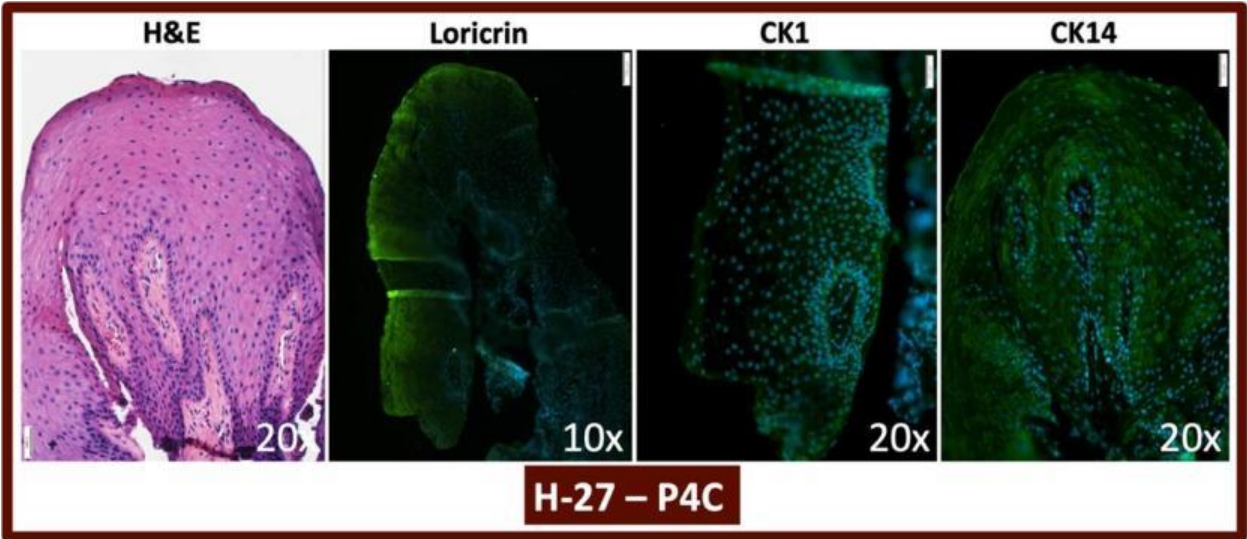
Figure 3.82 H-48 - P4C gingival sample combined histological stains.
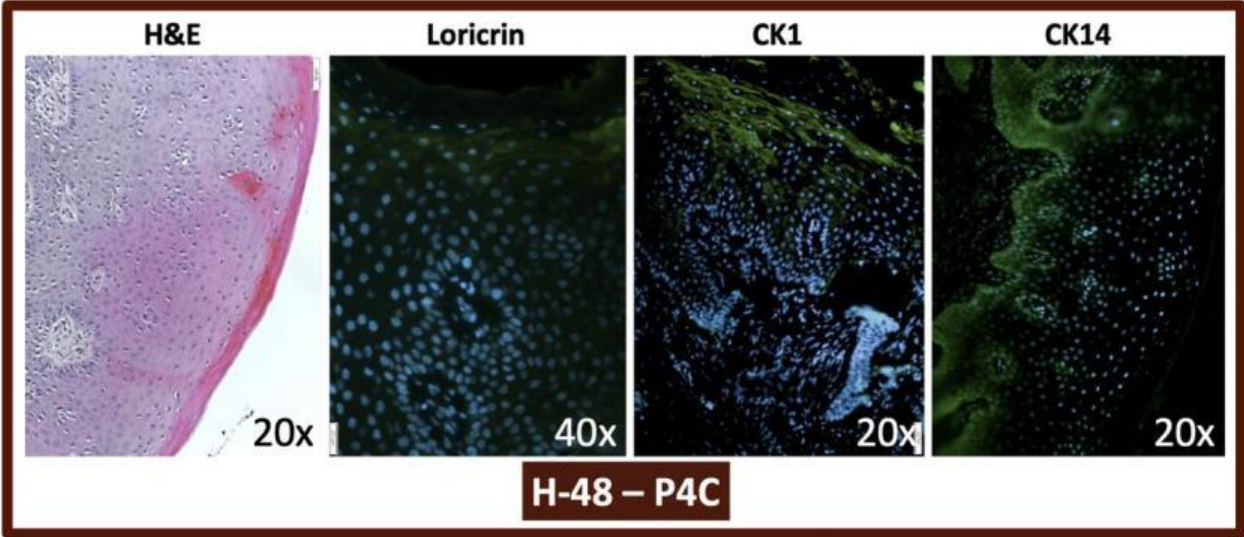
Chapter 4. Discussion

CHAPTER 4: Discussion

4.1 Rational

The results from a 2009 to 2012 National Health and Nutrition Examination Survey of the US Adult Population found that 46% of the participants had periodontitis, with 8.9% presenting with severe forms of the disease (Eke et al., 2012). Over the course of history, health care systems and access to care have improved significantly, extending life expectancies, and promoting an ageing demographic (Rowe et al, 2016). The prevalence, extent and severity of periodontitis has been shown to be associated with increasing age (Albandar et al., 1999, Nunn, 2003, Stanford & Rees, 2003). A recent study has calculated periodontal disease treatment economic costs to be approximately $200B in Europe and $150B in the US (Botelho et al., 2021). The combined ageing demographic and periodontitis severity will only further increase the economic burden on society. Further research on the pathogenesis and underlying mechanisms to prevent periodontal disease is warranted.

The gingival epithelium represents the first line of defense for the periodontium against harmful chemical, physical, and/or microbiological insults (Groeger & Meyle, 2019). The oral cavity consists of approximately 700 microbial communities (Aas et al, 2005). In gingival health, a symbiotic relationship is established between the host immune system and the oral microbiome. Periodontal disease is initiated after microbes establish a biofilm along the tooth surface. As a result of the microbial challenge, keratinocytes release cytokines that ultimately chemotactically attract neutrophils from the blood stream to the epithelium (Kornman et al 1998). This represents early gingivitis lesions. If the dental plaque biofilm persists, then an established periodontal lesion will develop. An established lesion presents histologically with an increase in lymphocytes, connective tissue loss, and fibroblast alteration (Page and Schroeder,

1976). The high turnover rate of the gingival epithelium will replace the damaged keratinocytes and barrier by the host-microbial challenge within one to two-weeks (Dabija-Wolter, 2013) This is a reversible condition that can return to gingival health once the etiology has been removed via improved oral hygiene or professional debridement. If not removed, the disease will progress to periodontitis and include irreversible alveolar bone destruction.

In addition to the complex host-microbial interactions, periodontitis is suspected to develop because of a barrier defect. A recent study described this defect analogous to the gastrointestinal barrier dysfunctions underlying inflammatory bowel disease (Takahashi et al, 2019). The gastrointestinal barrier junctional proteins are weakened after stimulation by proinflammatory mediators causing a "leaky gut" condition permitting further microbial invasion, destruction, and further inflammation (Bruewer et al 2006). Interactions between the epithelium and microorganism influence the integrity of this barrier. Periodontopathic microorganisms associated with periodontitis have been observed to cause either directly or indirectly the disruption of key epithelial junctional proteins (Takahashi et al, 2019). An animal study (Fujita et al, 2012) demonstrated the down regulation of claudin-1 after exposure to lipopolysaccharide virulence factor. This exposure led to an epithelial barrier defect from the decreased tight junction formation. The host development of a barrier defect may predispose this individual to periodontitis necessitating further investigation.

The objective of this study was to broaden the understanding of the role of the epithelial barrier, with specific focus on the protein loricrin, in relation to the pathogenesis of severe periodontitis. Loricrin is an integral structural protein that makes up 70% of the cornified envelope, an essential element of the epithelial barrier. Dermatological research on epithelial related disorders has demonstrated correlations between both a mutant loricrin phenotype and

downregulation of loricrin in epithelial related disorders (Catunda et al., 2019). Cytokeratins are key intermediate epithelial proteins with site specific expression (Rao et al, 2014). As important keratinocyte scaffold proteins, cytokeratins have a role in ensuring physical integrity against mechanical stress and permit resilience of the epithelium (Bragulla and Homberger, 2009). Altered expression of cytokeratins is associated with an array of epithelial integrity disorders. For example, genetic mutations of CK5 and CK14 are known to cause the severe skin disorder, Epidermolysis Bullosa Simplex (Schuilenga-Hut et a, 2003). As such, cytokeratins may serve as important diagnostic markers in other epithelial barrier defect disorders.

This study explored possible underlying links between periodontal disease and epithelial barrier defects due to altered loricrin, CK1, or CK14 phenotypic expression.

4.2 Patient Selection

University of Alberta Periodontology Patients that were undergoing various periodontal surgeries were asked to participate in this research. These patients were diagnosed with having gingival health, P3C or P4C periodontitis. Residents of the program completed a clinical and radiological assessment to determine the diagnosis using the 2017 American Academy of Periodontology Classification. The colour, contour, and consistency of the gingiva, bleeding on probing, and attachment loss (i.e., clinical recession or radiographic bone loss) distinguished gingival health from active periodontitis.

Gingival health presents with coral pink, firm, and scalloped gingiva. Further, healthy patients have an absence of interdental recession, minimal bleeding upon probing and no radiographic bone loss (Chapple et al., 2018). These patients may be present at a periodontal clinic as part of their restorative phase of treatment planning (e.g., crown lengthening procedure, orthodontic tooth exposure).

P3C and P4C periodontitis are severe forms of periodontitis. These two variants of severe periodontitis are differentiated on the basis of their clinical complexity. Both P3C and P4C present with erythematous and/or cyanotic, swollen, and rolled gingiva. There is the presence of severe interdental clinical attachment loss of ≥ 5 mm, bleeding on probing, and radiographic bone loss extending to the middle third of the root and beyond (Papapanou et al., 2018). The distinction between P3C and P4C is the increased prosthodontic rehabilitation complexity due to the number of teeth lost due to periodontitis. P3C patients are identified as having severe periodontitis with ≤ 4 lost teeth due to periodontitis. P4C patients have had ≥ 5 teeth lost due to periodontitis (Papapanou et al., 2018). As such, their prosthodontic rehabilitation complexity is increased due to greater number of teeth requiring replacement.

A total of 5 Healthy, 5 P3C, and 5 P4C gingival discard tissue samples were collected from patients. The samples were derived from 7 female and 8 male patients. The average age of the participants was 61 years. Systemically, the majority were healthy with no contraindications to treatment. Two patients were light smokers (i.e., <20 cigarettes per day, as per Johnson & Hill, 2004) and two had Types II Diabetes Mellitus.

Samples were collected as the patients were undergoing various periodontal procedures at the University of Alberta Graduate Periodontal clinic. Crown lengthening was the most common procedure where samples were collected (n=7), followed by dental extractions (n=4). The least common procedures were osseous resective surgery (n=2), open flap debridement (n=1), and orthodontic tooth exposure (n=1). Collected tissues were immediately fixed and then processed, sectioned, and analyzed histologically.

4.3 Histological Results

4.3.1 Inflammation confirmation with H&E staining

H&E staining provided a comprehensive overview of each gingival sample collected. The orientation of the gingival epithelium relative to the basement membrane and underlying connective tissue was garnered with this stain. Of most importance, the presence and absence of inflammatory signs were determined and compared amongst Healthy, P3C, and P4C gingiva.

Overall, the Healthy gingival samples had fewer inflammatory signs relative to P3C and P4C gingival samples. As determined by counting, Healthy gingiva displayed the fewest number of inflammatory cells, whereas the P4C samples collected in this study had the most. Also, there was a greater presence of RBCs within the connective tissue of the P3C and P4C samples relative to the Healthy samples, where none could be detected. All these known signs of inflammation correlated with the clinical and radiological findings from these patients.

Lastly, the lengths of rete pegs were observed and measured. Of note, there were three rete peg length measurements that could not be discerned due to the tangential orientation of the tissue samples. These samples included, P3C sample ID H-14, and P4C sample ID R1H and sample ID H-48. With regards to the Healthy samples, the average rete peg length was 147.54 μm; the maximum length was observed in sample ID H-42 ($\bar{x} = 302.2$ μm) and the minimum length was present in sample ID H-34 ($\bar{x} = 67.9$ μm). The P3C gingival samples presented with an average rete peg length of 196.65 μm; the maximum length observed was in sample ID R4H ($\bar{x} = 270.6$ μm) and the minimum length was in sample ID H-12 ($\bar{x} = 103.5$ μm). Lastly, P4C gingival samples presented with an average rete peg length of 275.47 μm; the maximum length observed was found in sample ID M1H ($\bar{x} = 309.2$ μm) and the minimum length was in sample ID H-27 ($\bar{x} = 254.4$ μm). Except for Healthy sample ID H-42, the rete peg length trend tended to

be longer in P4C and P3C samples relative to Healthy samples. The extension of rete pegs is a known histological sign of periodontal disease (Murakami et al, 2018). This change in rete peg dimension coincides with an increase in vasculitis, collagen fiber network destruction, and inflammatory cell infiltration (Murakami et al, 2018). This rete peg pattern may be in response to the host microbial challenge. An increased rete peg dimension increases the underlying connective tissue surface area contact with the epithelium. As a result, this could permit a rapid inflammatory response to the microbial challenging by reducing the epithelial distance for immune cells to target periodontopathogens.

The changes observed in the study confirmed the clinical findings of attachment loss and radiographic bone loss with inflammatory patterns within the epithelium. An increase in RBCs and perivascular correlated with an increase in inflammatory cells were found within the P3C and P4C gingival samples. In periodontal disease, the microbial challenge in the sulcus is confronted by the immune cells. Persistent presence of periodontopathic bacteria is known to trigger the immune cells to release cytokine signaling molecules such as Receptor activator of nuclear factor- κB ligand (RANKL) (Chen et al, 2014). RANKL is a signalling molecule for RANK to activate osteoclastogenesis leading to osteoclast bone destruction activity (Chen et al, 2014). In homeostasis, the third key molecules that regulate this process is osteoprotegerin (OPG) (Suda et al, 1999). OPG inhibits the overactivation of RANK by RANKL by binding to RANKL to limit osteoclast activation (Suda et al, 1999). In periodontal disease, B and T Lymphocyte inflammatory cells increase the release of RANKL, which offsets the RANKL to OPG ratio resulting in greater bone destruction (Chen et al, 2014). Relative to the healthy gingival samples, the P3C and P4C samples demonstrated an increase in inflammatory cell

presence. This supports the mechanisms of periodontitis pathogenesis where immune cell cytokine production leads to periodontal bone loss observed in the P3C and P4C patients.

4.3.2 Loricrin presentation amongst Healthy, P3C, and P4C gingival samples

Immunofluorescence staining for loricrin was completed to assess the distribution and expression in a semi-quantitative fashion for each sample. In general, loricrin was expressed at the stratum granulosum and corneum for all samples. Relative to the uniform presentation within Healthy gingiva, loricrin immunofluorescence staining presented with an interrupted, thinner pattern in both P3C and P4C gingival samples.

A semi-quantitative analysis was completed by measuring the average width of the loricrin expressing layer for each sample. Healthy gingival samples tended to have a thicker layer of expression and P4C gingival samples had the thinnest presentation. With regards to the Healthy samples, the average loricrin width was 60.1 μm; the maximum width was observed in sample ID H-23 ($\bar{x}$ = 102.2 μm) and the minimum width was present in sample ID H-39 ($\bar{x}$ = 26.1 μm). P3C gingival samples presented with an average loricrin expression width of 25.28 μm; the maximum width observed was in sample ID H-14 ($\bar{x}$ = 36.0 μm) and the minimum width was in sample ID H-44 ($\bar{x}$ = 10.4 μm). Lastly, P4C gingival samples presented with an average loricrin layer width of 7.76 μm; the maximum loricrin width observed was found in sample ID H-27 ($\bar{x}$ = 9.4 μm) and the minimum width was in sample ID R1H ($\bar{x}$ = 4.8 μm). This may be suggestive of a change in barrier integrity.

A more uniform and wider loricrin was observed in healthy gingiva relative to P3C and P4C gingival samples. A thinner and less organized barrier may provide a barrier breach for pathogens to invade the epithelium. The pathogenesis of loricrin downregulation in atopic dermatitis (Catunda et al, 2019) may provide an explanation for this finding observed in the P3C

and P4C gingival samples. In atopic dermatitis, loricrin is downregulated as a result of sharing a common transcription co-activator with IL-4 (Bao et al, 2017). In response to inflammation, this cytokine upregulation will outcompete the transcription of loricrin. The host microbial challenge will trigger an immune response leading to increased production of IL-4 that may result in a down regulation of loricrin. As a potential result, a narrower or disorganized cornified envelope favouring periodontopathic invasion causing further periodontal destructive sequalae.

4.3.3 CK1 presentation between Healthy, P3C, and P4C gingival samples

CK1 expression patterns were evaluated through immunofluorescence staining procedures. As anticipated, the distribution of this cytokeratin was, for the most part, observed in the strata spinosum and granulosum. In all three patient groups, there were samples that demonstrated expression in the stratum corneum as well. A general trend was observed of a more uniform pattern in Healthy relative to a more interrupted immunofluorescent pattern for both P3C and P4C gingival samples. This may suggest some disruption in the normal differentiation pattern of the epithelium.

A less organized CK1 amongst the strata spinosum and granulosum may provide an additional path of least resistance for microbial invasion. CK1 is a prominent intermediate filament that has a major role in maintaining epithelial mechanical integrity. This disorganized CK1 intermediate structures observed P3C and P4C gingival samples could provide an additional mechanism to allow a deeper invasion of periodontal pathogens between the keratinocytes. As a potential result, the microbial host challenge persists deeper within the epithelium providing greater access to engage in destructive processes of the periodontium.

4.3.4 CK14 presentation between Healthy, P3C, and P4C gingival samples

CK14 expression patterns were also examined through immunofluorescence staining procedures. In general, the fluorescent signal was confined to the stratum basale for all three patient groups. However, there were some gingival samples in all three groups where CK 14 expression appeared in the stratum corneum as well. Further, there was one P4C gingival sample where the distribution of CK14 was expressed in all strata (H-27). The general trend for all gingival tissue samples was a uniform signal pattern. No discernible differences were observed amongst all three patient sample types for CK14 immunofluorescence.

4.4 Limitations and Future Research Directions

This research coincided with the worldwide COVID-19 pandemic. As a result, clinical activities and laboratory experiment opportunities were reduced due to the campus closures. This limited the scope of the research and analysis of these gingival samples.

Gingival samples were collected from patients that were, for the most part, systemically healthy. However, there were two patients that were smokers and two with type II diabetes mellitus. Both of these conditions are known risk factors for periodontal disease that affect disease progression (Tonetti et al., 2018). Specific to the epithelial barrier, both smoking and diabetes have links with epithelial related disorders (Naldi, 2016 and Duff et al., 2015). Harmful effects of cigarette toxins and hyperglycemia lead to increases in oxidative stress, pro-inflammatory cytokine expression, and vascular changes. As such, results obtained from the samples cannot negate possible confounding influences of these risk factors on the inflammatory status and epithelial integrity observed.

Immunohistochemistry is an important tool in providing information on the relative distribution and expression of an antigen being explored. The downside is the variability that

exists due to differences in tissue preservation and processing, and other factors not easy to always define. Reproducibility, specificity, and sensitivity of this protocol are all potential issues (Toki et al., 2017). Results may be subjective and can be open to interpretation. The average width of loricrin was evaluated on the basis of three separate measurement points for each tissue, using ImageJ. This is a semi-quantitative analysis for this protein. Interpretation of these results should be done with caution, as variability can be observed amongst each evaluator.

Results from this study provide a general analysis of barrier associated proteins, which may be linked to epidermal integrity, in Healthy, P3C, and P4C human gingival samples. Immunofluorescence analyses were used to evaluate epidermal expression in these gingival samples, with an emphasis on the integral structural proteins, loricrin, CK1, and CK14. Further analysis should strive to reproduce these findings, while also adding quantitative approaches to determine exact content. An attempt to quantify loricrin was completed earlier in this study through an enzyme-linked immunosorbent assay (ELISA) kit designed for human loricrin. Results were determined to be inconsistent and not reproducible. As such, the ELISA for loricrin quantification was not explored further during this study. Immunofluorescent analysis automation has been explored in recent studies. A study by Tozzoli et al. (2012) compared various automation software in completing histopathological analyses of human samples for rheumatoid arthritis. This automation process may provide an improved detection mechanism to reduce false negatives and false positives by standardizing the fluorescence intensity, improving intra- and inter-examiner reliability, and by improving assay pattern analyses. Additional literature support is needed to validate each software automation technique, however, the results presented in this study appear promising in the quantification of protein biomarkers.

Lastly and relative to animal studies, human histological studies are limited by virtue of how the samples are collected from each subject. Gingival sample discards were collected during various surgical procedures at different types of teeth (i.e., anterior versus posterior tooth) and surface (buccal versus lingual sites) along each tooth. A tooth and surface that is more accessible for efficient oral hygiene procedures will tend to present with less plaque. Although the patient may have an overall diagnosis of periodontal disease, the sample may present with less signs and symptoms and inflammation by virtue of the position and site. Animal studies permit consistent sampling quantity and location to allow for a more robust analysis comparison. In contrast, samples collected from human patients were limited as to what could be provided following the periodontal procedure being completed.

Chapter 5. Conclusion

CHAPTER 5: Conclusion

The aim of this study was to qualify the expression of loricrin, cytokeratin 1, and cytokeratin 14 in human gingival samples from patients diagnosed with P3C and P4C and compare this with tissue from healthy patients. The hypothesis was that if histological and immunohistological differences existed in the epithelium of healthy versus severe periodontal disease patients, then this may suggest a pathogen-mediated epithelial barrier breach due to loss of loricrin. In general, and relative to P3C and P4C gingival samples, loricrin presented with a more uniform expression pattern within the stratum granulosum and corneum of Healthy patients. Cytokeratin protein immunofluorescence analyses were completed to evaluate differences in differentiation, that may result from a barrier defect. CK1 expression appeared in a more uniform pattern in Healthy samples relative to an interrupted pattern in both P3C and P4C gingival samples. In contrast, no distinctions could be found amongst the three gingival sample types for CK14.

Despite the limitations of this study, this research explored the possible role of loricrin in relation to severe periodontitis pathogenesis. A reduced phenotypic expression of this integral epithelial barrier protein has been correlated to epidemiological related disorders. The primary risk factor in periodontal disease is known to be plaque in a susceptible host. Future studies should continue to explore this susceptibility to evaluate the potential for a barrier breach to contribute to the pathogenesis of this disease.

References

References

Aas, J. A., Paster, B. J., Stokes, L. N., Olsen, I., & Dewhirst, F. E. (2005). Defining the normal bacterial flora of the oral cavity. *Journal of clinical microbiology*, 43(11), 5721–5732. https://doi.org/10.1128/JCM.43.11.5721-5732.2005

Albandar, J. M., Brunelle, J. A., & Kingman, A. (1999). Destructive periodontal disease in adults 30 years of age and older in the United States, 1988-1994. *Journal of Periodontology*, *70*(1), 13–29. https://doi.org/10.1902/jop.1999.70.1.13

Bao L, Mohan GC, Alexander JB, Doo C, Shen K, Bao J, Chan LS. A molecular mechanism for IL-4 suppression of loricrin transcription in epidermal keratinocytes: implication for atopic dermatitis pathogenesis. Innate Immun. 2017 Nov;23(8):641-647. http://doi.org/10.1177/1753425917732823

Barros, S. P., Williams, R., Offenbacher, S., & Morelli, T. (2016). Gingival crevicular fluid as a source of biomarkers for periodontitis. Periodontology 2000, 70(1), 53–64. https://doi.org/10.1111/prd.12107

Berlin-Broner, Y. (2018). *Apical periodontitis as a contributive risk factor for atherosclerosis*. [Master dissertation, University of Alberta]. Education & Research Archives. https://doi.org/10.7939/R38G8G02Z

Botelho, J., Machado, V., Leira, Y., Proença, L., Chambrone, L., & Mendes, J. J. (2021). Economic burden of periodontitis in the United States and Europe: An updated estimation. *Journal of Periodontology*, *93*(3), 373–379. https://doi.org/10.1002/jper.21-0111

Bragulla, H. H., & Homberger, D. G. (2009). Structure and functions of keratin proteins in simple, stratified, keratinized and cornified epithelia. *Journal of anatomy*, 214(4), 516–559. https://doi.org/10.1111/j.1469-7580.2009.01066.x

Bruewer, M., Samarin, S., & Nusrat, A. (2006). Inflammatory bowel disease and the apical junctional complex. *Annals of the New York Academy of Sciences*, 1072, 242–252. https://doi.org/10.1196/annals.1326.017

Candi, E., Schmidt, R., & Melino, G. (2005). The cornified envelope: A model of cell death in the skin. *Nature Reviews Molecular Cell Biology*, *6*(4), 328–340. https://doi.org/10.1038/nrm1619

Caton, J. G., Armitage, G., Berglundh, T., Chapple, I., Jepsen, S., Kornman, K. S., Mealey, B. L., Papapanou, P. N., Sanz, M., & Tonetti, M. S. (2018). A new classification scheme for periodontal and peri-implant diseases and conditions - Introduction and key changes from the 1999 classification. *Journal of clinical periodontology*, 45 Suppl 20, S1–S8. https://doi.org/10.1111/jcpe.12935

Catunda, R., Rekhi, U., Clark, D., Levin, L., & Febbraio, M. (2019). Loricrin downregulation and epithelial-related disorders: A systematic review. *JDDG: Journal Der Deutschen Dermatologischen Gesellschaft*, *17*(12), 1227–1238. https://doi.org/10.1111/ddg.14001

Cekici A, Kantarci A, Hasturk H, Van Dyke TE. Inflammatory and immune pathways in the pathogenesis of periodontal disease. Periodontol 2000. 2014;64(1):57-80. doi: https://doi.org/10.1111%2Fprd.12002

Chapple, I. L. C., Mealey, B. L., Van Dyke, T. E., Bartold, P. M., Dommisch, H., Eickholz, P., Geisinger, M. L., Genco, R. J., Glogauer, M., Goldstein, M., Griffin, T. J., Holmstrup, P., Johnson, G. K., Kapila, Y., Lang, N. P., Meyle, J., Murakami, S., Plemons, J., Romito, G. A., … Yoshie, H. (2018). Periodontal health and gingival diseases and conditions on an intact and a reduced periodontium: Consensus report of workgroup 1 of the 2017 World Workshop on the Classification of Periodontal and Peri-Implant Diseases and Conditions. *Journal of Clinical Periodontology*, *45*, S68–S77. https://doi.org/10.1111/jcpe.12940

Chen B, Wu W, Sun W, Zhang Q, Yan F, Xiao Y. RANKL expression in periodontal disease: where does RANKL come from? Biomed Res Int. 2014;2014:731039. http://doi.org/10.1155/2014/731039

Christodoulou, N., Weberling, A., Strathdee, D., Anderson, K. I., Timpson, P., & Zernicka-Goetz, M. (2019). Morphogenesis of extra-embryonic tissues directs the remodelling of the mouse embryo at implantation. *Nature Communications*, *10*(1). https://doi.org/10.1038/s41467-019-11482-5

Dabija-Wolter, G., Bakken, V., Cimpan, M. R., Johannessen, A. C., & Costea, D. E. (2013). In vitro reconstruction of human junctional and sulcular epithelium. *Journal of oral pathology & medicine : official publication of the International Association of Oral Pathologists and the American Academy of Oral Pathology*, 42(5), 396–404. https://doi.org/10.1111/jop.12005

Diabetes Canada Clinical Practice Guidelines Expert Committee, Punthakee, Z., Goldenberg, R., & Katz, P. (2018). Definition, Classification and Diagnosis of Diabetes, Prediabetes and Metabolic Syndrome. *Canadian journal of diabetes*, 42 Suppl 1, S10–S15. https://doi.org/10.1016/j.jcjd.2017.10.003

Duff, M., Demidova, O., Blackburn, S., & Shubrook, J. (2015). Cutaneous manifestations of diabetes mellitus. *Clinical Diabetes*, *33*(1), 40–48. https://doi.org/10.2337/diaclin.33.1.40

Eke, P. I., Dye, B. A., Wei, L., Thornton-Evans, G. O., & Genco, R. J. (2012). Prevalence of periodontitis in adults in the United States: 2009 and 2010. *Journal of Dental Research*, *91*(10), 914–920. https://doi.org/10.1177/0022034512457373

Furue M. Regulation of Filaggrin, Loricrin, and Involucrin by IL-4, IL-13, IL-17A, IL-22, AHR,

and NRF2: Pathogenic Implications in Atopic Dermatitis. Int J Mol Sci. 2020 Jul 29;21(15):5382. https://doi.org/10.3390/ijms21155382

Fujita, T., Firth, J. D., Kittaka, M., Ekuni, D., Kurihara, H., & Putnins, E. E. (2012). Loss of claudin-1 in lipopolysaccharide-treated periodontal epithelium. *Journal of periodontal research*, 47(2), 222–227. https://doi.org/10.1111/j.1600-0765.2011.01424.x

Ganavi, B. (2014). Oral cytokeratins in health and disease. *The Journal of Contemporary Dental Practice*, *15*(1), 127–136. https://doi.org/10.5005/jp-journals-10024-1502

Gautier, J.-C. (2017). *Drug safety evaluation: Methods and protocols* (pp. 110–112). Humana Press.

Groeger, S., & Meyle, J. (2019). Oral mucosal epithelial cells. *Frontiers in Immunology*, *10*. https://doi.org/10.3389/fimmu.2019.00208

Hausmann, E., Allen, K., & Clerehugh, V. (1991). *What alveolar crest level on a bite-wing radiograph represents bone loss?* Journal of periodontology, 62(9), 570–572. https://doi.org/10.1902/jop.1991.62.9.570

Hienz, S. A., Paliwal, S., & Ivanovski, S. (2015). Mechanisms of Bone Resorption in Periodontitis. *Journal of immunology research*, *2015*, 615486. https://doi.org/10.1155/2015/615486

Hohl D, Mehrel T, Lichti U, Turner ML, Roop DR, Steinert PM. Characterization of human loricrin. Structure and function of a new class of epidermal cell envelope proteins. J Biol Chem. 1991 Apr 5;266(10):6626-36.

Ishida-Yamamoto A, Takahashi H, Iizuka H. Loricrin and human skin diseases: molecular basis of loricrin keratodermas. Histol Histopathol. 1998 Jul;13(3):819-26. doi: 10.14670/HH-13.819.

Ishida-Yamamoto A. Loricrin keratoderma: a novel disease entity characterized by nuclear accumulation of mutant loricrin. J Dermatol Sci. 2003 Feb;31(1):3-8. https://doi.org/10.1016/s0923-1811(02)00143-3

Johnson, G. K., & Hill, M. (2004). Cigarette smoking and the periodontal patient. *Journal of Periodontology*, *75*(2), 196–209. https://doi.org/10.1902/jop.2004.75.2.196

Kornman, K. S., Page, R. C., & Tonetti, M. S. (1997). The host response to the microbial challenge in periodontitis: assembling the players. *Periodontology 2000*, *14*, 33–53. https://doi.org/10.1111/j.1600-0757.1997.tb00191.x

Lang, N. P., & Bartold, P. M. (2018). Periodontal health. *Journal of Periodontology*, *89*(S1), S9–S16. https://doi.org/10.1002/jper.16-0517

Lindhe, J., Karring, T., & Araujo, M. (2015). In J. Lindhe, & N. P. Lang (Eds.) Clinical Periodontology and Implant Dentistry (6th ed., pp. 5-14). Wiley Blackwell.

Lukas, D., & Schulte, W. (1990). Periotest-a dynamic procedure for the diagnosis of the human periodontium. *Clinical Physics and Physiological Measurement*, *11*(1), 65–75. https://doi.org/10.1088/0143-0815/11/1/006

Lundy, F. T., & Linden, G. J. (2004). Neuropeptides and neurogenic mechanisms in oral and periodontal inflammation. Critical reviews in oral biology and medicine: an official publication of the American Association of Oral Biologists, 15(2), 82–98. https://doi.org/10.1177/154411130401500203

Magin TM, Vijayaraj P, Leube RE. Structural and regulatory functions of keratins. Exp Cell Res. 2007 Jun 10;313(10):2021-32. https://doi.org/10.1016/j.yexcr.2007.03.005

Murakami, S., Mealey, B. L., Mariotti, A., & Chapple, I. (2018). Dental plaque-induced gingival conditions. Journal of periodontology, 89 Suppl 1, S17–S27. https://doi.org/10.1002/JPER.17-0095

Naldi L. (2016). Psoriasis and smoking: links and risks. *Psoriasis (Auckland, N.Z.)*, *6*, 65–71. https://doi.org/10.2147/PTT.S85189

Nanci, A. (2018) Ten Cate's Oral Histology (Clinical Periodontology and Implant Dentistry (6th ed., pp. 599-606). Elsevier

Nithya, S., Radhika, T., & Jeddy, N. (2015). Loricrin – An overview. *Journal of Oral and Maxillofacial Pathology*, *19*(1), 64. https://doi.org/10.4103/0973-029x.157204

Nunn, M. E. (2003). Understanding the etiology of periodontitis: An overview of periodontal risk factors. *Periodontology 2000*, *32*(1), 11–23. https://doi.org/10.1046/j.0906-6713.2002.03202.x

Omary MB, Coulombe PA, McLean WH. Intermediate filament proteins and their associated diseases. N Engl J Med. 2004 Nov 11;351(20):2087-100. https://doi.org/10.1056/NEJMra040319

Page, R. C., & Schroeder, H. E. (1976). Pathogenesis of inflammatory periodontal disease. A summary of current work. *Laboratory investigation; a journal of technical methods and pathology,* 34(3), 235–249.

Papapanou, P. N., Sanz, M., Buduneli, N., Dietrich, T., Feres, M., Fine, D. H., Flemmig, T. F., Garcia, R., Giannobile, W. V., Graziani, F., Greenwell, H., Herrera, D., Kao, R. T., Kebschull, M., Kinane, D. F., Kirkwood, K. L., Kocher, T., Kornman, K. S., Kumar, P. S., … Tonetti, M. S. (2018). Periodontitis: Consensus report of workgroup 2 of the 2017 World Workshop on the Classification of Periodontal and Peri-Implant Diseases and Conditions. *Journal of Periodontology*, *89*, S173–S182. https://doi.org/10.1002/jper.17-

0721

Rao, R. S., Patil, S., & Ganavi, B. S. (2014). Oral cytokeratins in health and disease. *The journal of contemporary dental practice*, 15(1), 127–136. https://doi.org/10.5005/jp-journals-10024-1502

Rowe, J. W., Fulmer, T., & Fried, L. (2016). Preparing for Better Health and Health Care for an Aging Population. *JAMA*, 316(16), 1643–1644. https://doi.org/10.1001/jama.2016.12335

Salvi, G.E., Berglundh, T., & Lang, N.P. (2015). In J. Lindhe, & N. P. Lang (Eds.) Clinical Periodontology and Implant Dentistry (6th ed., pp. 560-571). Wiley Blackwell.

Schroeder, H. E., & Listgarten, M. A. (1997). The gingival tissues: The architecture of periodontal protection. *Periodontology 2000*, *13*(1), 91–120. https://doi.org/10.1111/j.1600-0757.1997.tb00097.x

Schuilenga-Hut, P. H., Vlies, P. v., Jonkman, M. F., Waanders, E., Buys, C. H., & Scheffer, H. (2003). Mutation analysis of the entire keratin 5 and 14 genes in patients with epidermolysis bullosa simplex and identification of novel mutations. *Human mutation*, 21(4), 447. https://doi.org/10.1002/humu.9124

Silva-Filho JL, Caruso-Neves C, Pinheiro AAS. IL-4: an important cytokine in determining the fate of T cells. Biophys Rev. 2014 Mar;6(1):111-118. https://doi.org/10.1007/s12551-013-0133-z

Stanford, T. W., & Rees, T. D. (2003). Acquired immune suppression and other risk factors/indicators for periodontal disease progression. *Periodontology 2000*, *32*(1), 118–135. https://doi.org/10.1046/j.0906-6713.2003.03210.x

Toki, M. I., Cecchi, F., Hembrough, T., Syrigos, K. N., & Rimm, D. L. (2017). Proof of the quantitative potential of immunofluorescence by mass spectrometry. *Laboratory Investigation*, *97*(3), 329–334. https://doi.org/10.1038/labinvest.2016.148

Takahashi, N., Sulijaya, B., Yamada-Hara, M., Tsuzuno, T., Tabeta, K., & Yamazaki, K. (2019). Gingival epithelial barrier: regulation by beneficial and harmful microbes. *Tissue barriers*, *7*(3), e1651158. https://doi.org/10.1080/21688370.2019.1651158

Tonetti, M. S., Greenwell, H., & Kornman, K. S. (2018). Staging and grading of periodontitis: Framework and proposal of a new classification and case definition. *Journal of Periodontology*, *89*, S159–S172. https://doi.org/10.1002/jper.18-0006

Tonetti, M. S., Jepsen, S., Jin, L., & Otomo-Corgel, J. (2017). Impact of the global burden of periodontal diseases on health, nutrition and wellbeing of mankind: A call for global action. *Journal of Clinical Periodontology*, *44*(5), 456–462. https://doi.org/10.1111/jcpe.12732

Tozzoli, R., Antico, A., Porcelli, B., & Bassetti, D. (2012). Automation in indirect immunofluorescence testing: A new step in the evolution of the autoimmunology laboratory. *Autoimmunity Highlights*, *3*(2), 59–65. https://doi.org/10.1007/s13317-012-0035-2

Appendix

A.1 Participant consent form

PARTICIPANT CONSENT FORM

Title of Study: The role of a Loricrin in aggressive periodontal disease

Principal Investigator: Dr. Liran Levin (780-407-5562)

Research/Study Coordinator: Dr. Raisa Catunda

Why am I being asked to take part in this research study?

You are being asked to be in this study because we are trying to learn about one of the important causes of aggressive periodontal (gum) disease. During your procedure, gum tissue is normally discarded. Instead, we would like to collect this tissue that is normally disposed of for our study. The study will not change anything that the Dentist/Hygienist would do normally, it would only involve saving the tissue that is normally discarded for our study.

We would also like to collect a very small amount of the liquid that surrounds your teeth.

Before you make a decision one of the researchers will go over this form with you. You are encouraged to ask questions if you feel anything needs to be made clearer. You will be given a copy of this form for your records.

What is the reason for doing the study?

We are studying Aggressive Periodontal Disease or AP. AP is a very bad form of gum disease that occurs in young people in their 20s and 30s. It is so bad that they can lose all of their teeth in a very short time. You can imagine that it is very traumatic for the young person. Not a lot is known about why AP occurs. We think it may be caused by a decrease in a component of the gums, called loricrin. We would like to use the tissue that is normally thrown away during your procedure to measure the amount of loricrin in people with or without AP.

Our gums are composed of many cells that form a tight seal against the millions of bacteria found in our mouth. The tight seal is created by a protein called loricrin holding the cells together. Some bacteria that are found in the mouths of people with AP can trick the gum cells into producing less loricrin. We think this results in a weakening of the tight seal, allowing bacteria to invade. The body then tries to kill the bacteria, but in the process, can also destroy the bone that holds teeth in place. The body's response to bacteria is called "inflammation". It is similar to what happens when you have a cut and it gets infected: it becomes red and swollen with fluid. The fluid around your gums contains elements of inflammation that we can measure. We think those elements will be increased in the gum fluid of people with less loricrin because they will be fighting the invading bacteria.

What will happen in the study?

For participants who have a healthy mouth and are undergoing a crown lengthening procedure, we ask that you allow us to save the tissue that is normally discarded as a result of the procedure. Collection of this tissue will not change the procedure you undergo in any way.

We then ask that you also allow us to collect a small amount of the gum fluid around your teeth. To do this, we will place the tip of a small square of paper against your gums to absorb the fluid. We will do this at several places in your mouth.

You will not feel any more discomfort than what occurs during the normal crown lengthening procedure, and the collection of the fluid will take less than 2 minutes.

For participants with Aggressive Periodontal Disease, when you come to the clinic for periodontal surgery or scaling and root planing ("deep cleaning") as part of your normal treatment plan, we already occasionally remove tissue that has inflammation. Normally, this tissue is discarded. We ask that instead, you allow us to save this tissue for our study. Collection of this tissue will not change the procedure you undergo in any way.

For the collection of fluid, we will place the tip of a small square of paper against your gums to absorb the fluid. We will do this at several places in your mouth.

You will not feel any more discomfort than what normally occurs during your regular treatment, and the collection of the fluid will take less than 2 minutes.

So basically, you will have the same exact procedure that you would have had, but instead of throwing away your tissue, we will collect it for our study. We will also collect a small amount of fluid from around your teeth.

What are the risks and discomforts?
Since you are undergoing the procedure anyway, there are no changes in risks or discomfort as a result of collecting the tissue compared with throwing it away. Placing the paper against your gums to absorb the liquid causes no discomfort and has no risks.

What are the benefits to me?
There are no specific benefits to you. However, by participating, you are contributing to our knowledge of how AP causes such bad gum disease and tooth loss, and you may consider that this may help us treat AP patients better in the future.

What will I need to do while I am in the study?
Basically, there is no change in what you need to do. You will undergo the same exact procedure, except we will save instead of discard your tissue. It will take us less than 2 minutes to collect the gum fluid.

Do I have to take part in the study?
Participation in this study is entirely voluntary. If you decide to be in the study, you can change your mind and stop being in the study at any time during the procedure, and it will in no way affect the care or treatment that you are entitled to.

Are there other choices to being in this research study?
If you would like to participate, we will need to save the gum tissue instead of throwing it away as well as collect the fluid sample from your gum.
If you choose not to participate, we will just discard the tissue as done usually.

What will it cost me to participate?
There is no additional cost to participate in our study.

Will my information be kept private?
During the study we will be collecting health data about you. We will do everything we can to make sure that this data is kept private. No data relating to this study that includes your name will be released outside of the study doctor's office or published by the researchers.
When we collect your tissue and fluid, we will give it a random number. This random number will not be in your file, so no one will know that the sample is yours. We will also not document in your file that you were a participant in the study. The only other information that the lab researchers will have is your age (not your date of birth) and your gender. The researchers will also be told whether you are an AP patient or a healthy patient.

By signing this consent form, you are giving permission for the study doctor/staff to collect, use and disclose the information about you from your personal health records as described above (your age and your gender, and whether you are an AP patient or a healthy patient).
After the study is done, we will still need to securely store your health data that was collected as part of the study. At the University of Alberta, we keep data stored for 5 years after the end of the study.
If you decide not to participate in the study, we will not collect your health information or the samples.

What if I have questions?
If you have any questions about the research now or later, please contact Raisa Catunda at our office (780-407-5562).
If you have any questions regarding your rights as a research participant, you may contact the Health Research Ethics Board at 780-492-2615. This office is independent of the study investigators.
This study is being conducted/sponsored by the University Hospital Foundation. The Institution and study doctor are getting money from the study sponsor to cover the costs of doing this study. You are entitled to request any details concerning this compensation from the Principal Investigator (Dr. Levin).

CONSENT

Title of Study: The role of a Loricrin in aggressive periodontal disease

Principal Investigator(s): Dr. Liran Levin   **Phone Number(s):** 780-407-5562
Study Coordinator: Dr. Raisa Catunda   **Phone Number(s):** 780-407-5562

	Yes	No
Do you understand that you have been asked to be in a research study?	☐	☐
Have you read and received a copy of the attached Information Sheet?	☐	☐
Do you understand the benefits and risks involved in taking part in this research study?	☐	☐
Have you had an opportunity to ask questions and discuss this study?	☐	☐
Do you understand that you are free to leave the study at any time, without having to give a reason and without affecting your future dental care?	☐	☐
Has the issue of confidentiality been explained to you?	☐	☐
Do you understand who will have access to your records, including personally identifiable health information?	☐	☐
Do you want the investigator(s) to inform your dentistthat you are participating in this research study? If so, give his/her name _____	☐	☐

Who explained this study to you? _____

I agree to take part in this study:

Signature of Research Participant _____

    (Printed Name) _____

Date:_____

Signature of Witness _____

I believe that the person signing this form understands what is involved in the study and voluntarily agrees to participate.

Signature of Investigator or Designee   _____ Date _____

THE INFORMATION SHEET MUST BE ATTACHED TO THIS CONSENT FORM AND A SIGNED COPY GIVEN TO THE RESEARCH PARTICIPANT